

"Dunărea de Jos" University of Galati
Doctoral School of Mechanical and Industrial Engineering



PhD THESIS

ABSTRACT

**ASSESSMENT OF TRIBOLOGICAL BEHAVIOR
OF SEVERAL LUBRICANTS BASED ON RAPESEED OIL
AND NANOADDITIVES
(HEXAGONAL BORON NITRIDE AND GRAPHENE)**

PhD candidate
eng. Dionis GUGLEA

Scientific coordinator
Professor eng. Lorena DELEANU, PhD

Series I 6: Mechanical Engineering no. 65

Galați
2022



UNIUNEA EUROPEANĂ

Human Capital Operational Program

Priority axis 6 - Education and skills

Project: Scholarships for entrepreneurship education among PhD students and postdoctoral researchers (BeAntreprenor!)

Contract no.51680/09.07.2019 POCU/380/6/13 – Code SMIS: 124539



Instrumente Structurale
2014-2020

"Dunărea de Jos" University of Galati

Doctoral School of Mechanical and Industrial Engineering



PhD THESIS

ABSTRACT

ASSESSMENT OF TRIBOLOGICAL BEHAVIOR OF SEVERAL LUBRICANTS BASED ON RAPESEED OIL AND NANOADDITIVES (HEXAGONAL BORON NITRIDE AND GRAPHENE)

PhD candidate

eng. Dionis GUGLEA

Chairman

Univ. prof. eng. Elena SCUTELNICU, PhD
"Dunărea de Jos" University from Galati

Scientific coordinator

Univ. prof. eng. Lorena DELEANU, PhD
"Dunărea de Jos" University from Galati

Official Referee

Univ. prof. eng. habil. Răzvan RÎPEANU, PhD
Petrol-Gas University of Ploiesti

Official Referee

Univ. prof. eng. habil. Viorel PALEU, PhD
Technical University "Gheorghe Asachi" Iași

Official Referee

Univ. prof. eng. Luminița MORARU, PhD
"Dunărea de Jos" University of Galati

Series I 6: Mechanical Engineering no. 65

**Galati
2022**





The series of doctoral theses publicly defended in UDJG starting from October 1, 2013 are :

ENGINEERING SCIENCES field

- Series I 1: Biotechnoly
- Series I 2: Computers and information technology
- Series I 3: Electrical engineering
- Series I 4: Industrial engineering
- Series I 5: Materials engineering
- Series I 6: Mechanical engineering
- Series I 7: Food engineering
- Series I 8: Systems engineering
- Series I 9: Engineering and Management in Agriculture and Rural Development

ECONOMIC SCIENCES field

- Series E 1: **Economy**
- Series E 2: **Management**

HUMAN SCINCE fiels

- Series U 1: **Philology - English**
- Series U 2: **Philology - Romanian**
- Series U 3: **History**
- Series U 4: **Philology - French**

MATHEMATICS AND NATURAL SCIENCES field

- Series C: **Chemistry**

Acknowledgment

I would like to address words of thanks to those who offered me help and guided me throughout this doctoral thesis, supporting me so that, today, I can advocate it.

I would like to thank, first of all, professor Lorena Deleanu, PhD, who, as PhD supervisor, offered me all her knowledge and her constant guidance and encouragement, throughout the thesis preparation, as well as for my personal training.

I would like to express my sincere thanks to the commission for guidance and evaluation of the work, consisting of prof. phys. Gabriel Murariu, PhD, ass. prof. Doina Boazu, PhD and ass. prof. Constantin Georgescu, PhD, especially for the help provided on some very important details for me, which were related to the preparation of the doctoral thesis at a high level, as well as for the competent and highly professional guidance and recommendations.

Thanks to my colleague, eng. George Cătălin Cristea, PhD, currently a researcher at the "Elie Carafoli" National Aerospace Research Institute (INCAS) Bucharest, for the time offered in explaining how to work with the four-ball machine, as well as the testing methodology.

For the FTIR analysis, I thank professor chem. habilitated Constantin Apetrei, PhD, from the Department of Chemistry, Physics and Environment, Faculty of Sciences and Environment, "Dunărea de Jos" University of Galati.

Special thanks to my colleague and friend, eng. George Ghiocel Ojoc, PhD in mechanical engineering from 2022, for offering me support on the IT side and even hosting during the completion of the thesis.

Thanks to my colleague, eng. Traian Florian Ionescu, doctor in mechanical engineering from 2020, who offered me support during the pandemic time, in carrying out tests on the four-ball machine.

This doctoral thesis would not have been possible to develop without the support of lecturer eng. Dumitru Dima, PhD, from the Faculty of Sciences and the Environment, "Dunărea de Jos" University of Galati.

Last but not least, I want to thank lecturer eng. Alexandru Petrică, PhD, from the Faculty of Engineering, "Dunărea de Jos" University of Galati, for his help in using the optical microscope to measure wear scars and the ass. prof. eng. Răzvan Şolea, PhD, from the Faculty of Automation, Computers, Electrical and Electronics Engineering, "Dunărea de Jos" University of Galati, for the work on the calibration of the four-ball machine torque measuring equipment.

I thank Expur SA Bucharest, for providing the basic material, rapeseed oil, for this thesis.

I thank the team of the project "Scholarships for entrepreneurship education among doctoral students and postdoctoral researchers (BeAntrepreneur!" (Contract no. 51680/09.07.2019 POCU/380/6/13 - SMIS Code: 124539) for the support in disseminating the results of this work and for the courses, useful in a future research activity and project management.

With special esteem and gratitude, I thank my wife, as well as my parents, who were by my side every day, that have always surrounded me with their affection so that I could go to the end, no matter how hard it was; their patience gave me the strength to feel motivated, supporting me from all points of view throughout this period of studies.

Dionis Guglea

Table of Contents

Acknowledgement	3
Table of contents	4
Chapter. 1. Rapeseed oil as a lubricant and critical analysis of rapeseed oil lubricants	5
1.1. Additivation of vegetal oils.....	5
1.2. Properties of hexagonal Boron nitride.....	7
1.3. Applications of hexagonal Boron nitride (h-BN)	7
1.4. Hexagonal Boron nitride as an additive in lubricants.....	8
1.5. Experimental studies with h-BN as an additive in lubricants.....	8
1.6. Graphene as an additive in lubricants.....	9
1.7. Conclusions on lubricant additivation with h-BN and graphene	9
1.8. Conclusions and objectives of this study.....	11
Chapter. 2. Organization of the thesis	12
Chapter. 3. Lubrication regime evaluation for sliding ball-to-ball contact	13
3.1. The model for calculating the thickness of the fluid film	13
3.2. Lubrication regimes, calculated for sliding ball-ball contact, lubricated with rapeseed oil	16
3.3. Calculation of the minimum thickness of the fluid film	18
3.4. Conclusions on the theoretical regimes of rapeseed oil lubrication	19
Chapter. 4. The test campaign on the four-ball machine and elaborate lubricants	21
4.1. Evaluating the tribological characteristics of lubricants on four-ball machine	21
4.2. Test Procedure.....	22
4.3. Tribological parameters measurable by tests on the four-ball machine.....	23
4.4. Formulation of lubricants based on rapeseed oil and nano additives	25
4.5. Campaign of tests on four-ball machine	26
Chapter 5. Tribological evaluation of nano additive lubricants formulated with rapeseed oil	29
5.1. Tribological behavior of rapeseed oil on four-ball tester, in normal regime	29
5.2. The tribological behavior of rapeseed oil additivated with nano hexagonal Boron nitride, graphene and with the package with hexagonal Boron nitride and graphene, in normal regime	34
5.3. Analysis of Tribological Parameters in Severe Regime, for Rapeseed Oil and Rapeseed Oil Additivated Hexagonal Boron Nitride	41
5.4. Analysis of the tribological behavior of lubricants using 3D maps	43
5.5. Conclusions on the tribological behaviour of non-aditivated and additivated rapeseed oil	45
Chapter. 6. Flammability of rapeseed oil and rapeseed oil additived with 1% hexagonal Boron nitride on hot surfaces	47
6.1. Flammability of fluides and tests to assess it	47
6.2. Equipment and test procedure	48
6.3. Analysis of results	49
6.4. FTIR analysis for lubricant samples after flammability testing on hot surfaces	52
6.4.1. Apparatus and method of analysis	53
6.4.2. Results of the FTIR analysis.....	53
6.5. Conclusions on the flammability of rapeseed oil and the lubricant formulated with rapeseed oil and 1% h-BN, on a hot surface	58
Chapter. 7. Conclusions and personal contributions	59
7.1. Final conclusions.....	59
7.2. Personal contributions.....	64
7.3. Future research directions.....	66
<i>List of scientific papers elaborated by eng. Dionis GUGLEA</i>	<i>67</i>
<i>Bibliography.....</i>	<i>69</i>

Chapter 1

Rapeseed Oil as a Lubricant and Critical Analysis of Lubricants Obtained with Rapeseed Oil

1.1. Additivation of Vegetal Oils

In many applications, lubricants are obtained from petroleum, but the tendency is to be replaced by synthetic products or vegetal oils [116], the latter having the advantage of being more environmentally friendly [9], [163], but their additivation is still an object of study [45], [78]. Among the most usable plant resources for lubricants, from renewable and environmentally friendly resources, there are oils obtained from rapeseed (including here the Canadian variant, Canola), sunflower, soybean, leenseed, cotton, corn, castor, hemp, olive, palm, saffron, hazelnut etc.. Research has also been carried out in the last decade for the tribological characterization of more exotic oils that cannot be produced in large quantities, such as those obtained from rice or rice by-products, sesame, *Annona Muricata*, passion fruit, etc.

Today, vegetal oils are also processed to obtain environmentally friendly and non-toxic additives for lubricants [118]. The additives obtained can have a beneficial influence on the formation of films by adsorption to the metallic surface, the experimental results reported by Quinchia on the four-ball and ball-on-disc tribometers being promising.

The molecular chains of fatty acids and polar groups in vegetal oils help to physically fix them on the bodies in contact, even in severe exploitation [2]. From these studies and from the studies carried out by [16], [37], it follows that there is a composition in fatty acids, for which the tribological properties would be better, but today this concentration control is difficult to achieve in a technology for the market.

Vegetal oils, obtained from certain resources, can have compositions in somewhat wider ranges, depending on the geographical area, the nature of the soil and the climate, but they fall within 2...15%, which will influence the quality of the obtained lubricant to a relatively small extent [17], [64], [114], [182]. The amount of unsaturated fatty acids may reflect the ability of the vegetal oil to attach to the metallic surfaces, but also a higher probability of degradation and modifications through chemical bonding. The particular position of rapeseed oil and Canola oil is noted, with a high amount of mono-unsaturated fatty acids, highlights the peculiarity of the composition for rapeseed oil (European and Canadian - Canola type): a concentration of 6...10% saturated fatty acids, relatively low as compared to other vegetal oils, a concentration of more than 60% mono-unsaturated fatty acids and the presence of 25...30% of poly-unsaturated fatty acids. Other vegetal oils with similar concentrations of mono-unsaturated fatty acids (olive oil, sunflower oil) do not perform particularly well as lubricants and, therefore, the characteristic of this concentration of monounsaturated fatty acids (mainly, oleic acid) in rapeseed oil, being favorable to tribological applications.

In the beginning, those who formulated vegetal oil-based lubricants used principles and methods specific to petroleum products, but the resulting products did not meet the performance required by the industry. Even if the processes and methods have been tailored to the specifics of vegetal-base oils, they can be used in specific applications, often required by environmental protection legislation. There are several causes that lead to low efficiency of these lubricants. Classically, a lubricant has a base oil and addition agents or additives. Studies at the end of the last century proved that the additives used in mineral oils are not suitable in vegetal oils, especially because of the differences in the composition of the two types of oils. The role of additives in vegetal oils has been detailed in well-documented synthesis articles [158], [161].

Vegetal oil based lubricants have limited temperature ranges. Most vegetal oils can work well in the 60...70 °C range, only a few can work at 100...110 °C. Most of them are ineffective below 0 °C, but there are exceptions for -30 °C. In addition, their lifespan is reduced due to their susceptibility to natural or accelerated aging by temperature and/or environment.

In the last decades, vegetal oils have been improved through various technologies applied to both the culture and the resulting oil [144]. Thus, there are rapeseed oils with a low uric acid content, rapeseed and soybean oils with a high oleic acid content and castor oil that can be used at lower temperatures. The additive packages have been adapted to the composition and structure of vegetal oils and, thus, the performance of these oils has improved.

At the beginning of the introduction period of vegetal oil-based lubricants, additives from mineral oils were used. But mineral oils are generally nonpolar, while triglycerides in vegetal oils are polar. The same additive will react differently and unpredictably in vegetal oils as compared to mineral oils. It is recommended to use a solubilizing or dispersing agent, as the author of this study did, using guaiacol (supplied by Fluka Chemica), the chemical formula being noted with $C_6H_4(OH)OCH_3$ (2-methoxyxyphenol), Additives without metals, therefore without ash, are more soluble in vegetal oils. Additive packages for vegetal oils are few and must be adequately proportioned to keep the lubricant in the biodegradability class, required by the application. A synthetic presentation of lubricant additives is given in [179] and Georgescu C. et al. [44] reviewed additives used especially for vegetal oils.

Specialists also introduce the notion of friction modifiers [63], but these additives also have the role of reducing wear (because the excessive generation of wear particles leads to increased friction). These additives are often referred to as friction and wear modifiers [57], [100], [122], [151].

Additives, as friction and wear modifiers, can be solid substances (such as spherical particles, rolled or unrolled plates or "cloths", etc.). Chemically, there are metallic substances (generally, soft metals, such as Cu [20], [75], [131], Ag [81], [141], Zn, metal oxides such as CuO [150], ZnO [68], [69], TiO₂ [26], [53], [68], [77], MnO₂ [80], but also salts, hydroxides of Mg/Al/Ce [88], [89], hydroxides of Zn/Al/Mg [86], or metal compounds that have low shear strength, usually in hexagonal structure, such as sulfides of Mo and W, nitrides, such as hexagonal Boron nitride [1], [56].

Anti-wear and anti-friction additives are present in a lubricant in percentages of 2...3% in car lubricants. Some additives are not soluble in the base oil, such as Molybdenum disulfide, graphite, etc. Some additives, even of nano size, have a tendency to separate, agglomerate and, therefore, testing is necessary.

Bogatu et al. [18] concluded that vegetal oils have natural extreme pressure and anti-wear qualities and, therefore, they are less additivable as compared to mineral oils, fact that can be explained by the chemical structure of the compounds in vegetal oils and by other mechanisms of interaction between the lubricant and the additive, and lubricant and the metallic surface. The seizure load values of tested mineral oils were higher than those of vegetal oils.

Liu W. and Wang X., in the chapter "Nanolubricants Made of Metals" [92] from the book *Nanolubricants*, but also Qiao S. Z. et al. [117] admit that metals are most often used in tribological applications. Harder and less deformable metal alloys are intended for solid triboelements or coatings with sliding or rolling motion, while soft metals or their alloys, such as Au, Ag, Cu, Zn, Pb, Bi, Sn, In, are introduced into the lubricant in order to form continuous films or not, renewable or not, with the role of reducing wear and friction. The good behavior in contact results from their structure, usually face-centered, which has several sliding planes and, thus, have a low shear strength in the sliding direction. This sliding behavior is similar to that of a very high viscosity liquid lubricant.

Meng Y. et al. [99], in an extensive article on recent achievements in tribology, devoted a chapter to organic and inorganic nano additives, friction reduction mechanisms and protection of moving surfaces under load.

Along with graphene and MoS₂, other 2D materials, such as hexagonal Boron nitride (h-BN) [19], [55], [72], [152], double-layered hydroxides of Mg/Al [167], nano composites hybrids or mixtures of metals, oxides and/or metal salts [34], [157], Zn-Ni/Al₂O₃ [8], TiO₂/SiO₂ [58], Al₂O₃ and TiO₂ [4] or even organic salts [90], were introduced as anti-friction and anti-wear additives in lubricants.

Liu et al. [94] produced composite nanosheets of graphene and hexagonal Boron nitride using high energy mills in ammonia atmosphere, and investigated the tribological behavior of lubricants formulated with mineral oil as base oil. The stronger interaction between graphene nanosheets and h-BN has been shown to reduce wear and friction [93].

Manu B. R. et al. [97] carried out a valuable review of research in the field of 2D materials that includes graphene [49], but also oxidized graphene [108], hexagonal Boron nitride, MoS₂ [15], [119] and other 2D materials [67], [82], [83]. Other oil additives are metallic or non-metallic nanoparticles [146], [160], metallic or non-metallic oxides [115], [148] and inorganic nano composites [6].

Several researchers have mixed two or more of the compounds listed above as a package of oil additives, research being mostly done on motor oils.

In Rudnick's book (Lubricant Additives) [122], there is a chapter dedicated to the additivation of vegetal oils, which reflects the researchers' interest in improving the tribological behavior of this group of lubricants, vegetal oils + additives [99]. h-BN is described as a solid lubricant with a structure similar to graphite and WS₂, used for special applications [76], or, for example, as an additive in porous bearing lubricant [111].

1.2. Properties of Hexagonal Boron Nitride

Boron nitride is a compound of Boron and Nitrogen, refractory, thermally and chemically resistant, with the chemical formula BN [40]. The graphite-like hexagonal form, h-BN, is the most stable and soft among the allotropic forms of BN and it is used as a solid lubricant and an additive in lubricants [21].

Boron nitride exists in several allotropic forms, with different arrangements of Boron and Nitrogen atoms, giving rise to varying bulk properties of the material (Fig. 1.1).

Amorphous Boron nitride (a-BN) is similar to amorphous carbon. The other allotropic forms of Boron nitride are crystalline.

The hexagonal form (h-BN) is a stable crystalline form, also called graphitic Boron nitride. It has a layered structure, similar to graphite. Within each layer, there are strong covalent bonds between the Boron and Nitrogen atoms, but between the layers there are weak van der Waals forces [36].

Cubic Boron nitride (c-BN) has a structure similar to that of diamond.

The wurtzite form (w-BN) has the same structure as a rare hexagonal carbon polymorph. As in the cubic form, Boron and Nitrogen atoms are grouped into tetrahedra [14], [127]. Recent studies have measured the hardness of w-BN at 46 GPa, slightly higher than commercial Boron nitrides, but softer than the cubic form of Boron nitride [123], [140].

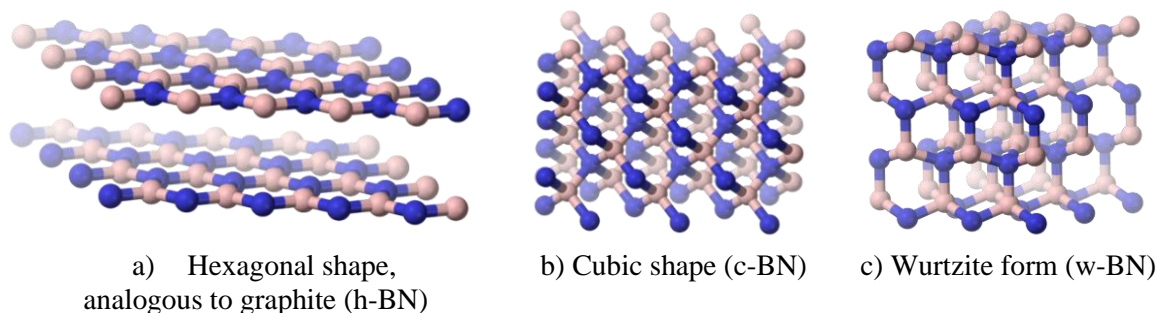


Fig. 1.1. Allotropic forms of BN [170]

1.3. Applications of Hexagonal Boron Nitride (h-BN)

Hexagonal BN (h-BN) is the most widely used allotropic form of Boron nitride. It is a good solid lubricant, both at low and high temperatures (up to 900 °C, even in oxidizing atmospheres) [127], [165]. As a solid lubricant, h-BN is useful where the electrical conductivity or chemical reactivity of graphite (as alternative lubricant) would be problematic. Another advantage of h-BN over graphite is that the lubrication process does not require water or gas molecules trapped between the layers. Solid h-BN lubricants can also be used in vacuum, in space applications. The lubricating properties of h-BN are used in cosmetics, paints, dental materials [170].

h-BN was firstly used in cosmetics around 1940s, in Japan. Due to its high price, h-BN was abandoned for this application. Its use was revitalized at the beginning of the 3rd millennium. And currently, h-BN is used by many cosmetic manufacturers and in tribological applications.

Hexagonal Boron nitride can be exfoliated in monolayers or in few atomic layers. Because of its structure analogous to that of graphene, atomically thin Boron nitride is sometimes called "white graphene" [130], [177].

Boron nitride is one of the best electrical insulators. Monolayer Boron nitride has a Young's modulus of 0.865 TPa and a tensile strength of 70.5 GPa and, in contrast to graphene, whose strength decreases dramatically with increasing thickness, few-layer Boron nitride sheets have a strength similar to that of monolayer Boron nitride [61], [112].

1.4. Hexagonal Boron nitride as an additive in lubricants

Hexagonal Boron nitride (h-BN) is a reference solid lubricant in the class of inorganic lubricants with lamellar structure, which also includes Molybdenum disulfide, graphite and other sulfides, selenides and tellurides of Molybdenum, Tungsten, Niobium, Tantalum and Titanium. Boron (B) and Nitrogen (N) atoms are covalently bonded to other atoms in the plane with an angle of 120° between two bonds (each boron atom is bonded to three nitrogen atoms and each Nitrogen atom is bonded to three Boron atoms). The hexagonally structured planes are bound together by weak van der Waals forces.

Frictional forces cause the Boron nitride particles to orient in the direction in which the planes are parallel to the sliding motion. The anisotropy of mechanical properties provides a combination of low coefficient of friction and high loading capacity of Boron nitride. Boron nitride forms a strongly adherent lubricating film on the surface of the substrate. The lubrication sheet ensures good wear resistance and resistance to detachment (compatibility).

The coefficient of friction of Boron nitride is in the range of 0.1-0.7, which is similar to that of graphite and Molybdenum disulfide. Impurities (e.g., Boron oxide) adversely affect the lubricating properties of Boron nitride.

The main advantage of Boron nitride, as compared to graphite and Molybdenum disulfide, is its thermal stability. Hexagonal Boron nitride retains its lubricating properties up to 2760 °C in an inert or reducing environment, and up to 870 °C in an oxidizing atmosphere. Boron nitride has a high thermal conductivity.

Some applications of hexagonal Boron nitride are: additive at nano scale in lubricating oils [1], [24], [56], [152], antifriction coatings, polymer based composites, second phase in antifriction coatings or metal-based composites, solid lubricant in metal forming, sintered ceramic parts for high temperature applications.

There is research in other Boron-based additives. For example, Bas H. et al. [10] studied the tribology of an engine oil, in which they added two types of Boron additives, each in different concentrations. The addition of boric acid (H_3BO_3) and h-BN reduced the friction coefficient by 10...50%, the optimum concentration being determined at 4 wt% for both boric acid and h-BN.

1.5. Experimental Studies with h-BN as an Additive in Lubricants

Abdullah M. I. H. C. et al. [1] investigated the effect of h-BN nano particles in SAE 15W-40 diesel engine oils, considering it to have a similar effect as extreme pressure (EP) additives. Testing was performed using a four-ball tribometer according to ASTM standard D2783/21 [184]. More adhesive wear was observed on the worn surfaces of the ball bearings, lubricated with SAE 15W-40 engine oil as compared to nano-oil lubrication. The results of the experimental studies demonstrated the potential of h-BN as an additive to improve the loading capacity of lubricating oil. The additivated lubricant was formulated by dispersing an optimal composition (0.5% vol) of 70 nm h-BN nano particles in SAE 15W-40 diesel engine oil using an ultrasonic homogenizer for 20 minutes with 0.5% surfactant (oleic acid) to prevent sedimentation of nano particles. The surfactant had no significant effect on the tribological performance of the lubricants.

In a documentation dedicated to 2D nano additives, including here hexagonal sheet-type structures, specific to graphite and graphene [87], [162], WS_2 [73], MoS_2 [153]. Xiao H. et al. [156] also include h-BN, as an additive alongside phosphorus additives [101], [102].

Shafi W. K. and Charoo M. S. [133] studied the rheology of sesame oil doped with h-BN nano particles. Tests were performed on a MCR102 rheometer Anton, at different temperatures (20 °C, 50 °C and 70 °C), the nanolubricant being characterized by a non-Newtonian behavior for the tested shear rates.

Yıldırım C. V. et al. [159] developed a nano lubricant by adding h-BN particles (65...75 nm, 99.85% purity) in the oil, helping the machining of Inconel 625 steel. Tribological parameters specific to the machining process were analyzed: lifespan of the tool, the roughness of the part and the tool, the wear of the tool and the temperature at the tool-workpiece interface. The results showed that a concentration of 0.5 vol% h-BN in the machining fluid resulted in reduced wear and higher tool durability. The cutting fluid containing 1 vol% h-BN produces the lowest tool interface temperature in

terms of cooling condition. The nano-fluid (1 vol%) reduces the temperature by 30.25%. Nano additives retain the oil particles, preventing the immediate release of cutting oil from the cutting area and, thus, it lubricates better. However, with increasing h-BN ratio in the coolant, there is a reduction in tool lifespan and an increase in surface roughness.

Bondarev et al. [19] used h-BN nanoparticles, with different morphologies (hollow particles, with smooth surfaces, butterfly or petal type particles, globular, formed by numerous h-BN nanosheets, added to a PAO6 lubricant; 100Cr6 metal surfaces in contact were tested in the presence of PAO6+BN lubricants with 0.1% and 0.01% Boron nitride as additive.

Thachnatharen et al. [147] introduced different concentrations of hexagonal Boron nitride (h-BN) into the lubricant, with an average particle size of 70 nm, in SAE 20 W50 Military grade diesel engine oil: 0.5 wt%, 0.25 wt%, 0.05 wt%, 0.025 wt%. The test parameters were 1200 rpm (4-ball machine spindle angular velocity), 392.5 N (force), 3600 s (test duration) and 75 °C (oil temperature). The lubricant with h-BN produced a 20.5% lower friction coefficient and a 9.47% smaller wear scar diameter as compared to those obtained with the base oil. The balls had a diameter of 12.7 mm.

1.6. Graphene as an Additive in Lubricants

Graphene, diamond and fullerenes have been studied as additives in lubricants by Cursaru D. et al. [30] and Lee et al. [85], Shahmohamadi et al. [134], Lee K. et al. [84].

Eswariah V. et al. [38] synthesized deoxygenated graphene, which has fewer network defects and is hydrophobic, dispersing well in oil. The wear scar diameter (WSD) decreased by 33% and the friction coefficient by 80% for 0.025 mg/mL graphene in engine oil. Without changing the rubbing surfaces, graphene reduced friction, but with increasing concentration, WSD and friction coefficient increased. The graphene was mixed with oleic acid for better dispersion in the base oil.

Lin J. et al. [91] studied the dispersion of graphene sheets in oil and tested several dispersing agents. Tests were done on the four-ball machine, at 1200 rpm and 147 N, at 75 °C, for 60 minutes. They concluded that stearic acid and oleic acid were the most suitable dispersants. 0.075 wt% was the optimal graphene concentration, reporting an improvement in wear and increased contact load capacity. Graphene nano platelets were mixed with stearic acid and oleic acid (mass ratio 3:5) in 40 mL cyclohexane by ultrasonication for 30 min at room temperature.

The conclusions of Lee and Hwang's study are as follows [85]:

- the addition of nano particles in lubricants improves their characteristics as compared to micro-sized additives; the nano particles in contact take part of the load and behave like very small rolling bodies [32], [35], [66],
- oils with fiber type particles (e.g. carbon nano tubes, PTFE) have higher friction coefficient values than those obtained with lubricants with spherical nano particles or all similar sizes, probably because of the way they make contact and the fact that spherical particles tend to roll more easily and to level the texture of surfaces in contact,
- the fibrous nano particles agglomerate more easily than the spherical ones, so that their thickness becomes greater than the thickness of the lubricant film, resulting in an increase in roughness, an embarrassment to the circulation of the lubricant, especially when entering in contact.

Graphene is considered an emerging lubricant [11], [12], [13]. However, the potential of graphene as a lubricant remains unexplored. Its properties can vary a lot, depending on the size of the sheets and their shape; thickness and defect density of graphene alter the mechanical and tribological properties.

However, the reported tests are of short duration and the results cannot be extrapolated over long periods of time, as required in actual applications. And, from these data, the need to test the formulated lubricant was highlighted because the results differ a lot, depending on the environment, test conditions, etc.

1.7. Conclusions on Lubricant Additivation with h-BN and Graphene

The following conclusions emerge from the studied documentation:

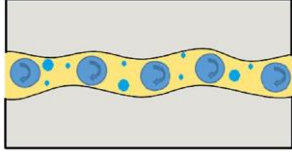
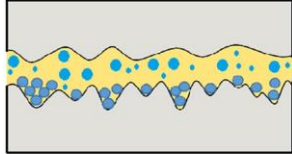
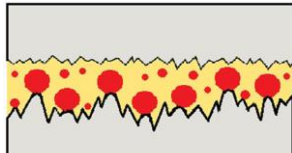

- good results are reported for the additivation of lubricant oils with friction and wear modifiers, but those with reference to additivated vegetal oils are very rare [135],

- the proposed experimental study has chances to formulate lubricants by adding nano h-BN, with improved tribological properties,

- the additive package (h-BN + graphene) has been proposed recently, only in a few articles but, from the consulted documentation, no researcher has tried to introduce this package into a vegetal oil. Liu Y et al. [94] produced a mixture of additives (h-BN + graphene) in mineral base oil, observing a better behavior at loads in the severe domain, increasing the seizure load value.

Table 1.1 provides a description of the mechanisms that occur in lubrication with fluids containing nano particles. The drawings are taken from [132], [163], but similar sketches are also given by Wu Y. Y. [155].

Tab 1.1. Mechanisms occurring in nanolubricant contacts [132]

Mechanism	Sketch	Benefits	Disadvantages
Rolling of nanoparticles between the surfaces of solid bodies		- Reduction of friction	- Fragmentation, - Scratching, - If the particles do not keep a shape favorable to rolling, friction increases
Texture leveling by filling very deep recess with particles		- Reduction of roughness parameters - Filling very deep recess	- Uneven deposits on the surface, - High asperities remain uncovered
Polishing (a light abrasive process)		- Surface finishing - The disappearance of very high and sharp peaks favors the appearance and maintenance of a continuous film of fluid	- Increasing wear and tear - Growing game
Generation of a protective tribolayer (continuous or not)		Reducing damage to solid parts Taking charge more evenly	- The film may be uneven, - film stability implies chemical reaction

Thampi et al. [149] concluded the following.

- The use of nanoparticles is reported by researchers to be beneficial for improving the tribological characteristics of lubricants. It is stated that the addition of 0.1...0.5wt% additive is sufficient to significantly improve the tribological properties but it does not provide arguments in favor or against other concentrations.

- Other authors have reported promising results for 1% to 3% nano additives. Obviously, the price of the lubricant is increasing and, often, the package of nano additives is limited by regulations regarding toxicity and/or biodegradability. Good results for the additive in a concentration of 1%wt were obtained by Cristea G.C [25], [27], [28], in soybean oil, Ionescu T.F. [68], [70] with rapeseed oil as base oil, Ilie F. [67], Paleu V. [107], [108], [109].

- The presence of nano additives in lubricants determines the development of specific mechanisms to protect the surfaces in contact, to reduce wear and friction [3], [113], [155]: the rolling of nanoparticles, the polishing mechanism, the mechanism of filling the bottom of the surface texture and the formation of a protective film. Following the analysis of recent works [42], [68], it was found that in the case of powder or nano plate additives, there is no continuous or discontinuous protective film, but only a mechanical fixation of the particles in the profile of the moving surfaces, which acts as

shock absorbers, as intermediate load takeovers, even in the conditions of their agglomeration or fragmentation.

- Nano additivation poses the question of the stability of dispersions, the synthesis of nano additives and their price.

In 2021, a paper appeared in *Tribology International*, in which the additive package (h-BN + graphene + ionic liquid) was introduced into a synthetic oil, polyalphaolefin 32, PAO, using the first two additives in low concentrations, 0.05 wt% graphene/0.1 wt% h-BN [101]. A ball-on-disc tribometer was used. This work, developed a few years after the theme for the doctoral thesis was set, proves that the interest in these additives was and is in the attention of researchers.

A model for a graphene-containing lubricant is presented by Zhang W. et al. [166], suggesting that graphene nanosheets attach to solid surfaces, “wrinkling” on contact, shifting, shearing or breaking, but maintaining a very thin graphene layer, in dynamics. Graphene concentration does not appear to significantly influence the friction coefficient, but the WSD decreases with increasing graphene concentration up to 0.06%, after which the increase has a very small slope, with the smallest scatter of values for 0.08% graphene, the range with 0.6...1% graphene giving WSD with small variation. The lowest value for COF was obtained for the oil with PAO+0.1% h-BN and PAO with h-BN and graphene. And this author noticed a disadvantage of these lubricants, the sedimentation of additives over time.

1.8. Conclusions and Objectives of This Study

From the studied literature, the following trends are observed:

- intensifying research for the use of rapeseed oil as an industrial lubricant, additivated or not,
- the formulation of lubricants based on vegetal oils with the attempt to highlight the peculiarities of their tribological and rheological behavior,
- the production and introduction of nano additives into lubricants with still contradictory results.

The objectives of this thesis are:

- theoretical evaluation of the lubrication regime for rapeseed oil, for working parameters (load, sliding velocity, temperature) and viscosity and calculation of the minimum thickness of the rapeseed oil film for the tested regimes, for an initial evaluation of the working regime (mixed or with fluid film),
- the design of a laboratory-scale technology for the additivation of rapeseed oil with h-BN, graphene and a package of h-BN and graphene,
- designing a test campaign that includes two regimes, normal working regime and severe regime, based on a set of variables (nano additive concentration, sliding speed and load on the 4-ball tribotester),
- evaluation of the tribological behavior by analyzing several parameters (friction coefficient, wear scar diameter and wear rate of the wear scar diameter, temperature in the lubricant bath at the end of the test),
- testing of friction and wear modifying additives (h-BN, graphene and h-BN+graphene) on the four-ball machine,
- evaluating the results and determining the influence of h-BN concentration, for working regime (with load and sliding speed in enlarged ranges), comparing the results for rapeseed oil, rapeseed oil with 1% h-BN and rapeseed oil +1% h-BN + 1% graphene,
- determination of flammability characteristics on hot surfaces (the highest temperature at which three repeated tests do not ignite the oil and the lowest temperature at which the oil ignites, at least one test out of three), for rapeseed oil and rapeseed oil + 1% h-BN,
- dissemination through participation in projects, international and national conferences, publication of articles.

Figure 2.1 presents the diagram of this thesis.

**Chapter 2
 Organization of the Thesis**

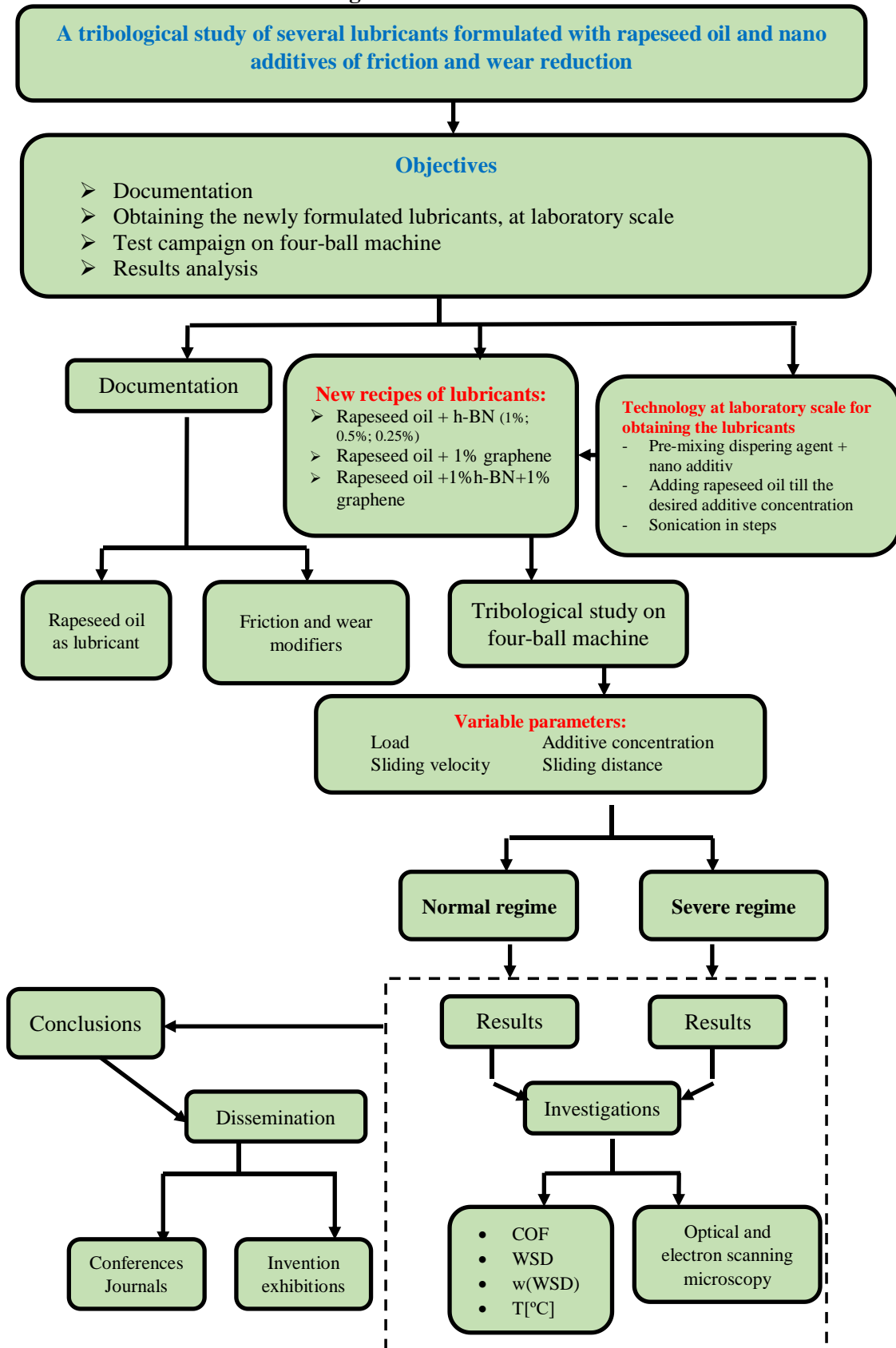


Fig. 2.1. Diagram of the thesis

Chapter 3

Evaluation of Lubrication Regime for Sliding Ball-to-Ball Contact

3.1. The Calculation Model of the Thickness of the Fluid Film

In a lubricated tribosystem, the fluid film that forms between the two bodies can have thicknesses that can vary between 10^{-10} m and 10^{-5} m [49], [318], [85]. The thickness of the fluid film is a parameter that characterizes, from a tribological point of view, a contact, in the case of this study, a point contact.

Hamrock and Dowson [142], [85] proposed a model for calculating the film thickness, both for the minimum value and for the thickness value near the plateau before the minimum thickness (also called the central thickness of the lubricant film).

From the study of the hydrodynamic lubrication model, it is known that lateral fluid losses reduce the lift for a given film thickness [85]. So, this phenomenon has an effect opposite to that observed in practice in hardly loaded contacts (formation of a load-bearing film).

Considering an isothermal process (specific to the stabilized regime), dynamic viscosity of the fluid in loaded contact remains a function dependent on pressure:

$$\eta = \eta_0 e^{\alpha \cdot p} \quad (3.1)$$

From the solutions obtained by numerical methods, two very important observations can be made (Fig. 3.1).

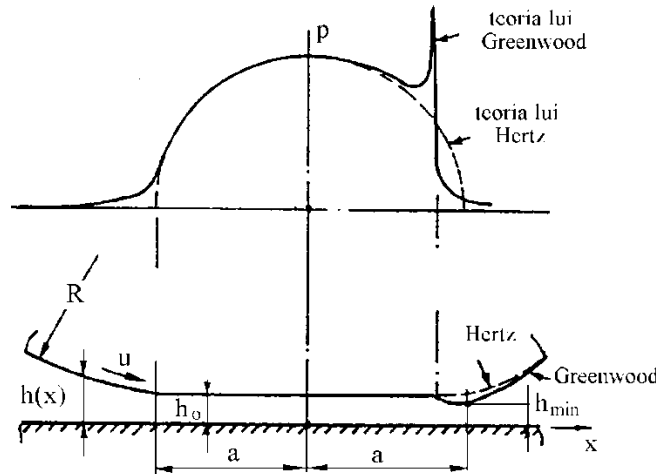


Fig. 3.1. The elastohydrodynamic contact [85]

Over most of the contact width ($2a$ in Fig. 3.1), the pressure is so high that the viscosity is several orders of magnitude higher than its value at atmospheric pressure. So, if the pressure gradient dp/dx must have realistic (not infinite) values, the film height variation must be very small, almost zero (denoted by h_0). From the mathematical model of EHD lubrication and the imposed boundary conditions, the film thickness should be very little variable over almost the entire high pressure area. As in heavily loaded contacts, the Hertzian pressure distribution is a satisfactory model of the actual pressure, there must be large pressure gradients near the edge of the loaded zone, towards its interior, to reduce the pressure to the atmospheric value.

At low pressures and viscosities, characteristic of the contact exit zone, large pressure gradients can only be achieved if the film thickness is reduced towards the exit zone. The numerical solution of the equation shows a pressure peak and a bulge of the bodies in contact towards the exit of the contact. For soft materials, this peak is greatly attenuated, it even disappears, the pressure distribution being asymmetric as compared to the Hertzian one, the maximum being shifted towards the contact exit zone [85], [318].

In conclusion, the film thickness and the contact lift were obtained by numerically solving the system consisting of: the Reynolds equation, the law of elastic deformations of solid bodies, the law of variation of viscosity with pressure.

For point contact, the following calculation formula is applied [85], [142], [244], being considered valid for a large number of combinations of materials in contact, including steel on steel, and for maximum pressures up to 4 GPa.

$$h_{\min} = 3.63 \cdot R_e \left(\frac{U \cdot \eta_0}{E' \cdot R_e} \right)^{0.68} \cdot (\alpha \cdot E')^{0.49} \cdot \left(\frac{W}{E' \cdot R_e^2} \right)^{-0.073} (1 - e^{-0.68 \cdot k}) \quad (3.2)$$

whre h_{\min} – minimum fluid film thickness; U – the relative velocity of the solids upon contact;

$$U = \frac{U_A + U_B}{2} \quad (3.3)$$

U_A and U_B are the velocities of the bodies A și B; η_0 – the dynamic viscosity of the fluid, at normal pressure; E' – the equivalent modulus of elasticity, ν_A, ν_B – Poisson's coefficients for bodies A și B; R_e – equivalent radius of curvature, α – pressure dependence coefficient of viscosity or piezoviscosity coefficient;

$$\alpha = \frac{0.0129 \cdot \ln(10^4 \cdot \eta_0)}{p_H^{0.25}}, [\text{MPa}^{-1}] [15], [50], [107] \quad (3.4)$$

p_H – Hertzian pressure; W – normal load in contact;

k – the ellipticity parameter;

$$k = a/b \quad (3.5)$$

with a – the semiminor axis of the contact ellipse; b – semimajor axis of the contact ellipse.

For sphere-sphere contact, $k = 1$.

In the four-ball tribotester, the load applied in the direction of the machine axis is distributed on the three fixed balls. The system has three sliding ball-ball contacts and three non-moving ball-ball fixed contacts. So, the contact between two balls is characterized by:

- load in contact

$$W = \frac{F}{3 \cdot \cos(\alpha)} = \frac{F}{3 \cdot \cos(35,264^\circ)} [\text{N}] \quad (3.6)$$

$U_A \neq 0$ (the upper ball, with the center on the axis of the machine)

- sliding speed

$$U = \frac{U_A}{2} = \frac{1}{2} \cdot \frac{2 \cdot \pi \cdot n}{60} \cdot \frac{R_A}{\sqrt{3}} [\text{m/s}] \quad (3.7)$$

where F – the load applied in the direction of the machine axis; n – the rotational speed of the main shaft of the machine, implicitly the angular speed of the fixed ball, attached to the shaft of the machine through a clamping system, in rpm.

Hamrock and Dowson, in a NASA technical report, determined the fluid film thickness as a function of following dimensionless factors [33], [60], [142]:

- the film thickness factor $H = \frac{h_{\min}}{R_e} \quad (3.8)$

- speed factor $U = \left(\frac{U \cdot \eta_0}{E' \cdot R_e} \right) \quad (3.9)$

- material factor $G = (\alpha \cdot E') \quad (3.10)$

- load factor $W = \left(\frac{W}{E' \cdot R_e^2} \right) \quad (3.11)$

- the contact shape factor (ellipticity factor), k .

For a contact between two identical spherical solids, equation (3.2) is rewritten as follows:

$$H = 3.63 \cdot U^{0.68} \cdot G^{0.49} \cdot W^{-0.073} \cdot (1 - e^{-0.68}) \quad (3.12)$$

In 1978, Hamrock and Dowson [60], proposed a classification of lubrication regimes according to the behavior of the materials in contact. Solids can be rigid or elastic and fluid can have constant or variable viscosity. By combining the solid variants with the fluid variants, four lubrication regimes are obtained:

- **isoviscous-rigid regime (IVR)** (rigid solids – fluid with constant viscosity),
- **piezoviscous-rigid regime (PVR)** (rigid solids – fluid with variable viscosity),
- **isoviscous-elastic regime (IVE)** (elastic solids – fluid with constant viscosity),
- **piezo-visco-elastic regime (PVE)** (elastic solids – fluid with variable viscosity).

The design first evaluates what type of lubrication regime is generated based on the design data, knowing the properties of the fluid lubricant and those of the solid triboelements.

The method of calculating the lubrication regime is done with the help of a set of parameters [142]:

- the lubricant film parameter $\bar{H} = H \cdot \left(\frac{W}{U} \right)^2 \quad (3.13)$

- the viscosity parameter $G_V = \frac{G \cdot W^3}{U^2}$ (3.14)

- the elasticity parameter $G_E = \frac{W^{8/3}}{U^2}$ (3.15)

- the ellipticity parameter, k , (kept constant) (3.16)

H is the fluid film thickness factor given in relation (3.12).

For each type of regime, the particular relations for calculating the dimensionless thickness of the fluid film are [142], [244], [318]:

- - the isoviscous-rigid regime

$$(\bar{H}_{\min})_{IVR} = 128 \cdot k^{\pi/2} \cdot \left[0.131 \cdot \arctg\left(\frac{k^{\pi/2}}{2}\right) + 1.683 \right]^2 \left(1 + \frac{2}{3} \cdot k^{-\pi/2}\right)^{-2} \quad (3.17)$$

- the piezoviscous-rigid regime

$$(\bar{H}_{\min})_{PVR} = 1.66 \cdot G_V^{2/3} (1 - e^{-0.68 \cdot k}) \quad (3.18)$$

- the isoviscous-elastic regime

$$(\bar{H}_{\min})_{IVE} = 8.70 \cdot G_E^{0.67} \cdot (1 - 0.85 \cdot e^{-0.31 \cdot k}) \quad (3.19)$$

- the piezo-elastic regime

$$(\bar{H}_{\min})_{PVE} = 3.42 \cdot G_V^{0.49} \cdot G_E^{0.17} \cdot (1 - e^{-0.68 \cdot k}) \quad (3.20)$$

The identification of the lubrication regime is important for evaluating the energy consumed by friction and for estimating the probability of a change in the lubrication regime in case of a change in the state of the surface due to wear and/or a change in some parameters (temperature, load, speed).

Having identified the lubrication regime and calculated the dimensionless thickness of the fluid film, with the relation specific to the lubrication regime, (3.17) – (3.20), its actual minimum thickness is:

$$h_{\min} = \left((\bar{H}_{\min}) \cdot R_e \cdot \left(\frac{U}{W}\right)^2 \right) \quad (3.21)$$

The method described below is also presented theoretically by Stachowiack [142] and Olaru [105]. The determination of lubrication regimes is based on the following assumptions:

- lubrication regime is stabilized (constant temperature, constant viscosity at working pressure and temperature (therefore, also in calculation),
- the model of the lubricated contact is a point contact, ball on ball with sliding, and it is isothermal,
- the contact is fully lubricated (there is enough fluid so that in the analyzed volume of the contact there are only the materials of the spheres and the lubricating fluid),
- it is considered that the contact failure does not occur.

The creation of the map of lubrication regimes, for a point contact, is done in a double logarithmic coordinate system, with the dimensionless elasticity parameter G_E on the abscissa and the dimensionless viscosity parameter G_V on the ordinate. In Fig. 3.2, a map of the lubrication regimes for rapeseed oil is given, at the lubricant temperature of 37.8 °C.

The method of drawing maps of the lubrication regimes, for a contact determined in shape by ellipticity ($k = 1$ for sphere – sphere contact) includes the following steps:

1. calculation of the dimensionless parameter of the fluid film thickness $((\bar{H}_{\min})_{IVR})$, with the relationship (3.17),

2. the parameter $((\bar{H}_{\min})_{IVR})$, as calculated in step 1, equals the dimensionless parameter of the lubricant film $((\bar{H}_{\min})_{PVR})$, given by relation (3.18) and the dimensionless viscosity parameter is determined $G_{V,1}$:

$$G_{V,1} = \left[\frac{((\bar{H}_{\min})_{IVR})}{141 \cdot (1 - e^{-0.0387 \cdot k^{\pi/2}})} \right]^{1/0.375} \quad (3.22)$$

3. For $k = 1$ imposed, with the dimensionless value of the fluid film thickness $((\bar{H}_{\min})_{IVR})$, calculated in step 1, and with the value of the dimensionless speed parameter $G_{V,1}$ calculated in step 2, the elasticity parameter is calculated $G_{E,1}$:

$$G_{E,1} = \left[\frac{((\bar{H}_{\min})_{IVR})}{3.42 \cdot G_{V,1}^{0.49} \cdot (1 - e^{-0.68 \cdot k})} \right]^{1/0.17} \quad (3.23)$$

It is obtained the point $A_{1,1}$, of coordinates $G_{E,1}$ și $G_{V,1}$, which is the first point of the boundary curve between the lubrication regimes PVE and PVR. The border between the IVR regime and the PVR regime is drawn, through a horizontal line through the point $A_{1,1}$ to the ordinate axis.

4. With the same values for the parameters k and $((\bar{H}_{\min})_{IVR})$, the elasticity parameter is calculated $G_{E,2}$:

$$G_{E,2} = \left[\frac{((\bar{H}_{\min})_{IVR})}{8.70 \cdot (1 - 0.85 \cdot e^{-0.31 \cdot k})} \right]^{1/0.67} \quad (3.24)$$

5. With the same parameters from step 4, along with the value of $G_{E,2}$, a new viscosity parameter is calculated $G_{V,2}$:

$$G_{V,2} = \left[\frac{((\bar{H}_{\min})_{IVR})}{3,42 \cdot G_{E,2}^{0.17} \cdot (1 - e^{-0.68 \cdot k})} \right]^{1/0.49} \quad (3.25)$$

It results the point $A_{1,2}$, of coordinates $G_{E,2}$ and $G_{V,2}$. The point $A_{1,2}$ is the first point of the separation curve between the PVE and IVE lubrication regimes. The points $A_{1,1}$ și $A_{1,2}$ join with a straight line and the boundary between the IVR regime and the PVE regime is obtained. The boundary between the IVR and IVE regimes is drawn, through a vertical line through the point $A_{1,2}$ to the abscissa axis.

Another value is chosen for $((\bar{H}_{\min})_{IVR})$, higher than the previous one and repeat the steps from step 2 to step 5, obtaining the points $A_{i,1}$ și $A_{i,2}$. Punctele $A_{1,1}, A_{2,1}, \dots, A_{i,1}$ join, the resulting curve being the border between the PVR and PVE regimes. The points $A_{1,2}, A_{2,2}, \dots, A_{i,2}$ determine by a straight line the boundary between the PVE and IVE regimes.

3.2. Lubrication Regimes, Calculated for Sliding Ball-Ball Contact, Lubricated with Rapeseed Oil

For the rapeseed oil (identified by its dynamic viscosity at temperature t), the lubrication regime for the test regimes was calculated. The test regime is customized by the sliding velocity and the force applied to the machine axis, i.e. on the fixed ball. Calculations were performed for sets (F, v) , with the values that were also used for the test campaign: for sliding speed $v = 0.23$ m/s, $v=0.38$ m/s, $v=0.53$ m/s, $v = 0.69$ m/s and $v= 0.84$ m/s and load ($F = 100$ N, $F = 200$ N and $F = 300$ N).

The author used an Excel program, created together with associate professor eng. Constantin Georgescu, PhD [110], [111], which quickly calculates the minimum fluid thickness and parameters necessary to draw the maps of lubrication regimes. Material and lubricant characteristics can be entered (viscosity, as a value dependent on a constant temperature – that is characteristic of the stabilized regime, and pressure through α), sliding speed, load.

The map of the lubrication regimes was drawn under the assumption that the operation of the lubricated contact is done in a stabilized regime, i.e. without variations in external load and speed, and in isothermal conditions. If the graph of rapeseed oil temperatures in the ball cup bath is analyzed, it can be seen that the selected temperature values are also found in the experimental data: approximately 40 °C for the load of $F=100$ N, in the speed range of 0.23...0.53 m/s, approximately 50 °C, in the same speed range of 0.23...0.53 m/s, but the load of $F=200$ N and 300 N, 60 °C for the speed of 0.69 m/s at $F=200$ N and $F=300$ N and for speed $v=0.84$ m/s at $F=200$ N.

For point contact, for the rapeseed oil in the four-ball tribotester, the lubrication regime is **piezo-viscoelastic (PVE)**. Positioning of determined points for each set $(F, v, \eta_{lubrifiant}^{(t)})$ is very close to the boundary between the PVE regime and the IVE regime.

The balls used in the test campaign are polished ($R_a = 0,03$ μm), made of chrome alloy steel (a brand intended mainly for bearing balls), having a diameter of 12.7 mm. The maximum pressure in contact, calculated with Hertz relation is 2185 MPa for the load $F=100$ N, 2753 MPa for $F=200$ N and 3151 MPa for $F=300$ N.

Table 3.1. Dynamic viscosity for rapeseed oil at different temperatures [243], [98], [81]

Temperature [°C]	Dynamic viscosity [cP]
37.8	0.0449
48.7	0.0303
60	0.0214

Table 3.1 presents the values of the dynamic viscosity of rapeseed oil, selected from the literature, for certain temperatures. The dependence of dynamic viscosity on temperature is similar for vegetal oils and, although at room temperature some oils have higher values (as in the case of Lesquerilla oil, with a viscosity ~ 3 times higher at ambient temperature), at 100...110 °C, their viscosities are only slightly higher than that of rapeseed oil and sesame oil. The problem is that the source of Lasquerilla and sesame oil is not in large quantities, as is the case with rapeseed oil.

Figure 3.3 shows a detail of the map in Fig. 3.2, with the same legend, to better observe the positioning of the test regimes on the four-ball tribotester.

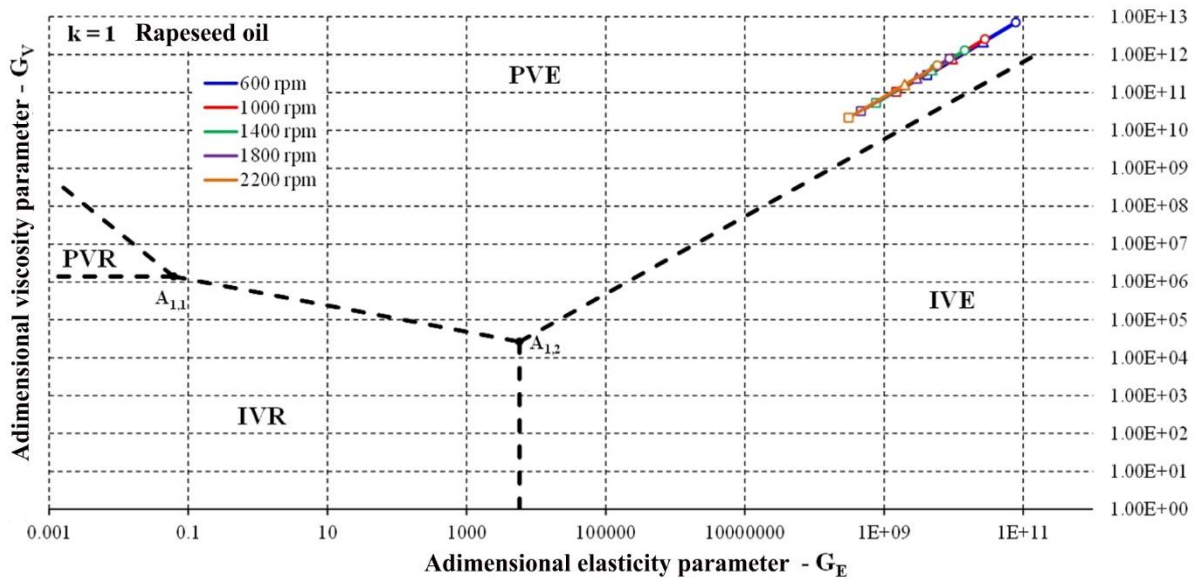


Fig. 3.2. Map of lubrication regimes for rapeseed oil, with ellipticity parameter $k = 1$, isothermal regime (37.8 °C). **Legend:** glide velocities: blue 600 rpm ($v=0.23$ m/s), red 1000 rpm ($v=0.38$ m/s), green 1400 rpm ($v=0.53$ m/s), magenta 1800 rpm ($v=0.69$ m/s) and brown 2200 rpm ($v=0.84$ m/s), the symbols for the load on the axis of 4-ball machine: o for $F=100$ N, Δ for $F=200$ N and \square for $F=300$ N

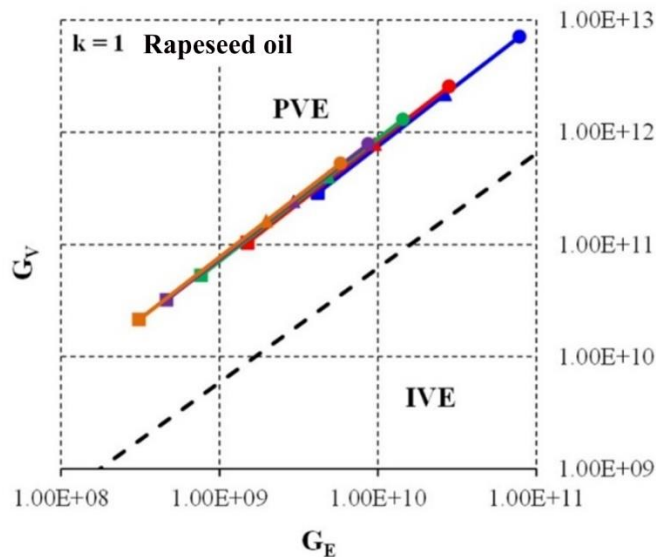


Fig. 3.3. Detail of the map of lubrication regimes for rapeseed oil, from Fig. 3.2

3.3. Calculation of the Minimum Thickness of the Fluid Film

If rapeseed oil is used in a stable regime at 60 °C, it can be seen that the load has only a small influence on the theoretical minimum film thickness, which means that the load variations in this range allow for having almost the same regime for the tribosystem. Thus, if one compares the value of h_{\min} for $F=300$ N with the one for $F=100$ N (with the same speed of 0.83 m/s, at 60 °C), increasing force produces only a 12% decrease in h_{\min} .

Fig 3.4 shows plots of minimum film thickness for rapeseed oil, h_{\min} , as a function of sliding speed and load on the four-ball machine shaft.

After the test campaign on the four-ball machine, the average friction coefficient for two tests has values lower than 0.1, meaning that a full film could be generated as predicted by the lubrication regime map for 60°C.

Calculated with relations (3.20) and (3.21), the minimum fluid film thickness for rapeseed oil for the same speed and force ranges as tested ones on the four-ball machine is given in Fig. 3.5 and Fig. 3.6. The minimum fluid film thickness is more influenced by the relative contact velocity and the fluid viscosity, i.e., the velocity parameter U.

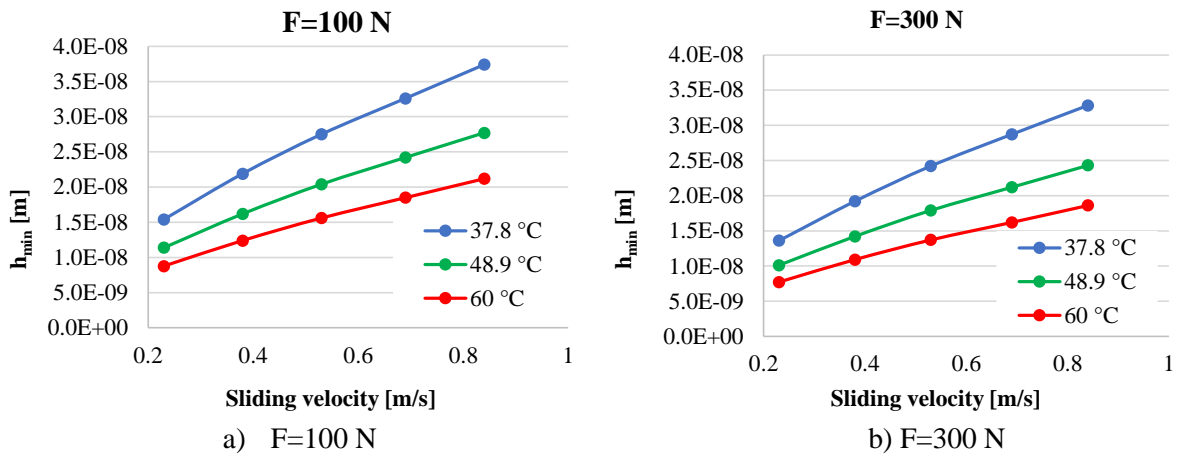


Fig. 3.4. Dependence of the minimum thickness of the fluid film, theoretically calculated as a function of the sliding speed and temperature stabilized for a) 100 N, b) 300 N (for a point contact)

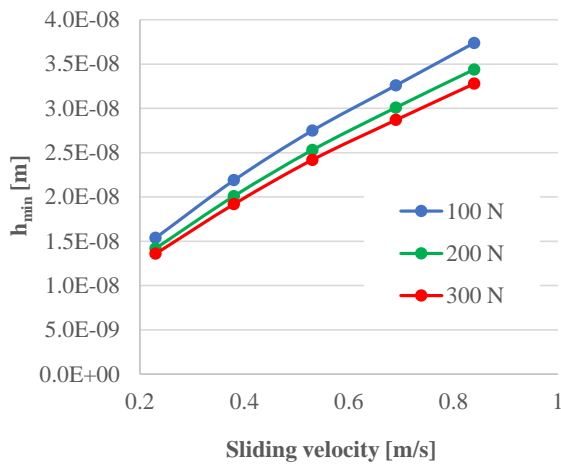


Fig. 3.5. The minimum thickness of rapeseed oil film, at the temperature of 38.9 °C (stabilized regime), depending on the sliding speed

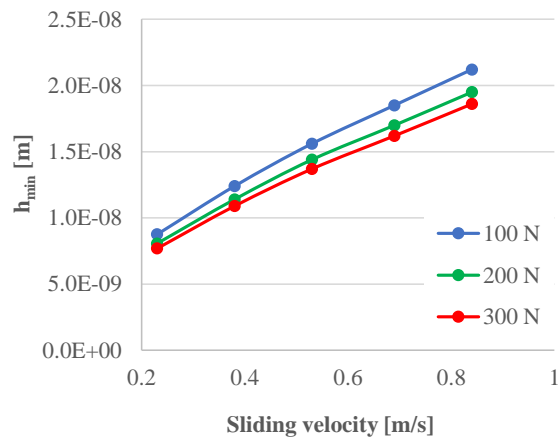


Fig. 3.6. The minimum thickness of rapeseed oil film, at a temperature of 60 °C (stabilized regime), depending on the sliding speed,

If one analyzes the two graphs in Fig. 3.5 and Fig. 3.6, it is found:

- the shape of the curves is similar,
- the minimum theoretical thickness of the fluid film is of the order of 10^{-8} m (micronic, even smaller),

- the influence of contact force is lower as compared to the influence of sliding speed on the minimum thickness of the rapeseed oil film,
- at the three temperatures analyzed for rapeseed oil in contact, the highest minimum thickness is obtained for the highest sliding speed ($v = 0.84$ m/s) and decreases slightly with force and for 60 °C,
- temperature has a strong influence on the minimum thickness of rapeseed oil, $h_{min(38.9^\circ\text{C})}$ is about one and a half times larger than $h_{min(48.9^\circ\text{C})}$,
- velocity has less influence at higher temperature or in other words, it has less influence for fluids with low dynamic viscosity.

The thickness of the fluid film is influenced to a lower extent by the force [85], [142].

With the same results for lubricant film thickness, graphs can be drawn to highlight the dependence of film thickness on temperature and another parameter, for example load or sliding speed. The same conclusion can be formulated: over the studied temperature range, the theoretical operating regime of the tribosystem does not change. For $F=300$ N, it is observed that the largest film thickness is obtained for the highest sliding speed, a trend that is consistent with the model and calculations performed by Dowson and Higginson [85]

3.4. Conclusions on the Theoretical Regimes of Rapeseed oil lubrication

The lubrication regimes, characterized by the set (F, v) , were positioned on the maps, with the same force and speed values as in the test campaign and for three temperatures (37.8 °C, 48.9 °C and 60 °C). Rapeseed oil generates a piezo-viscoelastic (PVE) lubrication regime in the four-ball tribosystem.

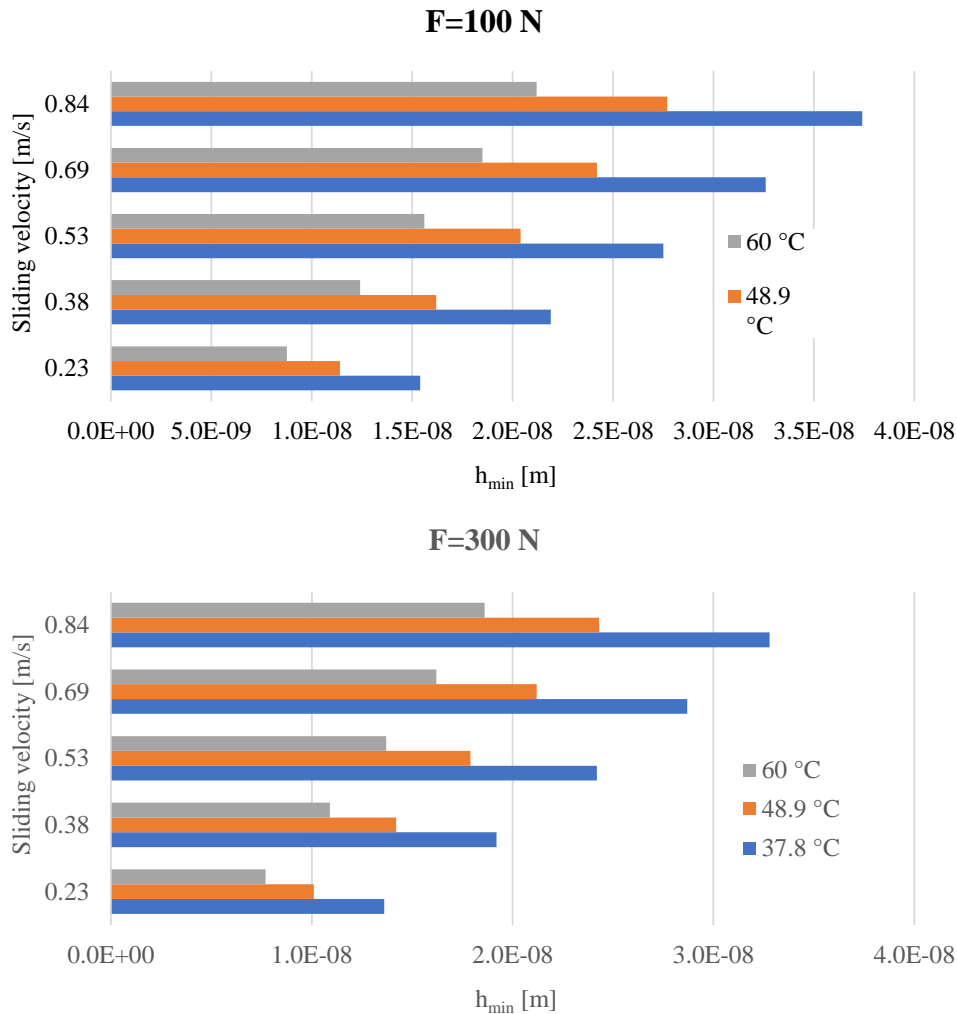


Fig. 3.7. Comparison of theoretical minimum lubricant film thickness values for ranges of sliding speed, temperature and load

Using the dynamic viscosity of rapeseed oil at certain temperatures (determined at the end of the test) and the piezo-viscosity coefficient, as reported in the literature, the theoretical minimum film thickness was calculated. For rapeseed oil, the calculated thicknesses of the fluid film are very close and comparable to the roughness value Ra of the initial surfaces in contact. The minimum theoretical thickness of the rapeseed oil film was calculated for the parameters of the working regime (similar to the one in the actual tests (F=100...300 N, v=0.23...0.84 m/s and the temperature of the rapeseed oil in the ball cup 38.9 °C to 60 °C).

From running the theoretical model, described above, for ranges of force, sliding speed and temperature, it is found (Fig. 3.7):

- rapeseed oil can form a film under certain operating conditions; it is recommended that the metal surfaces in contact be as smooth as possible, in order not to have asperities that interrupt the lubricant film;

- the influence of temperature: the increase in the temperature of the lubricant in contact causes the reduction of the viscosity of the fluid, this process participating in the reduction of the minimum theoretical thickness of the fluid film,

- the influence of the sliding velocity, at the same temperature and the same force in contact, is manifested by the increase of the minimum thickness with the increase of the speed,

- the influence of the load: when the contact force increases at the same temperature and speed, the minimum thickness decreases, but the influence of the load is smaller than the influence of the sliding speed.

If one considers the roughness reported by [103] for SKF balls for the 4-ball tester, Ra=0,018...0,035 μm, and the relation for evaluating the lubricated regime, through the parameter λ

$$\lambda = \frac{h_{\min}}{\sqrt{R_{q1}^2 + R_{q2}^2}} = \frac{h_{\min}}{1.15 \cdot \sqrt{R_{a1}^2 + R_{a2}^2}}, \quad (3.26)$$

where h_{\min} – the minimum thickness of the lubricant film, [m]; R_{q1} , R_{q2} – the average square deviations of the roughness heights of the two surfaces in contact, [μm], [142], the values from Table 3.2 are obtained. The denominator has values between 0.02927 and 0.05692 μm.

Tab 3.2. Theoretical values of the parameter λ

Caz	Viteză [m/s]	Forță [N]	Temperatura [°C]	h_{\min} [μm]	λ	
					min	max
Caz 1	0.23	100	37.8	1.54×10^{-2}	0.270	0.5185
Caz 2	0.84	300	37.8	3.28×10^{-2}	0.5762	1.1206
Caz 3	0.23	100	60	0.876×10^{-2}	0.1539	0.299
Caz 4	0.84	300	60	1.86×10^{-2}	0.326	0.6354

From these theoretical calculations it would result that the working regime of the tribosystem would be mixed or boundary, but, as can be seen from the values of the friction coefficient, experimentally obtained, for some sets (v, F) of tests, this parameter drops to 0.05...0.08, values specific to the fluid film regime (EHD). This fact is argued by the fact that elastic deformations and wear change the contact configuration (especially, the equivalent radius of curvature increases and also, the roughness of wear scars becomes coarse), which favors the generation of the film.

Chapter 4

Test Campaign on the Four-Ball Machine and Formulated Lubricants

4.1. Evaluating the Tribological Characteristics of Lubricants on Four-Ball Machine

Tests and measurements for tribological characteristics, carried out in the laboratory, are recommended for newly formulated lubricants, but also for quality control of products already on the market [50], [65], [142], being widely applied in industrial and research activities.

For lubricants (synthetic, mineral or vegetal oils) with the properties improved by including additives, testing is necessary for the following reasons:

- Introduction of new oils on the market, in different groups and levels of quality and recommendations for their use [121], [122],
- verification of the base oil and their characteristics given by additives,
- verification on delivery,
- the existence of sources of contamination with water or other impurities, which alter the tribological behavior,
- comparison of several lubricants under the same test conditions.

The price of research studies for a lubricant increases significantly for tests made in nearly actual conditions, as compared to the initial ones, carried out in the laboratory. In order to reduce research costs, specialists [31], [50], [142] recommend starting research in the laboratory, on simple tribotesters, and with rigorously controlled conditions. These testers do not fully simulate the set of conditions in which the actual system is exploited. But the tribotesters are useful because they allow a rigorous control of the parameters and a correct and continuous monitoring of them.

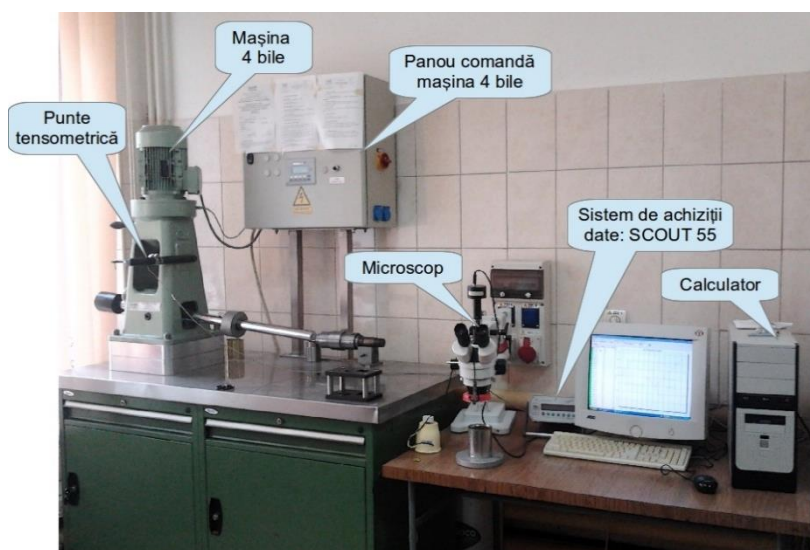


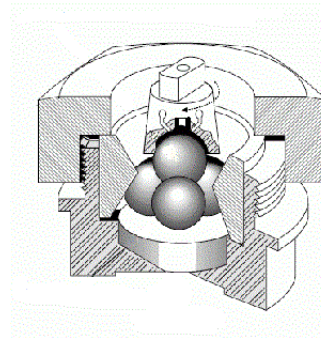
Fig. 4.1. Four-ball machine and data acquisition system (overview)
(Laboratory "Lubritest" of the "Dunărea de Jos" University of Galati)

Figure 4.1 shows the four-ball machine from the "Mechanics and Tribology of the Superficial Strata" research center of "Dunărea de Jos" University of Galati, with a maximum load of 6000 N (made by Hansa Press und Maschinenbau GmbH, Germany). The machine is composed of: electric motor that can vary the rotational speed of the main shaft from 10 rpm to 5800 rpm, the machine body, the loading system, the panel for adjustment and monitoring, bench-support. The system for measuring and monitoring the resisting (friction) moment was made at the "Dunărea de Jos" University of Galati and calibrated by the author.

Figure 4.2 shows the ball cup and the load lever assembly. Measurable parameters are the time of sliding, the diameter of the wear scar (WSD) and the temperature in the lubricant bath; with the values of the recorded friction moment, the coefficient of friction can be calculated, taking into account the friction force arm. The four-ball machine may be served by a microscope, for measuring wear scars, usually with an accuracy of ± 0.01 mm, and by an automatic stopwatch, which can record the time with an accuracy of 0.2 s.



a) Ball cup with fastening components and tightening lever



b) The system for fixing the four balls during the test

Fig. 4.2. Assembly of the 3 balls

The diameter of the 4 balls involved in one test is 12.7 mm. The balls are made by SKF, of bearing steel (chromium alloy steel AISI 52100 — EN 10027 100CR6 (1.3505), mark 20), specially treated, having: a small diameter tolerance (± 0.0005 mm), a deviation from the shape of $0.5 \mu\text{m}$, a diameter variation of $0.5 \mu\text{m}$ per ball and $1 \mu\text{m}$ on a set of four balls, high hardness (60... 66 HRC) and a special surface quality ($R_a = 0.02...0.032 \mu\text{m}$).

4.2. Test Procedure

SR EN ISO 20623:2018 [185] specifies three different test conditions as follows: A – test for the wear load index (LWI), B – test for the wear-and-load curve and C – test for wear and seizure.

In explaining the test procedure, the notations and names are consistent with [185].

The general procedure consists of the following operations:

a. After checking that the machine and the ball cup is clean, place the ball cup on the assembly device. Put three clean balls in the bucket, hold them in place with the fixing ring and secure the assembly by tightening the nut with a moment of $68 \text{ Nm} \pm 7 \text{ Nm}$. Enter enough sample liquid (8 ml to 10 ml) to cover the fixed balls at least by 3 mm. Place the tightening ring, screw down the tightening nut and check if the lubricant level exceeds the fixed balls. Four new balls and a fresh amount of the test fluid shall be used for each test. A clean ball shall be fixed in the upper ball clamping device and checked that it cannot be rotated by hand in the fastener. The ball cup assembly is centrally mounted, under the main shaft, the fixed balls being in contact with the fourth. Place the mounting disc between the axial bearing and the cup so that, when the cup is left in place, it sits firmly on the disc and is free to rotate with it. For machines with a loading lever arm, the masses consist of a set of rings of different values that are located on the notches processed in the lever of the machine. Notches are identified with the force applied if the mass is located in a given position. Adjust the friction recorder according to the instructions.

b. Apply the load using the loading device fixed to the machine (charging lever plus weights), being careful to avoid loading with shock as it can deform the balls permanently. Check that the lower three balls center on the upper ball. It is permissible for rotation to start before applying the load, but the starting condition must be specified in the test report. The timer and the recording device must be switched on when the whole load is applied. It has the effect of reducing damage to the contact areas during the first rotations of the upper ball and avoiding vibrations.

c. Start the engine to operate at desired rotational speed, the timer and the friction recorder if required. For machines equipped with integrated timers, as is the case with the four-ball machine in the Research Center "Mechanics and Tribology of the Superficial Layer", select the required duration of the test. Actuate the motor switch and timer simultaneously; the friction recorder must also be switched to open at the same time if possible. Let the machine run for the set time interval, by stopping it using an integrated timer.

d. Disconnect the recorder and remove the load from the balls by removing the applied load (lifting the lever arm and locking it in place). Disconnect the friction recording device. Remove the cup

from the machine. Drain the amount of tested lubricant from the cup and rinse the assembly with a cleaning solvent. Remove the balls, wash them with cleaning solvent, dry and put them in a properly marked container to hold safely and subsequently to measure the diameters of the wear scars. Register the values from the friction recorder.

e. Clean the locking nut, the locking ring etc., to be ready for the new test. Remove the clamp fixing the upper ball from the machine and remove the ball from its recess with the help of a device made of hardened steel and a hammer. Clean the fixing clamp carefully.

f. Repeat the above procedure using four new balls and a portion of new fluid to test for each test, for all the different values for load and velocity, as required to complete a specific test campaign. Figure 4.6 shows moments from the test procedure (here for rapeseed oil additivated with h-BN).



a) Ball cup preparation b) Adjustment of the working regime (time and velocity) c) Extraction of lubricant and balls from the cup, after testing

Fig. 4.3. Moments in the test procedure

4.3. Tribological Parameters Measurable by Tests on the Four-Ball Machine

This research had as objective the study of several tribological parameters (coefficient of friction, as evolution in time and average value, and two parameters dependent on the average diameter of the wear scars on fixed balls).

The frictional force was measured with a system consisting of a tensometric bridge (connected between the arm of the four-ball machine and the ball cup arm), whose signal was taken over by a data acquisition system (scout type) and then transmitted to a computer. The frictional force is displayed in real time on the computer screen. The data acquisition and their processing were done with the CATMAN® EXPRESS 4.5 software. Details are also given in [25], [139]. Starting from the values of the frictional force, the friction moment and the coefficient of friction were determined.

In the particular case of the test on the four-ball machine, wear and seizure can also be assessed by the wear rate of the wear scar diameter because it is easy to calculate and compare to tests performed on the same tribosystem (only by changing the lubricant and/or the working regime).

The wear rate of wear scar diameter is calculated, in this work, with the formula

$$w(\text{WSD}) = \frac{\text{WSD}}{F \cdot L} \quad [\text{mm}/(\text{N} \cdot \text{m})] \quad (4.1)$$

in which WSD is the average diameter of the wear scar for a performed test, F is the load applied to the axis of the machine and L is the sliding distance, determined as the product of the calculated sliding velocity and the duration of the test).

Figure 4.5 shows the COF graph for all values recorded by the data acquisition system during the test (here 7200 values, i.e. a sampling of 2 values per second). This sampling was kept for all tests carried out, regardless of the duration or distance of the test. This representation is difficult to evaluate in practice and specialists use moving average over various data ranges. In this work, the moving average was calculated with 100 successive values (the black curve in Fig. 4.5).

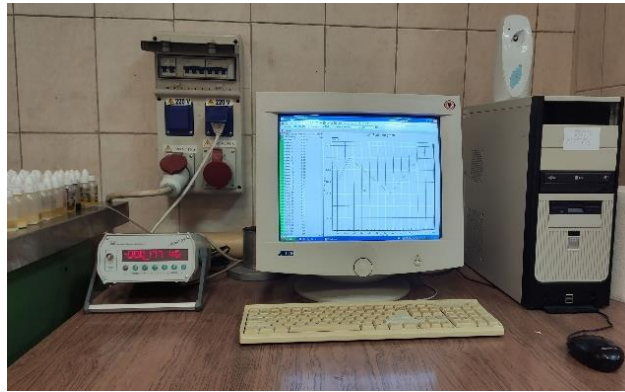
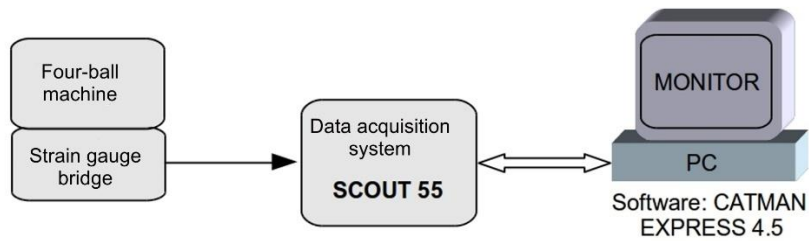


Fig. 4.4. Schematic block of the data acquisition system as it was performed by Şolea [25], [139]

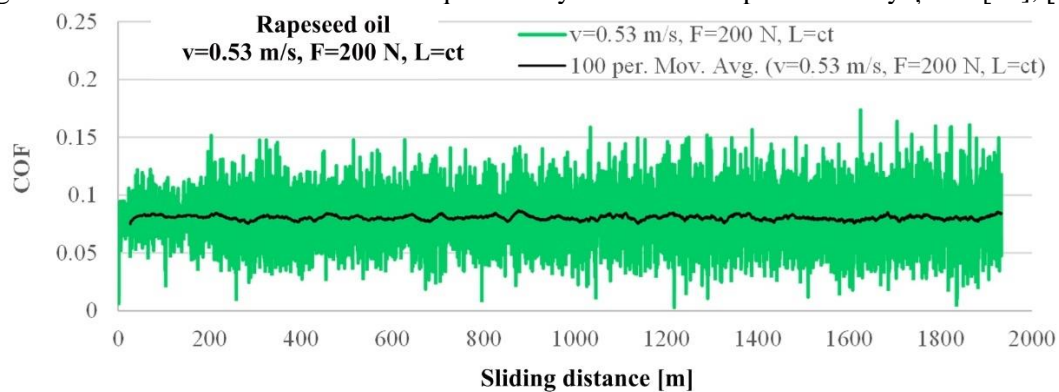


Fig. 4.5. COF graph for all values recorded by the data acquisition system (example is for a test with non-aditivated rapeseed oil, tested at the sliding velocity of 0.53 m/s and with a force $F=200$ N on the axis of the four-ball machine)

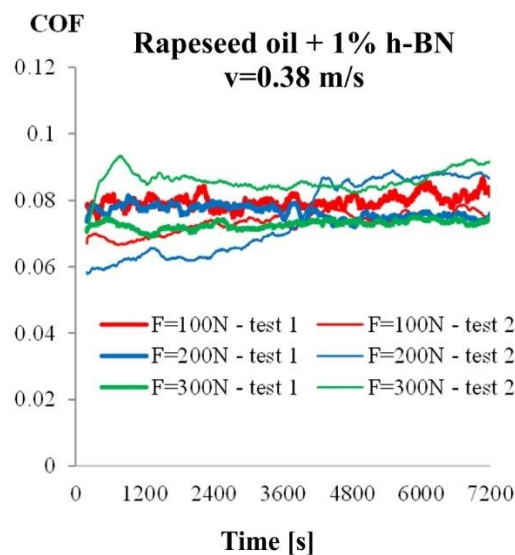


Fig. 4.6. A graph of coefficient of friction (COF) for two tests performed under the same conditions

The repeatability is exemplified in Fig. 4.6: COF curves are relatively close and similar in shape. From the experience of the author and the team who worked on the four-ball machine [29], [43], [68], [139], it was found that for sliding motion systems, 2...3 tests are enough to obtain reliable results.

4.4. Formulation of Lubricants Based on Rapeseed Oil and Nano Additives

The lubricants tested for this research are based on raw rapeseed oil, from Expur SA Bucharest, unaditivated or added with nano particles of h-BN, in various concentrations (0.25 wt%, 0.5 wt% and 1 wt%), graphene (1 wt%), and a package of additives (1 wt% graphene + 1% h-BN).

The fatty acid composition of the tested rapeseed oil is given in Table 4.1 and was performed at Expur SA Bucharest, with the help of a chromatograph. Fatty acids vary in the length of the chain and in the degree of unsaturation, hence resulting in differences in rheological and tribological behavior.

Table 4. 1. The composition of theui of rapeseed oil tested (analysis by Expur SA Bucharest)

Acid	Symbol	Concentration, %wt
Myrrhic acid	C14:0	0.06
Palmitic acid	C16:0	4.60
Palmitoleic acid	C16:1	0.21
Heptadecanoic acid	C17:0	0.07
Stearic acid	C18:0	0.18
Oleic acid	C18:1	1.49
Linoleic acid	C18:2	60.85
Linolenic acid	C18:3	19.90
Arachidic acid	C20:0	7.64
Gondoic acid	C20:1	0.49
Others		1.14

The nano additives used in this PhD thesis were provided by the company PlasmaChem [172]:

- **hexagonal Boron nitride (h-BN)** (Fig. 4.7a); powder with a particle size of 100-1000 nm, mean value 500 ± 100 nm, specific area of 23 ± 3 m²/g, purity > 98.5%, nitrogen content > 55%, contents of elements, in %: O< 1; C< 0,1, B₂O₃<0,1,
- **nano graphene** (Fig. 4.7b): nano foils with a thickness of 1.4 nm and particle size up to 2 μm, specific area 700-800 m²/g, purity 91 at.%, of the telemente: O<7 at%; N<2 at%.

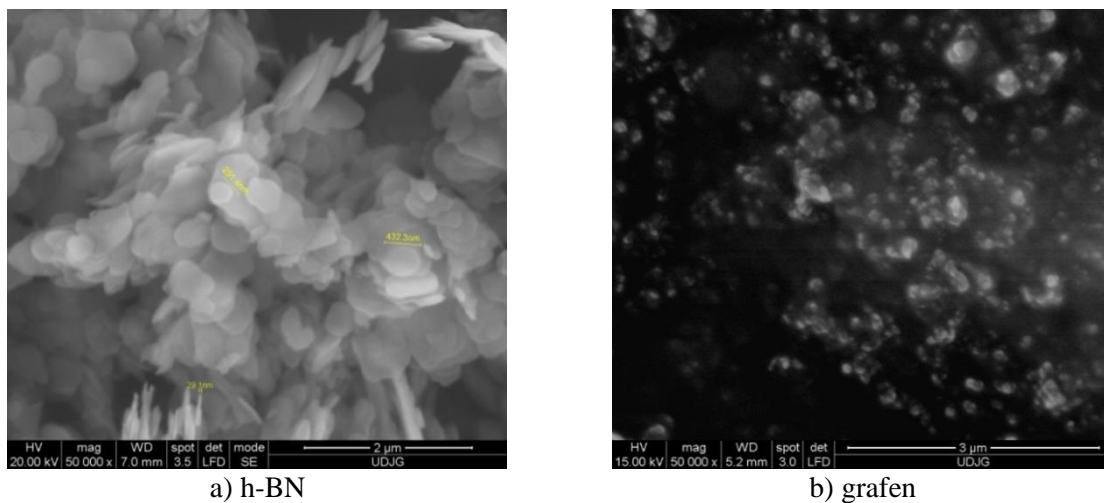


Fig. 4.7. Appearance of h-BN nanoparticles, provided by PlasmaChem [172]

Such additives to reduce friction and wear are prone to form agglomerations and it is difficult to achieve a dispersion of them in the base oil, which will last over time.

The SEM images show the nano additives used for the formulation of rapeseed oil-based lubricants and were obtained under the scanning electron microscope, FEI Quanta 200, which has a resolution of 4 nm, the magnification power of 10^6 times, of the "Dunărea de Jos" University of Galați.

The fatty acid composition of rapeseed oil used in this study is given in Table 4.4. The high concentration of linoleic acid and linolenic acid, both unsaturated fatty acids which can argue for good tribological behaviour under conditions of limit or mixed regimen, is observed.

Autor has designed a laboratory scale technology to achieve a good dispersion of nano particles of additives. Nano-additive lubricants were obtained in a small amount of 200 ml each. The steps followed in this technology at laboratory scale were similar to those presented by Cristea G. C. [25] and by Ionescu T. F. [68]:

The steps taken in the formulation of the tested lubricants were as follows:

- mechanical mixing of the nano additive and an equal quantity of guaiacol (dispersant supplied by Fluka Chemica) with the formula $C_6H_4(OH)OCH_3$ (2-methoxyphenol), over a period of 20 minutes; this dispersing agent is compatible with both the additive and vegetable oils; the mass ratio between the additive and the dispersing agent being 1:1, to the nearest 0,1 mg,
- continuous addition of rapeseed oil, measured to obtain 200 g of additive lubricant, with the desired concentration of nano additive,
- mixing with a magnetic homogenizing device for 1 hour,
- for the additive package 1% graphite+1% h-BN the same was done, so the lubricant contains 1% graphite+ 1% h-BN +2% guaicol+96% rapeseed oil (by mass),
- sonication + cooling of 200 g lubricant for 5 minutes using the sonicator Bandelin HD 3200 (Electronic GmbH & KG Berlin); during sonication the lubricants are heated to approximately 70 °C; the cooling time was 1 hour; this sonication + cooling step is repeated 5 times to obtain a total sonication time of one hour. The parameters of the sonication regime, chosen by the author together with dr.ing. Dumitru Dima, from the Faculty of Sciences and Environment of the "Dunărea de Jos" University, are: power 100 W, frequency 20 kHz \pm 500 Hz, continuous regime.

4.5. Campaign of Tests on Four-Ball Machine

The author developed this campaign with the aim of highlighting the influence of the concentration of the additive and the working regimen.

The test parameters for each formulated lubricant were:

in normal regime (Table 4.2 and Table 4.4)

- loading force – 100 N, 200 N and 300 N (\pm 5%);
- sliding velocity 0.23 m/s, 0.38 m/s, 0.53 m/s, 0.69 m/s and 0.84 m/s, corresponding to the spindle rotational speed of the four-ball machine of 600 rpm, 1000 rpm, 1400 rpm, 1800 rpm and 2200 rpm (\pm 10 rpm),
- the same sliding distance $L = 1933.8$ m, corresponding to the test time - 60 minutes (\pm 1%) at a velocity of 0.537 m/s,
- for three sliding velocities (0.38 m/s, 0.53 m/s and 0.69 m/s) tests with a constant duration of 1 h were also carried out (it has resulted that tests carried out at $v = 0.53$ m/s and the duration of 1 h can be classified in both groups, i.e. the results are also for $L = ct$ and $t = ct$ and will be considered as a reference when comparing the two sets of tests),
- in the formulated lubricants, for h-BN the concentrations in rapeseed oil were 0.25%, 0.50% and 1% (wt), for graphene 1% (wt), and for the additive package, 1% (wt) h-BN+1% (wt) graphene.

in severe regime (Table 4.6): the parameters of a set of tests were: the load on the four-ball machine from 500 N to 900 N, in steps of 50 N (\pm 5%); sliding velocity 0.53 m/s, corresponding to a rotational speed of the machine main shaft of 1400 rpm (\pm 6 rpm); duration of a test - 1 minute (\pm 1%).

For rapeseed and lubricants additive with h-BN, a set of tests lasting 1 h, but with different sliding lengths, was performed.

Figure 4.8 shows the balls as obtained after the test. The ball to the right of the image is the fixed ball.

The tested lubricants have been poured into the fixed ball cup, so that the level of the lubricant is at least 3 mm higher than the highest point of the balls (approximately 10 ml). After each test, the ball fixture, tribotester and balls were cleaned with isopropyl alcohol and dried in a stream of air.

Table 4.2. Test parameters on four-ball machine, for the tests carried out

v [m/s]	0.23	0.38	0.53	0.69	0.84
ω [rpm]	600	1000	1400	1800	2200
L[m]	1933-constant				
Time [h/min/s]	2 h 20 min	1 h 24 min	1 h	46 min 40 s	38 min 12 s

Table 4.3. Test parameters on four-ball machine, for tests during 1h

v[m/s]	x	0.38	0.53	0.69	x
L[m]	x	1368	1933	2484	
Time[h]	1 h				



Fig. 4.8. Balls tested at different regimes

Measured and calculated parameters

The friction moment, T , between the upper ball, attached to the axis of the machine, and the lower fixed balls can be calculated by either of the two equations:

$$T = \mu \cdot 3Q \cdot r' = \frac{\mu \cdot F \cdot r}{\sqrt{3}} \quad (4.2)$$

$$T = F_R \cdot M \quad (4.3)$$

μ - the coefficient of sliding friction; F - the force applied to the axis of the machine, N; r' - the distance from the centre of the contact surfaces of the lower balls to the axis of rotation of the machine ($r' \cong r \cdot \sin 30^\circ = 3.175$ mm, r is the radius of the balls); Q - the normal force in the contact of the ball on the ball $Q \cong \frac{1}{3} \cdot \frac{F}{\cos 30^\circ} = \frac{2}{3} \cdot \frac{F}{\sqrt{3}}$, N; F_R the force read on the force measurement system, M - the arm of the force F_R , mm.

From the equations (4.2) and (4.3) it results:

$$\mu = \frac{2 \cdot F_R \cdot M}{3 \cdot Q \cdot r} \quad (4.4)$$

Diameters of the wear scars were measured using an optical microscope.

According to the procedure recommended in SR EN ISO 20623:2018 [185], for each test, three wear scars were obtained on the fixed balls. As a result of wear, two diameters were measured on each scar, one measured in the direction of sliding, the other perpendicular to the first. Resulting three wear scars, six measurements of the diameters were obtained and their average value was calculated. This value represents the diameter of the wear scar (WSD), which has been reported for each test [25], [31], [68].

Table 4. 4. Normal test campaign for L=constant

Lubricant	Additive concentration [%]	Force [N]	Sliding velocity [m/s]				
			0.230	0.383	0.537	0.691	0.84
Rapeseed oil	-	100	xx	xx	xx	xx	xx
	-	200	xx	xx	xx	xx	xx
	-	300	xx	xx	xx	xx	xx
Rapeseed oil + h-BN	1	100	xx	xx	xx	xx	xx
		200	xx	xx	xx	xx	xx
		300	xx	xx	xx	xx	xx
Rapeseed oil + 1% graphene	1	100	xx	xx	xx	xx	xx
		200	xx	xx	xx	xx	xx
		300	xx	xx	xx	xx	xx
Rapeseed oil + 1% graphene + 1%h-BN	1	100	xx	xx	xx	xx	xx
		200	xx	xx	xx	xx	xx
	1	300	xx	xx	xx	xx	xx

Table 4. 5. Normal test campaign for t=constant (1h)

Lubricant	Additive concentration [%]	Force [N]	Sliding velocity [m/s]		
			0.38	0.53	0.69
Rapeseed oil	-	100	xx	xx	xx
	-	200	xx	xx	xx
	-	300	xx	xx	xx
Rapeseed oil + h-BN	0.25	100	xx	xx	xx
		200	xx	xx	xx
		300	xx	xx	xx
	0.5	100	xx	xx	xx
		200	xx	xx	xx
		300	xx	xx	xx
	1	100	xx	xx	xx
		200	xx	xx	xx
		300	xx	xx	xx

Table 4. 6. Severe test plan

Tested lubricant	v [m/s]	Forța [N]								
		500	650	600	650	700	750	800	850	900
rapeseed oil	0.53	xx	xx	xx	xx	xx	xx	xx	xx	xx
rapeseed oil+1% h-BN	0.53	xx	xx	xx	xx	xx	xx	xx	xx	xx

The author evaluated the tribological behavior in severe regime as in Table 4.6 for two lubricants, rapeseed oil and rapeseed oil with 1% h-BN, analyzing the following parameters: coefficient of friction, wear scar diameter, temperature of the oil in the ball cup, at the end of the test, pfilm strength parameter (OFS).

Chapter 5

Tribological Evaluation of Lubricants Formulated with Rapeseed Oil and Nano Additives

5.1. Tribological Behavior of Rapeseed Oil on Four-Ball Tester in Normal Regime

Analysis of the coefficient of friction

The author of this work performed tests for both $t=ct$ (1 hour) and $L=ct$ (1933 m). This sliding distance corresponds to the test rotational speed at the middle of the studied range, $v=0.53$ m/s, a value common in specialized works and in SR EN ISO 20623:2018 [185] and ASTM D2596:2010 standards [187]. This grouping of tests, according to the load and duration, was also carried out because some tribological parameters, such as WSD, could not be compared directly in the case of tests with constant duration and different sliding speeds. However, a tribological assessment in this case was carried out using another parameter, the wear rate of WSD, $w(WSD)$, which takes into account the tested sliding distance.

Figure 5.1 shows the evolution of COF for rapeseed oil, tested on the four-ball machine, for 1 hour [164], [130], [129].

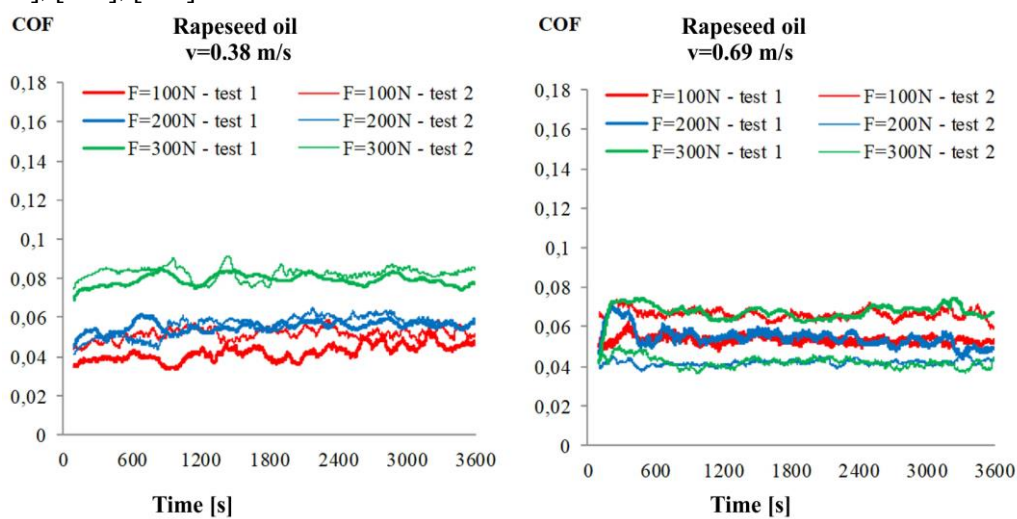


Fig. 5.1. Evolution over time of the coefficient of friction (COF), depending on load, and the sliding velocity, on the four-ball machine for two tests with the same parameters (F,v), for rapeseed oil

It is noticed that the difference between two tests with the same parameters is small and that the COF oscillations are small, and therefore, from the point of view of rubbing rapeseed oil is advisable for the range of studied parameters ($F=100\dots300$ N and $v=0.38\dots0.69$ m/s). The representation in Fig. 5.2 is achieved by a moving average with 100 values. The graphs show lower COF values at the force of 100 N, and higher values, for larger forces, 200 N and 300 N. At the highest speed, $v=0.69$ m/s, COF evolves for all forces in a very narrow range. So, for this working velocity, $v=0.69$ m/s, the load has a minor influence. In other words, the use of rapeseed oil at higher working speeds (if the technological process allows), is beneficial for the technical system because it reduces the energy needed to defeat friction.

Figure 5.3, shows the average of the values of the coefficient of friction (COF) during the test, for rapeseed oil, for the two tests carried out.

The increase in speed to $v=0.69$ m/s resulted in agglomeration of the COF values in a smaller range. If at a speed of 0.38 m/s, the COF is between 0.04 and 0.09, at the speed of 0.69 m/s, COF is registered between 0.05 and 0.08. The coefficient of friction of rapeseed oil is a little sensitive to load at high speeds. Small values obtained for COF (0.04...0.08), indicates the formation of a continuous film of fluid.

Tests with $L=constant$ were performed for five sliding velocities. The increase in this range being justified by the results represented above and by the fact that vegetal oils are used in higher speed ranges than the one initially tested. Tests were performed on the four-ball machine, where $L=constant$ (1933 m), for three forces, namely $F=100$ N, $F=200$ N and $F=300$ N, respectively, with five different speeds, namely: $v=0.23$ m/s, $v=0.38$ m/s, $v=0.53$ m/s, $v=0.69$ m/s and $v=0.84$ m/s.

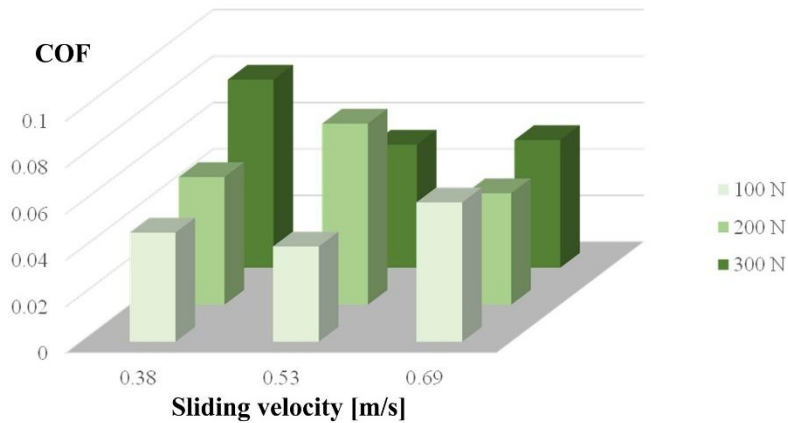


Fig. 5.2. Evolution of COF for non-additive rapeseed oil

At $t=ct$, the sliding distance is shorter for the lower velocity and higher for the higher velocity than that obtained for $v=0.53$ m/s.

For $L=ct$, it was found that the largest variations of COF were obtained for $F=100$ N. For the other forces, the COF evolution is made in a narrow range, both for the same repeated test and for tests with different parameters. In the case of using rapeseed oil as lubricant, it would be recommended that the load of the point contact to be greater than 2185 MPa (Hertz pressure in contact), corresponding to the force applied to the four-ball tribotester of 100 N. The average of the values from two tests is given in Fig. 5.4. One may notice that the values are above 0.1 for low velocities, which results that, at these velocities, the lubrication regime is mixed or boundary. For higher velocities, the values decrease to 0.08 and even lower, with the result that, for these regimes, a full film of lubricant is generated.

At the same velocity and force, for the charge $F=100$ N, the differences between the COF values for $t=ct$ and $L=ct$ are somewhat higher, but at higher load (e.g. $F=300$ N), $COF=0.081$ for $t=ct$ and $COF=0.096$ for $L=ct$.

The evolution of COF during $L=ct$ tests is given in Fig. 5.5. It is observed that the most uniform evolution of the COF is for $v=0.38$ m/s and $v=0.53$ m/s, regardless of the load. For the other speeds, the COF has more oscillating evolutions for the low load ($F=100$ N), the largest differences between the curves of the two tests being obtained for $v=0.23$ m/s.

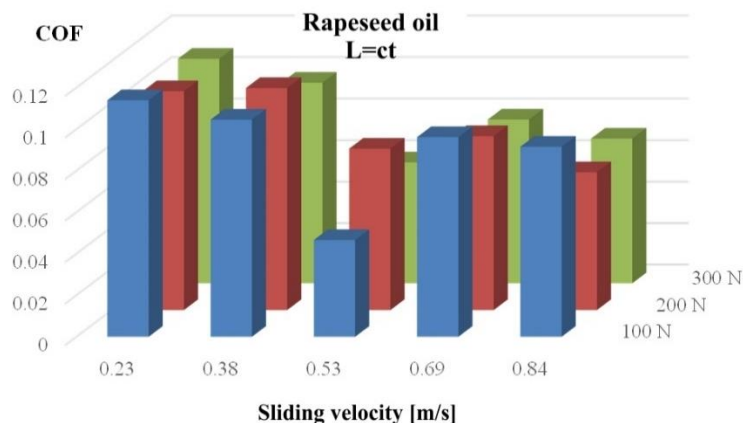


Fig. 5.3. Evolution COF for non-aditivated rapeseed oil, for $L=ct$

Wear evaluation

In this work the evaluation of wear is done by analyzing 2 parameters: average diameter of the wear trace (WSD) and the wear rate of the average diameter of the wear trace, denoted by $w(WSD)$.

The average wear scar diameter, determined according to SR ISO 20623:2018 [458], for tests of 1 hour, is plotted in Fig. 5.4. At the same velocity, the WSD increase is more pronounced for $v=0.69$ m/s, from $F=100$ N to $F=200$ N. Since the sliding distances are different for different velocities, it is not

recommended to make a comparison between the values obtained for different velocities. This comparison can be made for tests performed with $L=ct$.

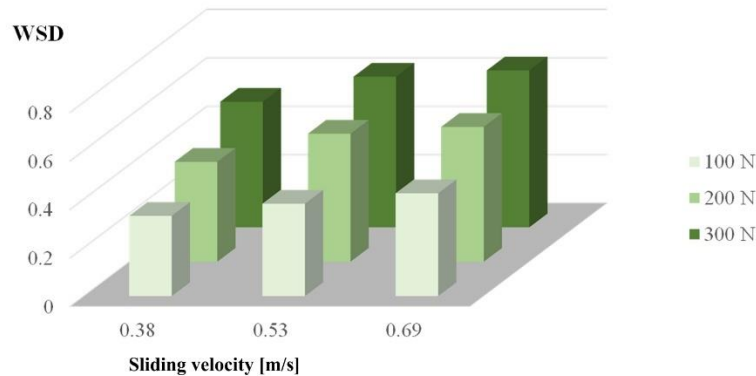


Fig. 5.4. WSD evolution for unaditivated rapeseed oil $t=ct$

In Fig. 5.5, photographs of wear scars are given for two tests carried out under the same conditions ($v=0.53$ m/s and $F=300$ N). It is noticed that the wear scars are very similar in size and from the point of view of the surface quality, which reflects the accuracy of the machine and its good adjustment, but also the high quality of the balls.

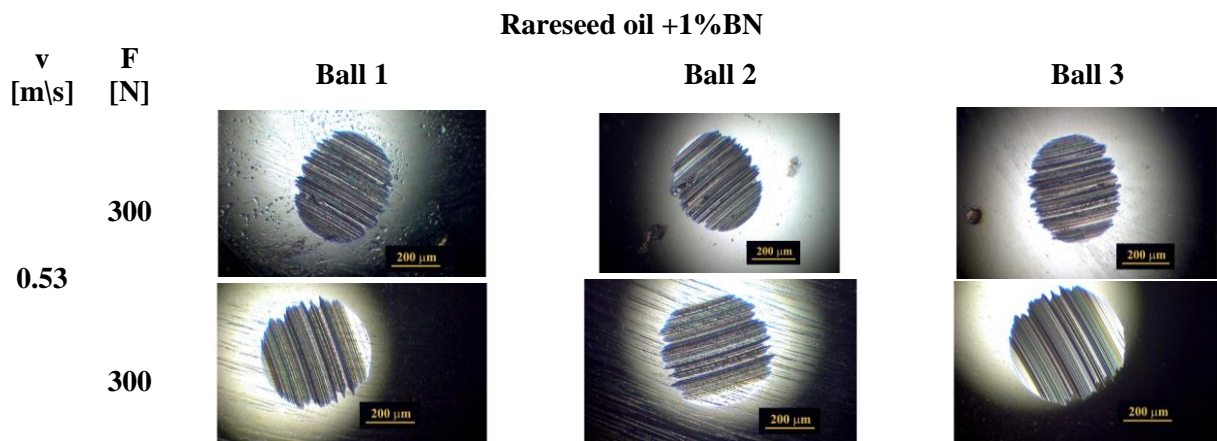


Fig. 5.5. Photographs obtained with optical microscope ($t=ct$ and $L=ct$, reference sliding length test, $L=1933$ m)

In Fig. 5.6, the averages of wear scar diameters (WSD) are represented for tests performed at $L=ct$. In this case, comparisons can be made between the WSDs resulting from the tests at different velocities. The conception of a test campaign of this kind belongs to the author and, as far as the open literature in the field has been studied, no wear studies have been presented on this principle ($L=ct$), for the four-ball machine.

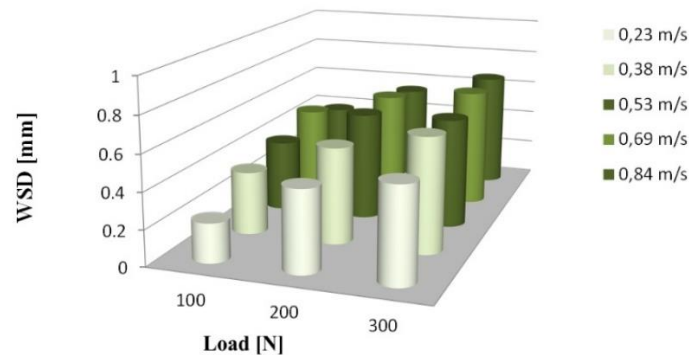


Fig. 5.6. Evolution of WSD, for rapeseed oil, for $L=ct$ tests

Analyzing the values in Fig. 5.6, it is found that the WSD is slightly increased at the speed for low velocities ($v=0.23$ m/s and $v=0.38$ m/s). For the other velocities, WSD varies very little with the velocity, from which it follows that the wear in contact is not dependent on speed, achievable if there is a continuous film of lubricant. The COF analysis resulted in this, as evidenced by the low COF values (0.04...0.08). In other words, the domain of WSD values obtained in this test campaign can be divided into 2 zones:

- an area where WSD varies both with speed and load; in conjunction with COF values, this load and speed dependence is specific to the mixed or boundary lubrication regime,
- an area where WSD is more load-dependent and without a clear influence on the sliding velocity; correlating with very low values of COF values, it follows that this area is characterized by a complete film lubrication regime.

In Table 5.1, WSD values obtained for $t=ct$ and $L=ct$ are given for two test velocities, i.e. $v=0.38$ m/s and $v=0.69$ m/s. For $v=0.38$ m/s, it is observed that for any of the three tested forces, WSD is larger for the longer sliding length. The $L=1933$ m test has a sliding length 29.22% longer than the 1-hour test. If the same percentages are calculated for WSD, you get 6% extra for $F=100$ N, 23% extra for $F=200$ N and 19.5% more for $F=300$ N, compared to the WSD values for $t=ct$. This increase in WSD proportional to the length of the slip indicates a process of abrasive wear, in the presence of lubricant that does not form a continuous film (very likely the lubrication regime is mixed or limit). For $v=0.69$ m/s the difference between the WSD values for the two types of tests is very small. This may result from statistical scattering of the results and from the accepted deviations of ball sizes, measured force values and revolutions. For example, for the 1-hour tests, WSD is 3.4% lower than the WSD obtained with $L=ct$, for $F=300$ N. It can be said that in this case the wear represented by WSD does not depend on the sliding distance, which is plausible if the lubricant generates a continuous film during the test.

Table 5.1. WSD values for tests of 1 h and tests with $L=ct$

		WSD [mm]							
		0.23		0.38		0.53	0.69		0.84
Velocity [m/s]									
Force [N]		L [m]							
		t=ct L=828	L=ct L=1933	t=ct L=1368	L=ct L=1933	t=ct	t=ct L=2484	L=ct L=1933	t=ct L=3024
100	-	0.218	0.331	0.352	0.381	0.424	0.479	-	0.387
200	-	0.446	0.412	0.537	0.528	0.556	0.608	-	0.548
300	-	0.529	0.518	0.644	0.621	0.647	0.669	-	0.662

Figure 5.7 must be carefully analyzed because keeping the test time at 1 h determines different sliding distances (see Table 5.1) and, therefore, only the values for the same velocity can be compared.

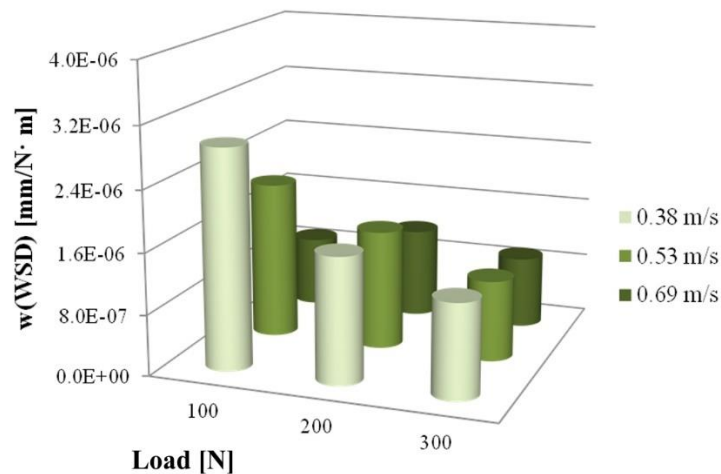


Fig. 5.7. Wear rate of WSD, for rapeseed oil, for tests with $t=ct$

Instead, for tests with $L=ct$, WSD can be compared at any velocity. In order to compare wear processes at different speeds and sliding lengths, the WSD wear rate graph was drawn for the results of the $t=ct$ tests. It is noted that the highest values were obtained for $v=0.38$ m/s, which means that the abrasive wear process (of removing material) is more accentuated at low speeds, since they do not favor the generation of complete lubricant film.

The wear rate of WSD decreases with increased load, which recommends using such a system at somewhat higher forces. In the range of $v=0.53...0.69$ m/s and $F=200...300$ N, WSD does not have a clear speed dependency and only decreases slightly with the load. Figure 5.6 shows the average values of WSD, for $L=ct$, for rapeseed oil as a lubricant. In this case, for $L=ct$ (1933 m), WSD can be compared between different velocities. It is observed that the smallest values were obtained for $F=100$ N, at $v=0.23$ m/s, but for high values of force and velocity ($F=200$ N and $F=300$ N) and ($v=0.69$ m/s and $v=0.84$ m/s), the values are very close.

The graph of the wear rate of WSD for tests with $L=ct$ is given in Fig. 5.8. For $F=100$ N, the increase in the wear rate of WSD has the highest slope, resulting in the abrasive wear process being more intense at low forces due to the vibrations of the machine. For $F=200$ N and $F=300$ N, the slope of this parameter is lower, depending on the velocity. The graph shows that rapeseed oil would be better to use at higher speeds and loads. Attention! These recommendations are valid only for this type of contact (point contact), in practice they can be found in ball bearings and ball screws.

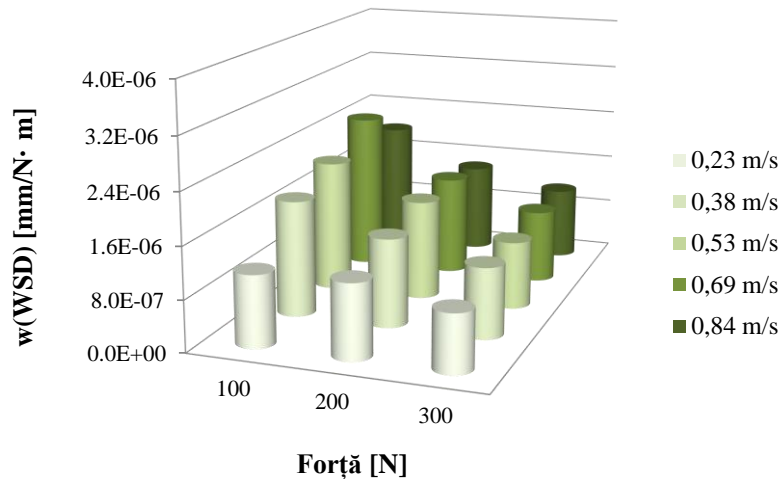


Fig. 5.8. Evolution $w(WSD)$ for unaditivated rapeseed oil for $L=ct$

Temperature in the lubricant bath (rapeseed oil)

Figure 5.9 shows the evolution of the lubricant temperature in the ball cup, for tests of 1 h, at sliding speeds of 0.38 m/s, 0.53 m/s, 0.69 m/s, forces of 100 N, 200 N, 300 N.

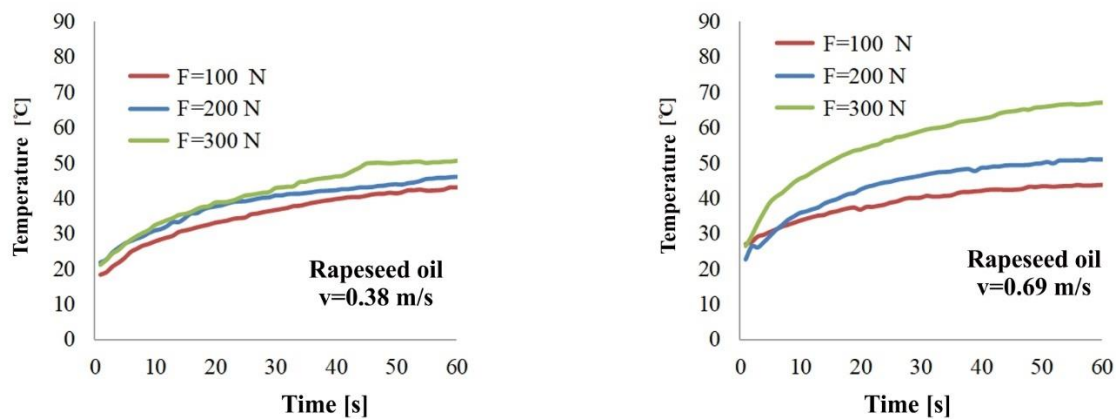


Fig. 5.9. Temperature evolution in the oil bath, for unaditivated rapeseed oil

It is important to point out that rapeseed oil does not reach temperatures that favor oxidation or other degradation processes of vegetable oil [9], [139]. The temperature curves of rapeseed oil in the ball cup are ordered upwards, according to the increase in force. At $v=0.38$ m/s, the temperature curves evolve in a band of 5-8 °C. This band increases to 10...15°C for $v=0.53$ m/s. For this velocity, the curves for $F=100...200$ N are side by side. The temperature evolution band increased to 20...23°C, for $v=0.69$ m/s.

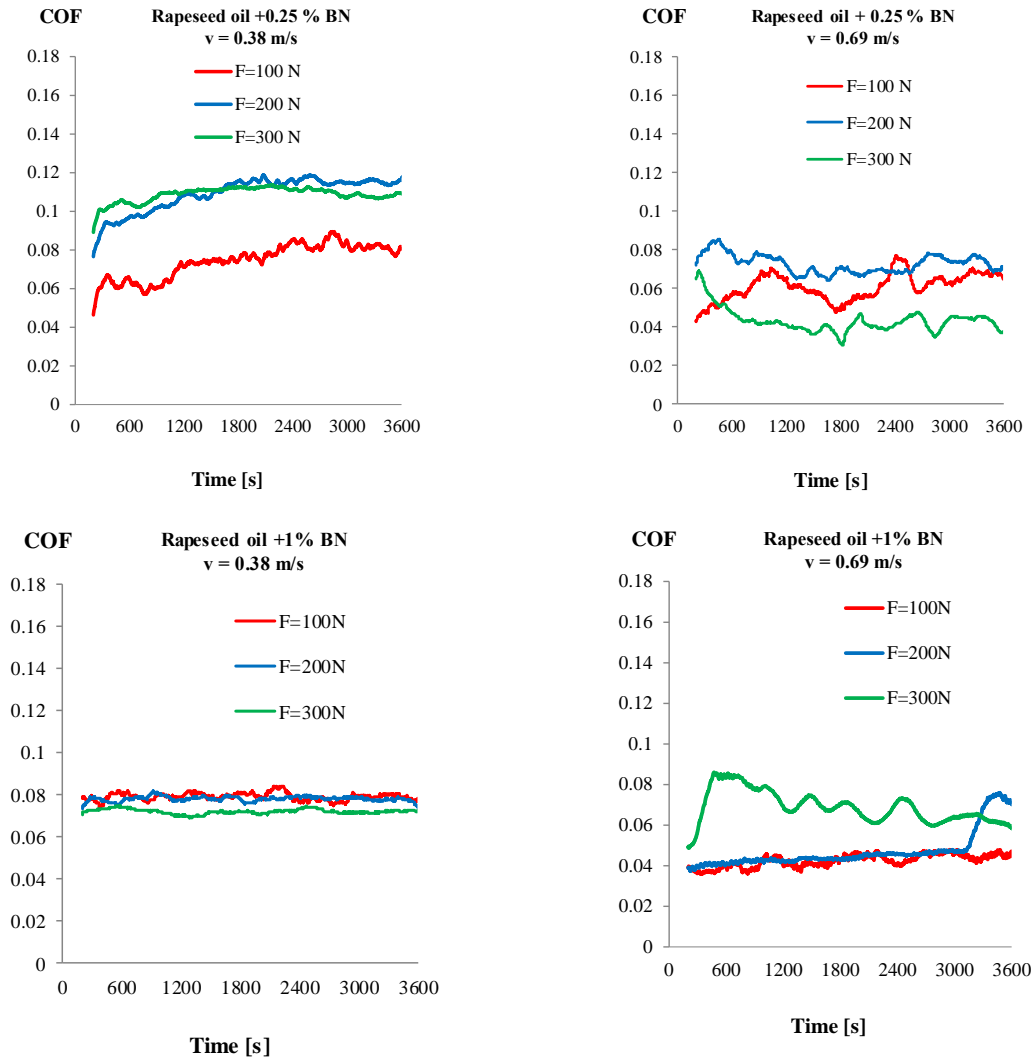


Fig. 5.10. Coefficient of friction of h-BN additive rapeseed oil with different concentrations (here, 0,25% wt and 1,0% wt), test 1h

5.2. Tribological Behavior of Rapeseed Oil Additivated with Hexagonal Nano Boron Nitride Coefficient of friction

Figure 5.10 shows the evolution COF for L=ct tests for h-BN additive lubricants, for different concentrations of the nanoadditive (0.25% wt, 0.5% wt and 1% wt). In these graphs from Fig. 5.10, a single test is presented for each concentration, velocity and force to better evacuate the evolution of COF and the influence of nanoadditive concentration. Higher COF values were obtained for the lowest concentration of nanoadditive (0.25 % wt), as can be seen from Fig. 5.10. This could be argued by the fact that being too few particles of nano additives, they are pressed, unevenly agglomerated on the texture of the contact surfaces, allowing in some places also direct contact between metal surfaces. In terms of COF, both concentrations of 0.5% wt and 1% wt h-BN are favorable for reducing friction. Figure 5.11 presents only the evolution of COF for the additive concentration of 1% wt: increasing the

velocity makes COF to decrease for all tested force, meaning high velocity is favorable to generate complete fluid film (EHD film).

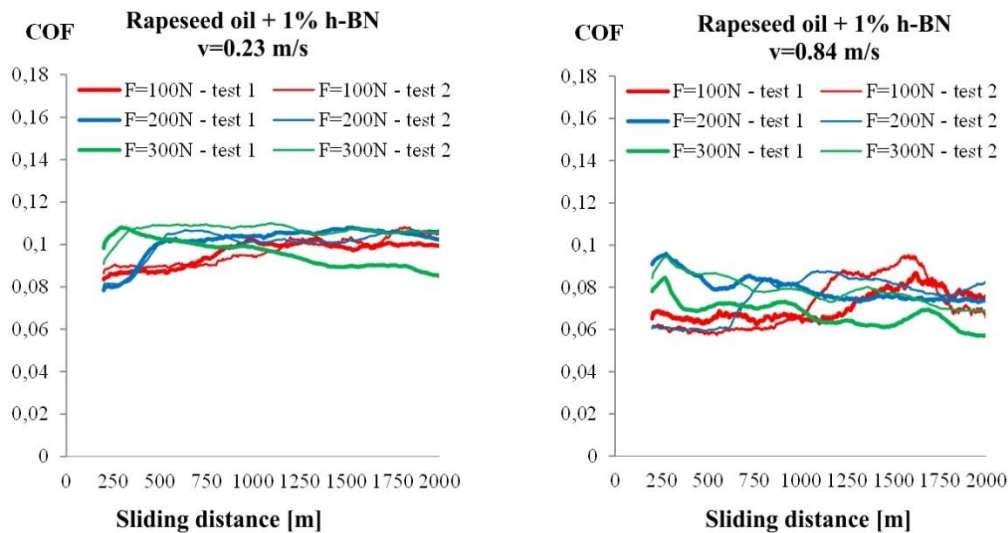


Fig. 5.11. COF for rapeseed oil +1% h-BN ($L=ct$)

But analyzing in conjunction the data for COF and WSD, for nano-additivated lubricants, the author considered that the best behavior for these two test parameters (force and speed tests of 1 h) was the additive oil with 1% h-BN. Therefore, tests for this lubricant were also carried out for $L=ct$, for a larger sliding velocity range (0.23 m/s to 0.84 m/s).

Analysis of wear parameters for additivated oil

In this study, WSD and $w(WSD)$ will be taken into account for establishing the influence of additive concentration.

Because all the tests in this campaign lasted an hour, the sliding distance is different for each velocity. It follows from this that a comparison of WSD, for different velocities does not really reflect the influence of a parameter as load or additive concentration, for all velocities.

Instead, the wear rate of WSD, $w(WSD)$, makes possible to compare regimes with different test velocities, because it is taken into account, in its calculation, the value of the sliding distance, as it results from the product $L=v \times t$, v being the velocity and t – the time. That is why WSD analysis will be done for each speed.

From Fig. 5.12, the following conclusions can be drawn:

- at $v = 0.38$ m / s, the best results (WSD the lowest), was obtained for the oil with 1% h-BN, so the additive lubricant protects the solid bodies through the additive. For the other 2 concentrations (0.25% and 0.5% h-BN), the WSD values are higher than those obtained for rapeseed oil. This would be explained by the fact that a small amount of additive does not ensure uniform distribution on the contact surface of the particles. Hence areas where wear is localized on solid bodies, not enough particles to interpose between solid bodies.
- at $v = 0.53$ m/s, the trend is the same, i.e. values a little more here and there of WSD, compared to those obtained with rapeseed oil, only for the concentration of 1% hBN. For lower concentrations the results are similar, but with greater wear and tear compared to rapeseed oil.
- at $v = 0.69$ m / s, it is noticed that it has the same tendency as at speed $v = 0.53$ m / s.. Although the sliding distance is greater, the WSD values are similar to those at $v=0.53$ m/s, which reflects the better protection of surfaces at higher speeds, probably also because a thicker lubricant film can form.

From these graphs the author can recommend the use of additive lubricant with 1% hBN, to reduce the wear of triboelements.

Figure 5.12 qualitatively shows WSD dependence on load and speed, for the lubricant with 1% hBN. It can be seen from the images obtained under the optical microscope that the wear is of an abrasive nature, more pronounced for high loads.

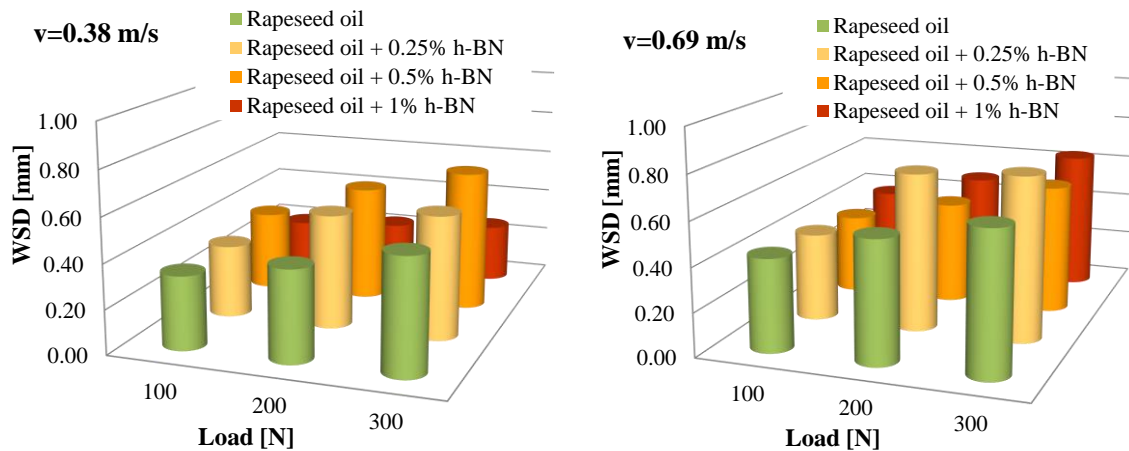


Fig. 5.12. WSD depending on load and nano-additive concentration, for each tested velocity (all tests lasted 1 h)

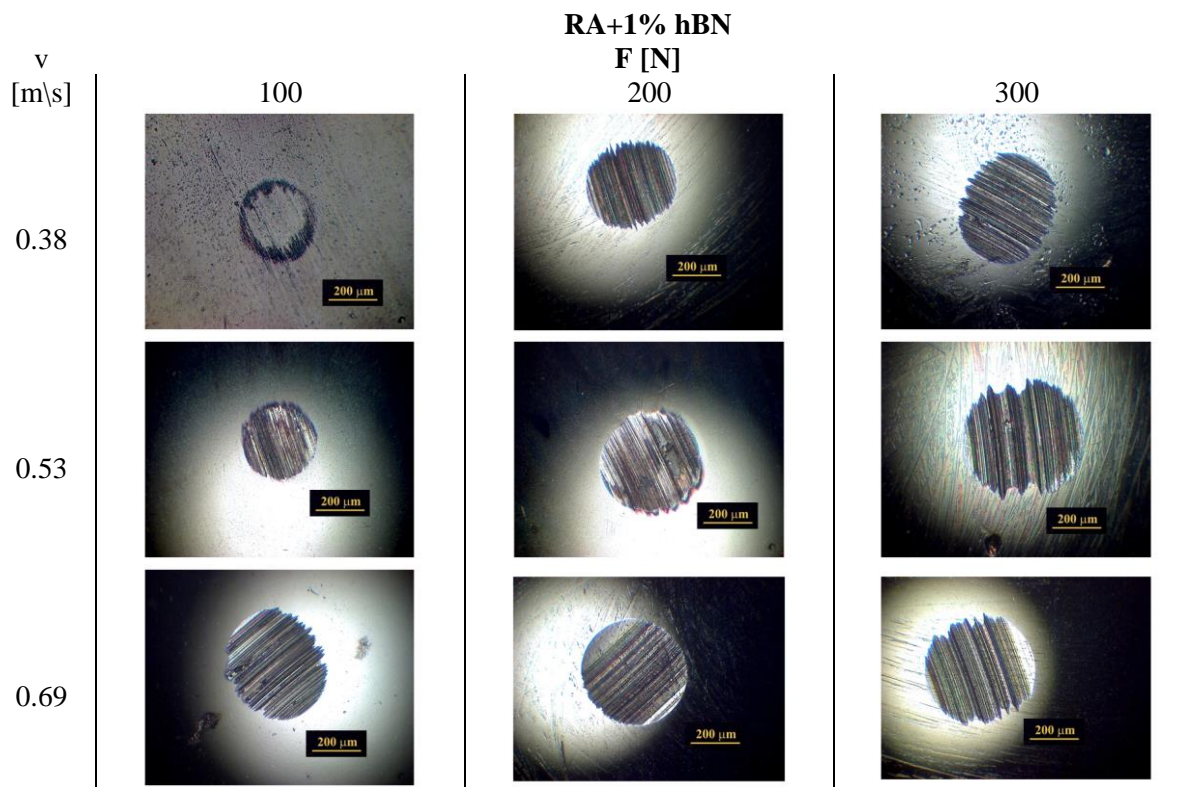


Fig. 5.13. Optical microscope images for WSD when lubricated with rapeseed oil +1%BN

The wear rate of WSD could be analyzed for each velocity, but also the values for different velocities could be compared (Fig. 5.13). The results look different from the WDS graphs in the same coordinates. The general trend $w(WSD)$, for the velocities $v=0.38$ and $v=0.69$ m/s, is not similar, i.e. higher values for the $F=100$ N regime for lower velocity, and higher values for small additive concentration (0.25% wt), this would be explainable because at low loads the nanoparticles are not fixed in the textures of the surfaces of solid bodies and so, they act only by the rolling effect between the two surfaces and could be more uneven distributed as compared to greater concentrations. At $v=0.69$ m/s,

for rapeseed oil, there is an increase in the wear rate at $F=200$ N, and then a decrease to $F=300$ N. This indicates a change in the wear process. The increase in load from 100 N to 200 N shows the intensification of the abrasive wear process. The increase of the load to 300 N, favored the reduction of wear because the increase of the load also contributes to the generation of a fluid film (which, obviously, also reduces friction and wear). If one compares the values of the graphs, it is noticed that the additive produces values of the wear rate, less sensitive to the load, but more sensitive to the concentration of the additive. For additivated lubricants, the tendency to reduce $w(WSD)$ is almost linear.

For rapeseed oil, the wear analysis for tests done at $L=ct$ was performed on the set of wear scar diameter values (WSD) (Fig. 5.14) and on the set of values for wear rate of wear and tear trace ($w(WSD)$) (Fig. 5.15).

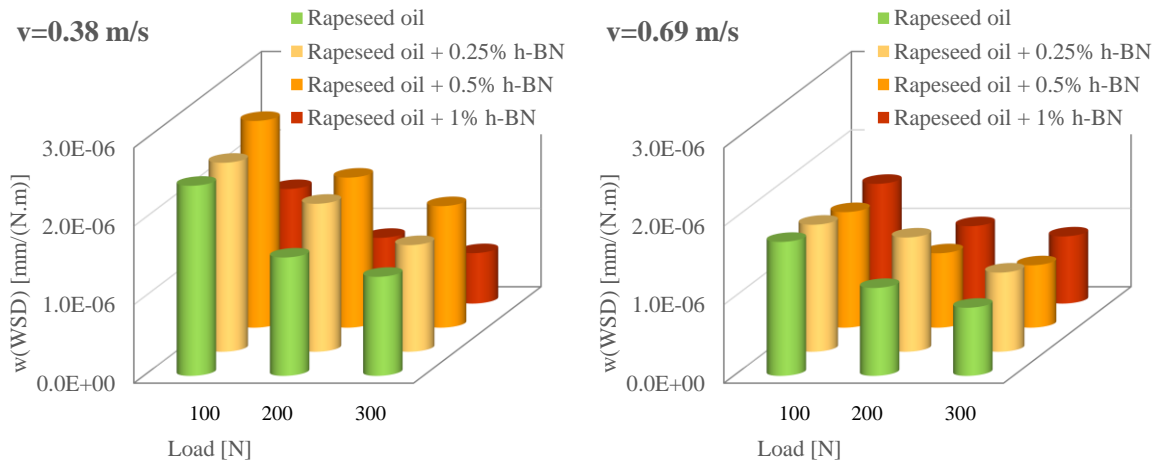


Fig. 5.14. $w(WSD)$ depending on the load and nanoadditive concentration, for each speed tested (all tests had a duration of 1h)

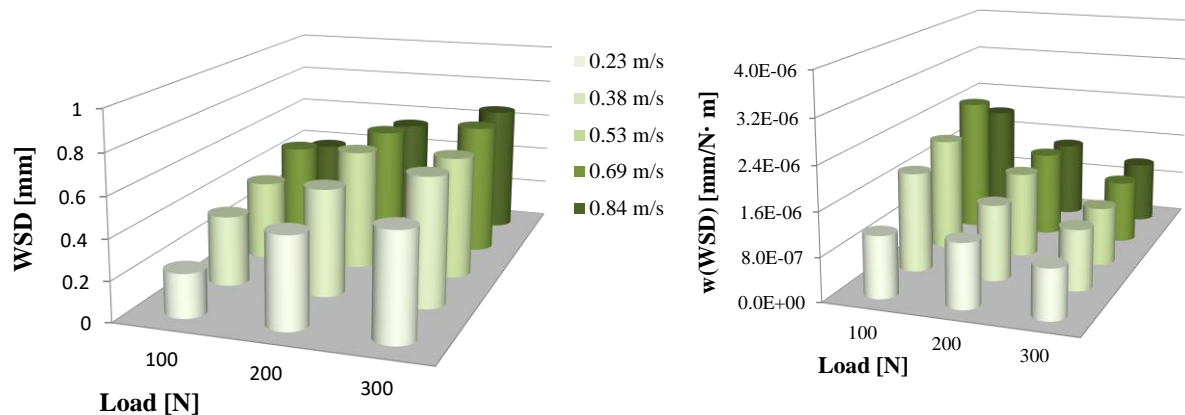


Fig. 5.15. WSD analysis for tests with rapeseed oil at $L=ct$ (both figures have the same legend)

Fig. 5.16. $w(WSD)$ analysis for tests with rapeseed oil at $L=ct$

The smallest value of WSD was obtained for $F=100$ N and $v=0.23$ m/s. For the same force, WSD increases more sharply with velocity, at its low values ($F=100$ N). At higher loads the dependence on the sliding velocity is weaker, especially at higher values ($v=0.69$ m/s and $v=0.84$ m/s). This could be explained by the fact that at higher velocities and loads, a fluid film is generated that no longer allows for mixed contact and, therefore, the wear no longer depends on the product (force \times velocity). For these sets of parameters, the greater wear, however, can be explained by the fact that the four-ball machine starts under load and, at the beginning of the movement, there is a mixed transient regime with wear proportional to the load and speed. Continued movement leads to the generation of the fluid film and it a significant reduction in the wear intensity.

The evolution of the wear rate of WSD (Figs. 5.14, 5.16 and 5.18) is also an argument for the presence of a lubricant film for higher speeds and loads. At $F=100$ N, this wear parameter has an almost linear evolution with the speed, with the highest slope, specific to the mixed regime. At $F=300$ N, the

wear rate of the WSD is too little sensitive with the speed, which means that the solid surfaces are no longer in direct contact until very short of time at the beginning of the test.

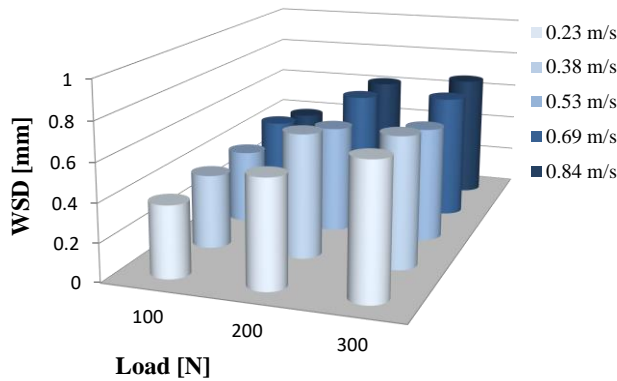


Fig. 5.17. WSD analysis for tests done with rapeseed oil additived with 1% h-BN, at L=ct (both figures have the same legend)

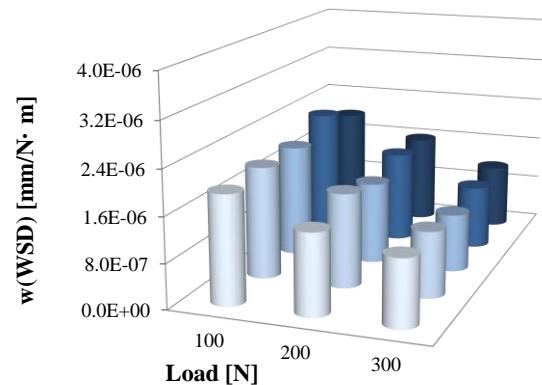


Fig. 5.18. W(WSD) analysis for tests with rapeseed oil additived with 1% h-BN at L=ct

The introduction of 1% h-BN into rapeseed oil altered WSD dependence on load and velocity, in the sense of having approximately the same dependence on load and without a clear dependence on velocity. The maximum values are approximately the same as for rapeseed oil, for the zone F=300 N, v=0.69...0.84 m/s (WSD tends to be of 0.6...0.66 mm). In terms of value, the WSD wear behavior has not been considerably improved by adding 1% h-BN, but the system has a close response over a larger range of working parameters, resulting that the system responds more evenly to variable regimes as compared to the respons of rapeseed oil.

The same trend is observed after testing the lubricant with 1% h_Bn + 1% graphene, but WSD is for the more severe range of working parameters below 0.6 mm. Comparing to the lubricant additivated only with 1% h-BN, at low velocities, this parameter is lower. The wear reduction mechanism can be complex, in this case, involving taking over the load by h-BN and graphene nano sheets, reducing friction and protecting roughness by fixing these sheets on the surface, even unevenly.

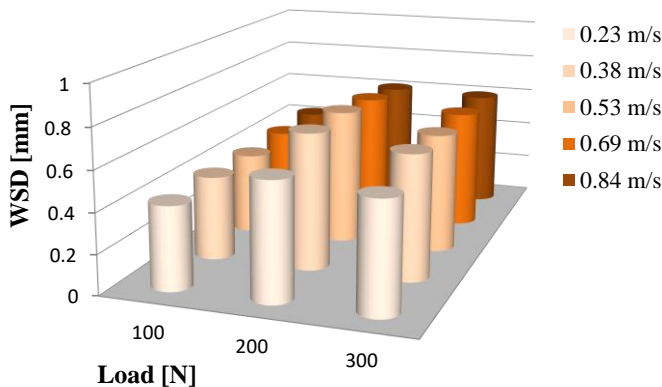


Fig. 5.19. WSD for tests done with rapeseed oil +1% h-BN+ 1% graphene at L=ct (both figures have the same legend)

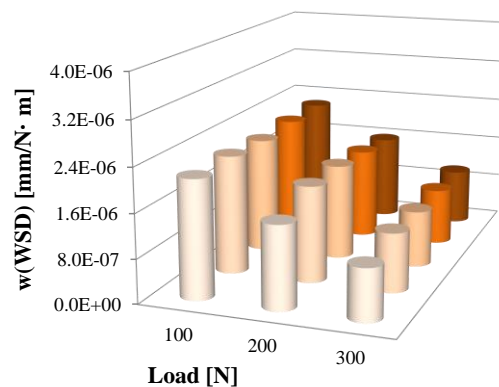


Fig. 5.20. w(WSD) for tests performed with rapeseed oil +1% h-BN+ 1% graphene, at L=ct

The graph for the wear rate of WSD (Fig. 5.19) shows small and very close values for F=300 N, with the result that for a point contact, this load will cause the smallest modifications in the wear rate of WSD. Comparing the graphs in Fig. 5.15 (rapeseed oil), Fig. 5.17 (rapeseed oil +1% h-BN) and Fig. 5.19 (rapeseed oil +1% h-BN+1% graphene), the last lubricant has the most advantageous wear rate of WSD, low at high load and without a visible velocity dependence.

Temperature in the lubricant bath for nano additive lubricants

The temperature in the lubricant bath is important because lubricants based on vegetal oils have a narrower working range and towards the minimum values, they are not stable at negative temperatures, in the sense that they precipitate waxes and some other components, and their maximum working temperature should not exceed the lowest oxidation temperature or thermal decomposition characteristic of one of the components (acids) of vegetal oil, even if it has a low concentration.

Figure 1.20 gives examples of temperature evolution of the additivated lubricant in the ball cup: at low velocity, the temperature is just slowly increased during the test, but for the highest velocity, the temperature is less dependent of load and increases in a very narrow band meaning that that interval friction in the fluid film and the friction among nanoparticles and solid surfaces generate heat enough to rise the fluid temperature.

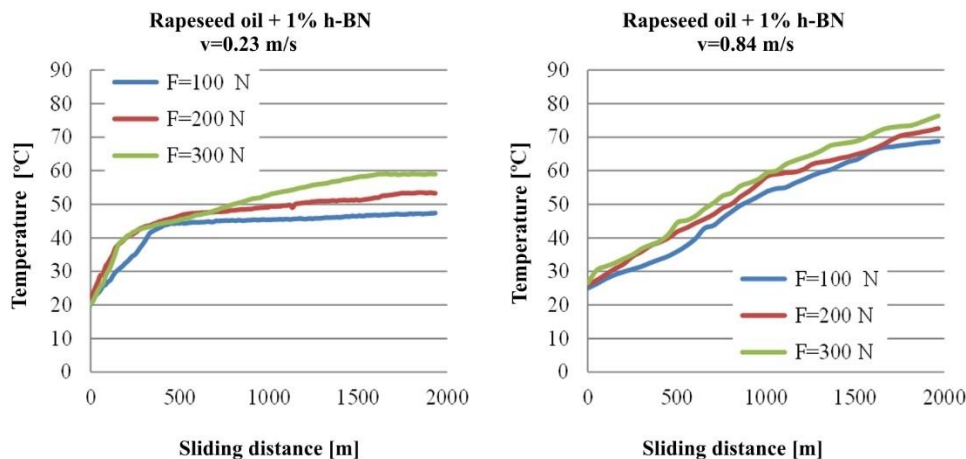


Fig 5.21. Temperature evolution in the ball cup, for rapeseed oil +1% h-BN, tests with $L=ct$

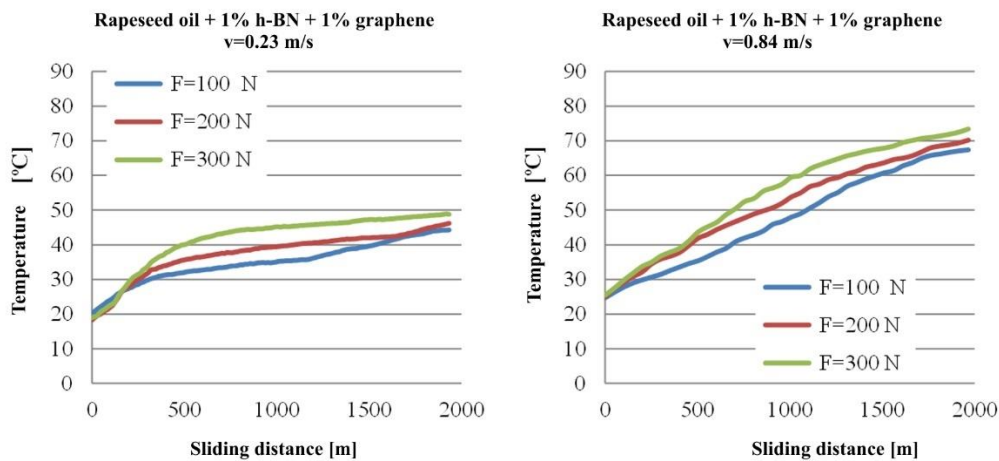


Fig. 5.22. Temperature evolution in the lubricant bath for rapeseed oil +1% h-BN + 1% graphene, tests with $L=ct$

The following analysis is based on Figure 22. As compared to simple rapeseed oil, the additivated lubricant has the final temperature in the bath increased, but it does not exceed the range of use of the base oil that goes to 90-100 °C (without oxidizing the rapeseed oil).

For the velocity of 0.38 m/s, the temperature in the ball cup, at the end of the test, is higher at low concentrations of h-NB because the low concentration allows for direct contact of the rubbing surfaces. But this temperature is lower for the concentration of 1% h-BN, thus demonstrating that the additive can help evacuate heat from the contact. For $F=300\text{ N}$ and $v=0.38\text{ m/s}$, rapeseed reaches 50 °C and the additivated oil with 1% h-BN reaches 60 °C, which means that it is not a problem for the lubricant to operate at this temperature.

At $v=0.69$ m/s and $F=300$ N, the rapeseed oil in the ball cup has 60 °C, at the end of the test, and the additivated oil with 1% h-BN has 67 °C.

In general, at the end of the test the temperatures increase with the load (more), but with the increase of the speed at the same load the temperatures do not increase spectacularly (only by a few degrees). This ordering of the evolution of temperatures according to speed and load does not change with the concentration of the additive, which would reflect that there is no change in the regime of the tribological system in contact, but only an accumulation of friction energy in the form of heat. The curves obtained for $F=300$ N are higher for higher speed ($v=0.69$ m/s).

The presence of the additive, only 1% wt h-BN, produced the more pronounced joining of the curves but still in the order of the applied load. In other words, the additive produced closer temperature values in the bath, not so differentiated according to the load, as measured in the case of rapeseed oil.

The h-BN and graphene package lowered the temperature curves below 50 °C for all speeds and loads, which had relatively smaller slopes than in the case of rapeseed oil, even a very low slope plateau trend, especially at low speeds. The exceptions were the tests performed with $v=0.84$ m/s, for which the maximum values remained around 70 °C.

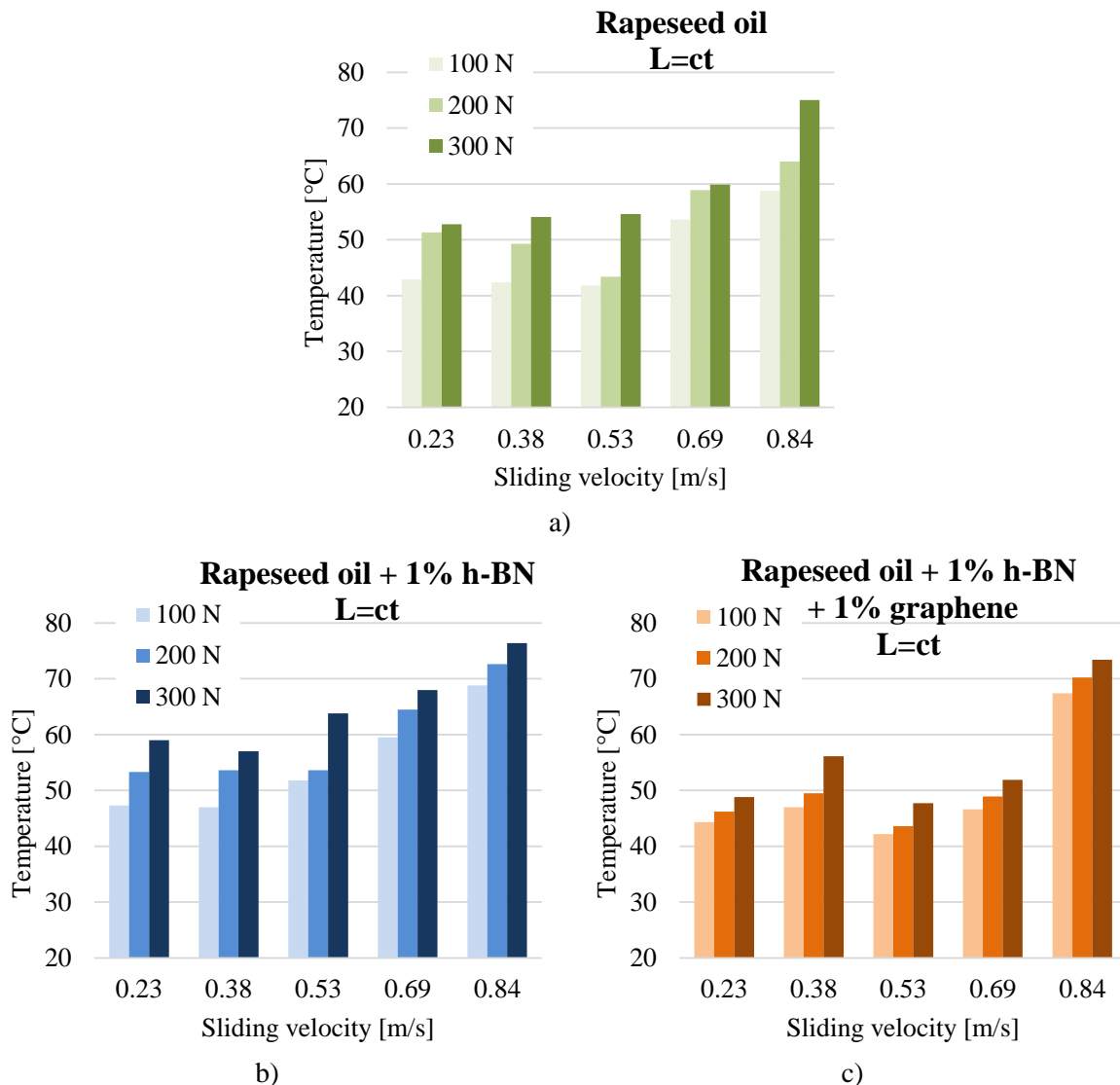


Fig. 23. Temperature in the oil bath at the end of the test

The representation of temperatures at the end of the test with $L=ct$ (Fig. 5.30 to Fig. 5.32) reveals the following:

- for rapeseed oil the temperature set for $F=100\text{...} 300\text{ N}$ is practically the same on the interval $v=0.23\text{...} 0,53\text{ m/s}$,
- for lubricant with 1% h-BN, this trend is maintained but with $5\text{...} 8\text{ }^\circ\text{C}$ higher,
- the package of additives (1% h-BN +1% graphene) has increased the range in which temperatures do not change at the same load, i.e. for $v=0.23\text{...} 0,69\text{ m/s}$.

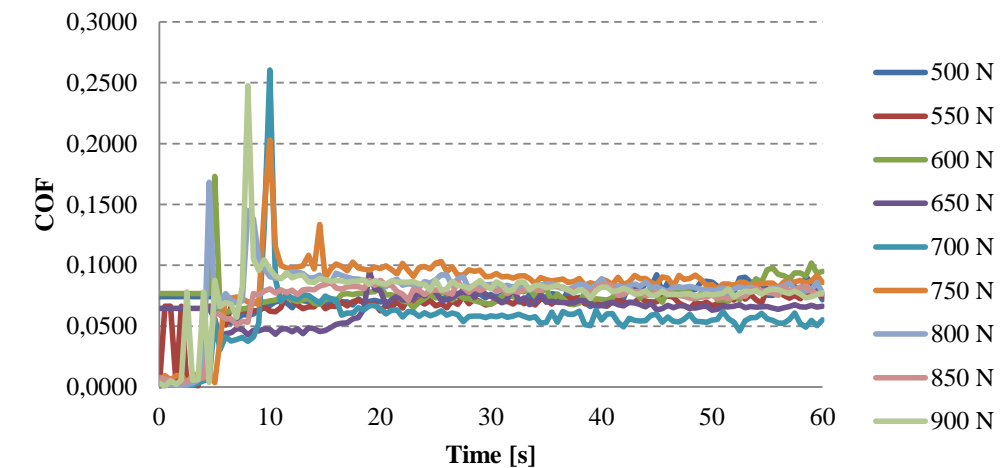
5.3. Analysis of Tribological Parameters in Severe Regime for Rapeseed Oil and Rapeseed Oil Additivated Hexagonal Boron Nitride

Analysis of the friction coefficient

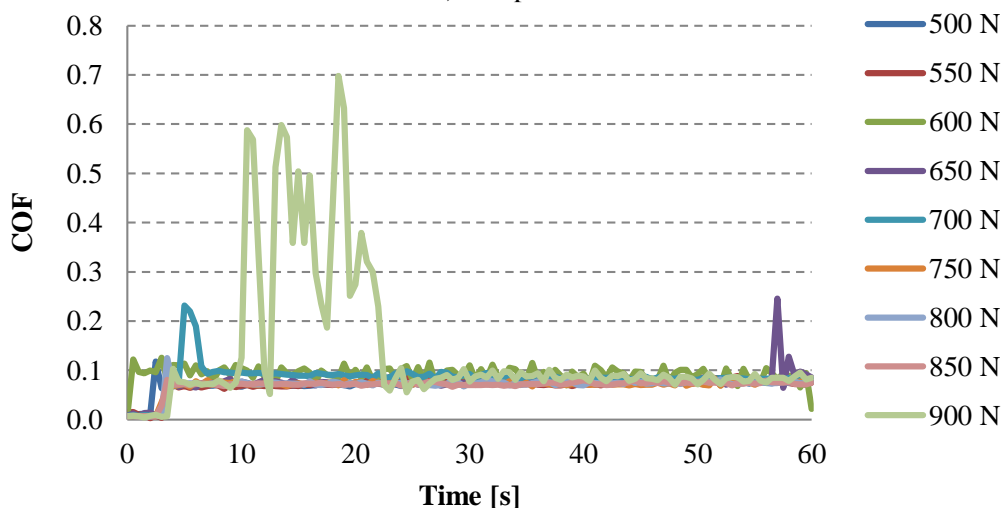
COF developments for severe regime are shown in Fig. 5.23.

From the evolution of the coefficient of friction in severe regime, it is observed

- large variations for $F=900\text{ N}$, which announces a friction in dry mode, with the possibility of gripping, given the oscillating values with large oscillations $\text{COF}=0.6\text{...}0.7$,
- the fact that the COF then returns to values around 0.1 shows that the surfaces have become accustomed by wear and the contact surface has increased so that the maximum pressure in contact has decreased.



a) Rapeseed oil



b) Rapeseed oil +1% h-BN

Fig. 5.24. Evolution of the coefficient of friction in severe mode

Analysis of wear parameters

By additivation with 1% h-BN the shape of the load-WSD curve changes substantially compared to that of unaditivated rapeseed oil (Fig. 5.24).

Rapeseed oil tends to linearly increase the WSD, with the increase of the load to 900 N, while the lubricant by 1% h-BN, maintains the WSD in a very narrow range (0.35-0.4 mm), up to 700 N, after which it has a steeper slope between 700-750 N. If the two curves are compared, it follows that the additive lubricant has a better response to the severe regime, up to 700 N.

Temperature at the end of the severe tests

The temperature of the lubricant in the oil bath, at the end of the test, in severe tests, has about the same tendency, with slightly higher values for the additive lubricant (a few Celsius degrees) (Fig. 5.25). This would be explained by the fact that in the mixed regime, with roughness in contact, the friction of the nanoparticles (rolling, sliding, dragging) is added to the mixed regime and the fact that the additive does not participate in the evacuation of heat to the same extent as the lubricant.

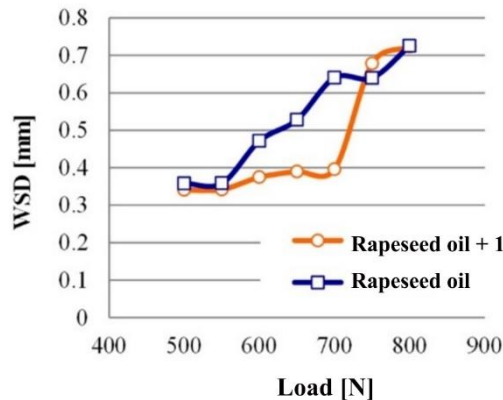


Fig. 5.25. Load curve-WSD

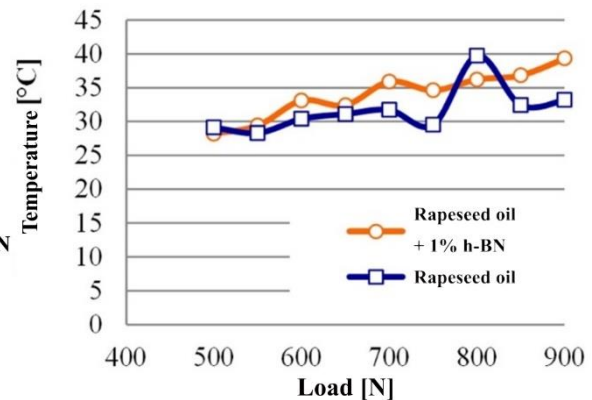


Fig 5.26. Temperature in the oil bath at the end of the test of rapeseed oil and rapeseed oil +1% h-BN

Parameter of the resistance of the lubricant film

Paleu V. et al. [106], [108] introduced the resistance parameter of the lubricant film (oil film strength, OFS) as a parameter for monitoring the process of deterioration of contact operation, also applicable to the 4-ball machine.

Figure 5.26 shows the evolution of OFS as a function of the load applied to the axle of the machine. Its value decreases to the critical value at 550 N for rapeseed oil, but for additivated lubricant, this decrease occurs at 750 N, which indicates a better behavior in severe regime as compared to non-additivated oil.

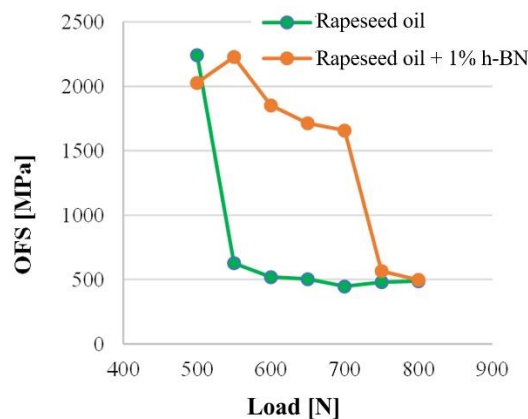


Fig. 5.27. OFS parameter for unaligned rapeseed oil and Rapeseed oil additived with 1 % h-BN

OFS is calculated with the relationship

$$OFS = \frac{W}{a(WSD)} = \frac{0.408 F}{a(WSD)} \text{ [MPa]} \tag{5.1}$$

in which W is the normal force in the contact between the balls, calculated as follows:

$$W = \frac{F}{3 \cdot \cos(\alpha)} = \frac{F}{3 \cdot \cos(35,264^\circ)} [N] \quad (5.2)$$

F being the force on the axis of the four-ball machine, a(WSD) is the calculated area of the wear trace, using the average value of the wear scar diameter, WSD

$$a(WSD) = \frac{(WSD)^2}{4} [mm^2] \quad (5.3)$$

Previous works [106]-[108] have reported that this parameter tends to have low values when the flu process begins. OFS correlates the parameters of contact in operation: the viscosity of the lubricant at working temperature (implicitly, the viscosity index), the quality of the surfaces in contact during operation, the shear resistance of the lubricant film. Paleu V. et al. [106] propose a critical value of 300 MPa for gripping.

5.4. Analysis of the Tribological Behavior of Lubricants with the Help of 3D Maps

In 1987, Ashby M. F. et al. [20] proposes wear maps for non-lubricating, steel-on-steel contacts because it can be highlighted the transition from one wear process to another, especially the transition from mild wear, acceptable in operation, to severe wear. On such a map one may also see transition areas, if the transition from one wear process to another is made quickly or on a larger range of variables.

The author of this study drew maps of the tribological parameters, coefficient of friction, wear by WSD and the wear rate of WSD, and the temperature at the end of the test (characterized by constant sliding distance), for the set of parameters (force-velocity), set that characterizes the working regime of the four-ball tribotester. The maps are drawn by cubic interpolation, in MatLab, the experimentally determined points being included in the surface.

The map of average values of friction coefficient, obtained on entire duration of each test, are given in Fig. 5.37. For rapeseed oil, COF has a range of values above 0.1, in the range $v=0.23...0.4$ m/s, the load dependence being poor, a range below 0.1 for high speeds and loads.

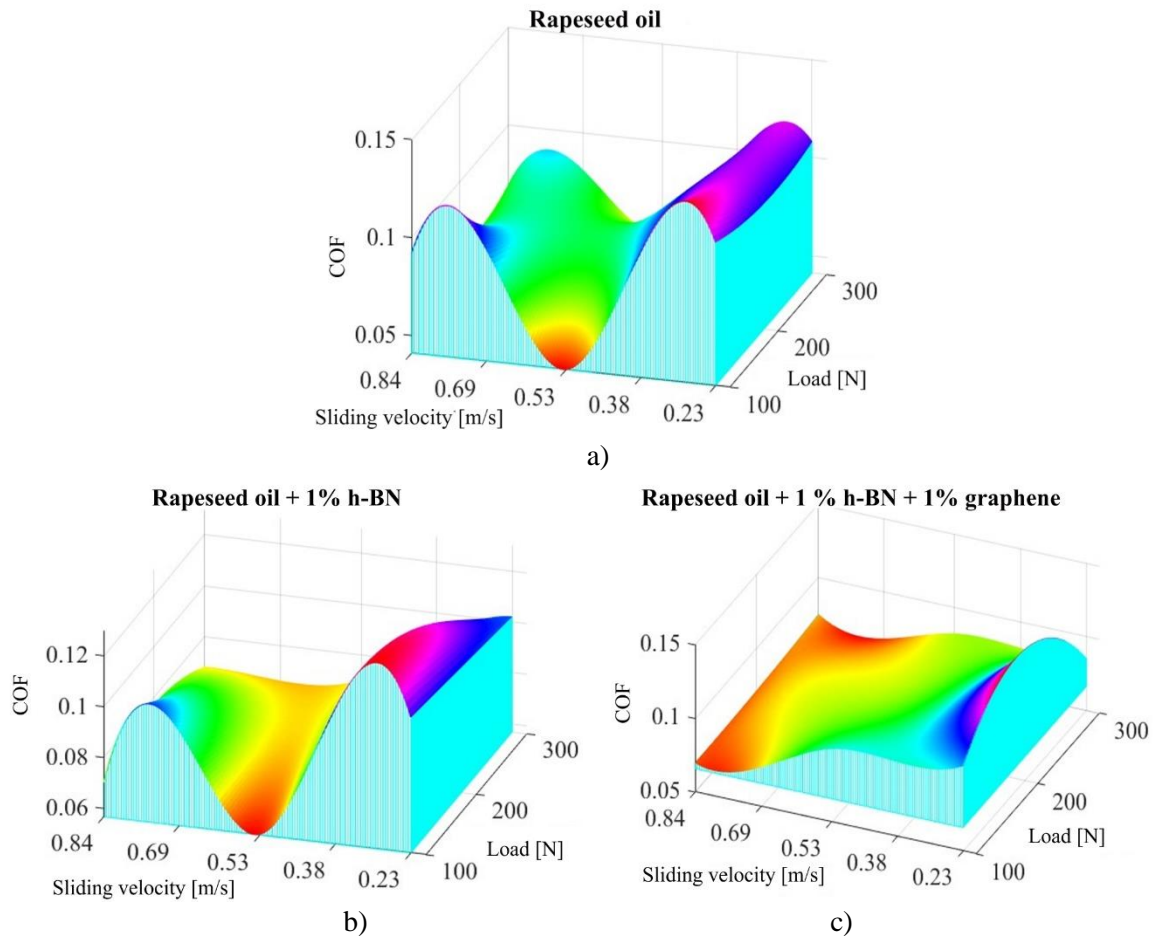


Fig. 5.28. Maps of the friction coefficient, in the force-velocity domain

The range with the lowest values was obtained around the speed of 0.53 m/s and up to 150 N. It is unlikely that a system will operate within such narrow limits of the working regime, technological processes, transport involve speeds and loads that flow on larger fields.

Additives changed the shape of the surfaces. The addition of rapeseed oil increased the range by minimum values towards higher loads but still around the speed of 0.53 m/s. The domedium with values around 0.1 is also in the range of low velocities and poorly dependent on the force applied to the four-ball triboster. The map for rapeseed oil additived with 1% h-BN +1% graphene seems more promising in the sense of lowering the COF surface for an extended range, towards the high speeds of the studied range. And for this lubricant formulated by the author, the dependence on force is weaker.

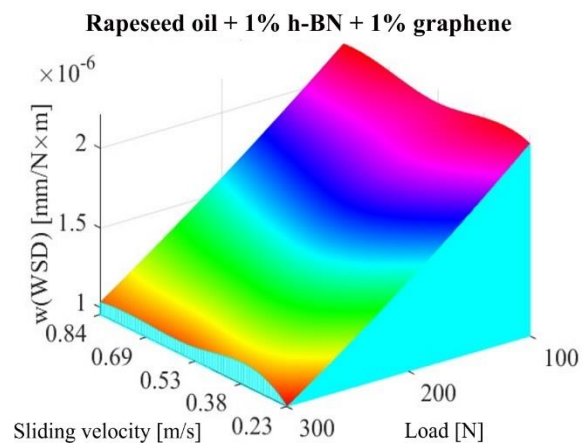
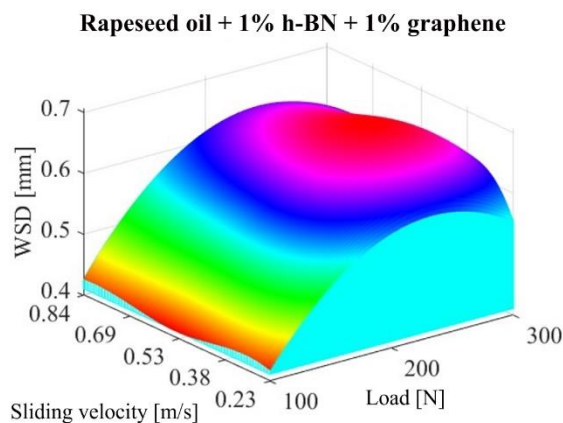
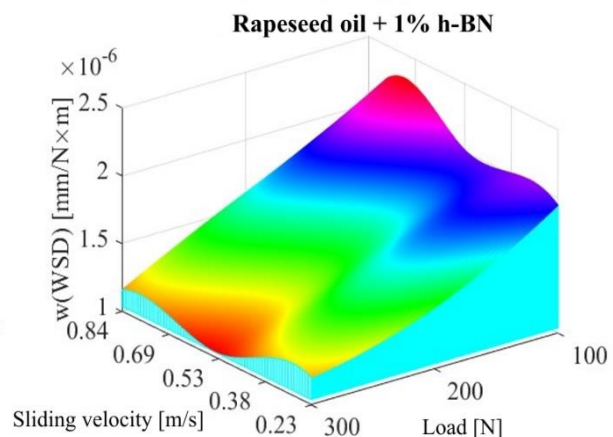
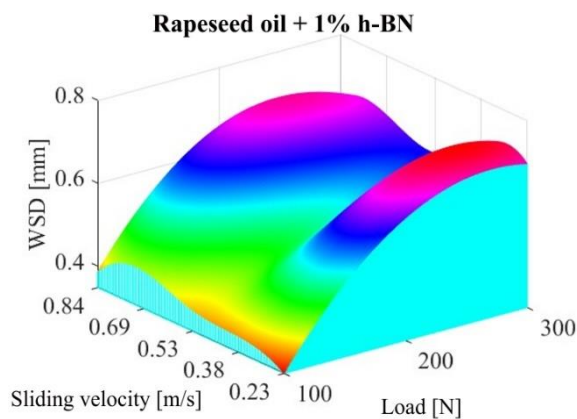
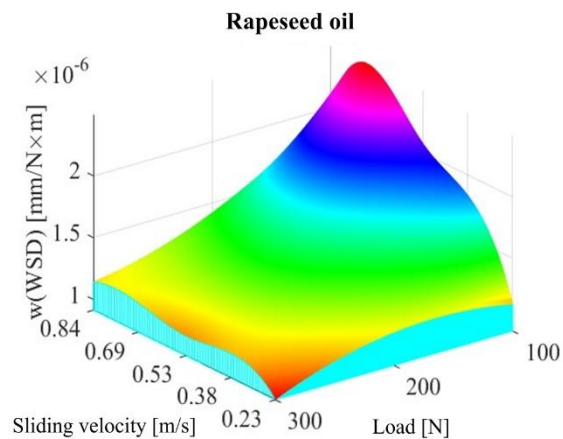
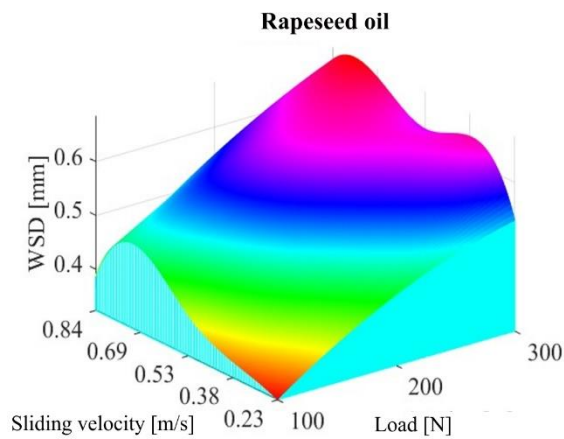


Fig. 5.29. Maps for WSD in the force-velocity domain

Fig. 5.30. Maps for w(WSD) in the force-velocity domain

curves has changed, for $F=300$ N being obtained lower values as compared to $F=200$ N. This is explained by the change of the working regime, from a mixed or boundary regime at lower velocity, towards a fluid film regime (partial or total), which is consistent with the EHD theory, formulated by Dowson and Higginson in 1967. This theory states that velocity has a greater influence in generating full-film regime in a tribosystem. For $v=0.69$ m/s, the COF evolutions are grouped in a much narrower range, which would argue that for this velocity and for the applied loads (100...300 N), there is a fluid film that separates the solid bodies in motion. This is also argued by the COF values, around 0.04...0.06.

At the concentration of 0.25% h-BN, the evolution of COF is more uneven than that of non-additivated oil. Variations occur at higher velocities over tens of seconds that could reflect the agglomeration of the particles in contact or their lack in contact and the increase in COF due to direct contact. COF values are higher than those obtained with the non-additivated oil, explained by the friction with the third body of the additive particles. At $v=0.38$ m/s, COF values were obtained around 0.1, a value that characterizes the mixed or boundary regime. Only at the velocity $v=0.69$ m/s, COF decreased in the range of 0.04...0.08, which shows that the particles circulate through the fluid or along with the fluid, without generating intense friction with solid bodies. For the concentration of 0.5% h-BN, COF values are grouped and lower for $v=0.38$ m/s and $v=0.53$ m/s. It is noticed that COF values for $v=0.69$ m/s are very small, much different from the other tests. Thus, this concentration is not favorable for decreasing friction in four-ball tester or similar systems.

At the concentration of 1% h-BN, COF evolution is in a narrow band for $v=0.38$ m/s and for $v=0.53$ m/s, but for the most severe normal regime ($F=300$ N, $v=0.69$ m/s), COF evolution is more non-uniform and there is a tendency to obtain higher values for the lower load. Here, too, based on the results obtained, it is recommended to repeat the tests to confirm this trend.

Influence of the concentration of the additive on the parameters of wear and seizure

Concentrations of 0.25% wt and 0.50% wt h-BN did not give satisfactory results, $w(WSD)$ values being higher than those of rapeseed oil, but for 1% wt nano additive, the values of this parameter are lower than those of the base oil, justifying the additive in this concentration (see Fig. 5.12).

In severe regime, the observed and measured tribological parameters show that the additive lubricant has a better behavior, reflected especially by WSD.

The first value where WSD decreases for rapeseed oil +1%h-BN appears at $v=0.38$ m/s and $F=300$ N. Starting with higher velocities, lower values for WSD appear for $v=0.53$ m/s and $F=300$ N, $v=0.69$ m/s and $F=100$ N, $v=0.39$ m/s and $F=300$ N, $v=0.84$ m/s and $F=300$ N.

At lower loads, namely for $F=100$ N and $F=200$ N, WSD values obtained with 0.25% and 0.5% h-BN in the base oil are higher with 2%-10%, but for the lubricant with 1% h-BN the wear rate decreases systematically. The WSD reductions, having small values of 1%-13%, may be included in experimental statistics.

The conclusion is that the additivation with h-BN becomes effective for the velocity $v=0.53$ m/s and higher, for all tested loads, and for the additive concentration of 1% wt. Better results in terms of COF and WSD were obtained with the additive package (1% h-BN + 1% graphene).

The wear results, using additivated rapeseed oil, do not show spectacular results for the parameters tested in this study, but the additivation improved enough wear parameters to be taken into account as promising lubricant based on rapeseed oil.

Chapter 6

Flammability of Rapeseed Oil and Rapeseed oil added with 1% Hexagonal Boron Nitride on Hot Surfaces

6.1. Flammability of Fluids and Tests to Assess It

The analysis of the consequences of fire in the work area is today much more complex and must highlight the short and long-term implications: costs of production interruption, the costs related to the health and safety of personnel, the impact on the environment and the image of the organization, etc.

The term fire resistant is poorly understood or interpreted relatively when it comes to fluids; it seems appropriate to specialists to standardize the terminology and revise the accepted test methods in order to assess the fire resistance of a particular fluid [48], [53]. There is no single property or test for a fluid that qualitatively quantifies its relative resistance to fire or ignition. Usually tests to assess the fire resistance of fluids are, in fact, "simulated incidents" so that the tests are a repeatable replica of the worst possible scenario in typical applications where a fluid is used next to a potential fire hazard. Fluids pass or do not pass these tests and those that pass them are included in recommendations [176].

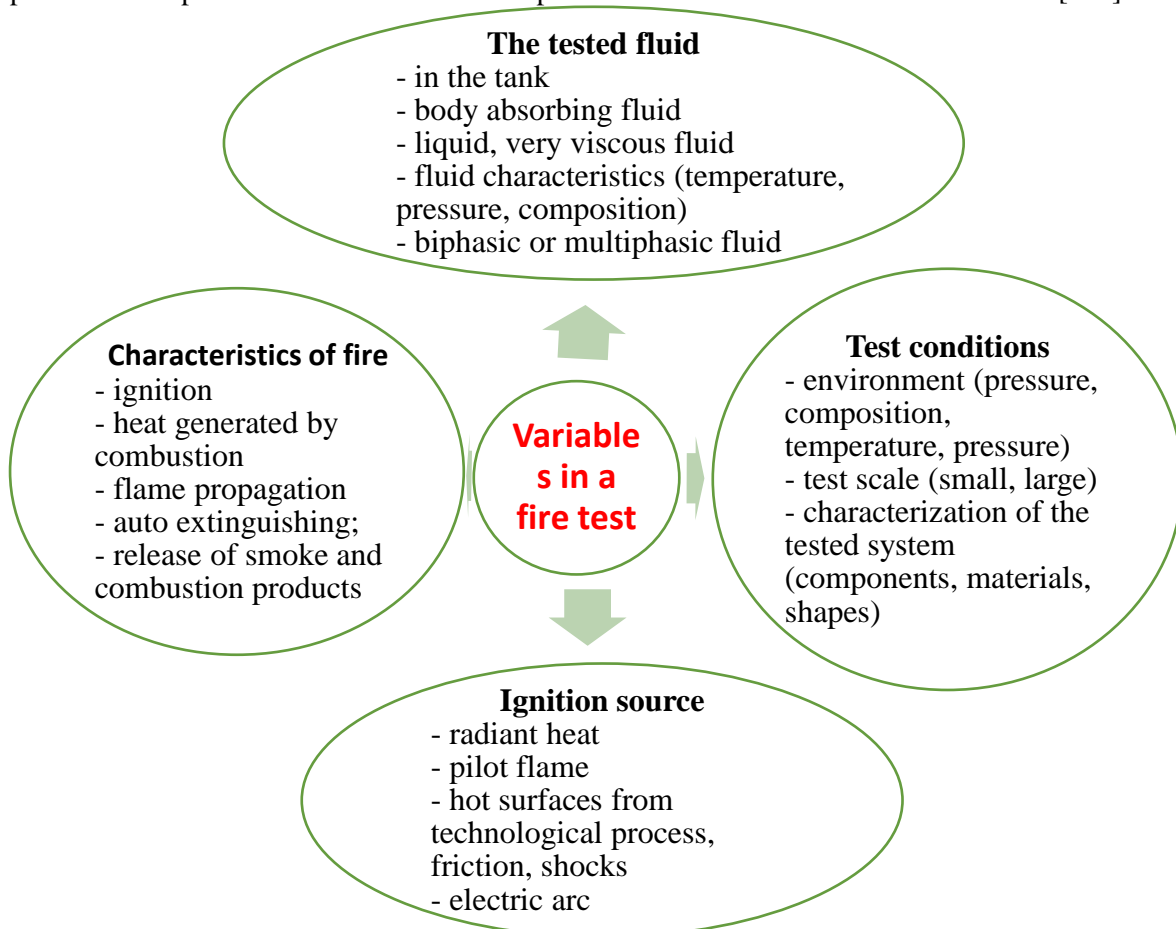


Fig. 6.1. Variables in fire tests, for fluids only, after [168]

Potential sources of ignition include not only red-heated or molten metal, sparks or flames, but also hot surfaces resulting from normal or accidentally severe operation. Fire-resistant fluids, even if safer, cost more than petroleum-based fluids and/or require changes in equipment or operating parameters.

A peculiarity of these tests to assess the flammability of fluids is that the result of the test is given as "pass" or "not pass". The fluid that has passed the tests is included in the recommendations of the specialists or in the approvals, but they are subject to regional regulations (in the USA: Approval Guide or List of Qualified Fluids, in the European Union: [173], [174], [175] or in national regulations:

The flammability characteristics of a fluid include [129]: smoke point [433], flash point, point of fire (combustion), self-ignition point or spontaneous combustion point, flammability point (or interval) on hot surface. Of particular interest is for the determination of these characteristics for organic structures and especially for hydraulic fluids and lubricants [145].

For vegetal oils, all these characteristics depend on the content of saturated fatty acids [free fatty acids]. An increase in the content of unsaturated fatty acids causes a drop in the flashpoint from 230 °C to a content of 0.01 % free fatty acids at 93 °C if this content approaches 100 %. Under the same conditions the flash-point shall fall from 330 °C to 193 °C and the burning point from 363 °C to 221 °C [37]. However, the fatty acid composition plays a minor role in modifying these three flammability assessment points when short and medium molecular chains exist.

The need to assess the risk of ignition in the case of fluids in order to ensure compatibility with safety requirements is present in European directives, one of the most importance being Directive 94/9/EC (the Explosive Atmospheres. ATEX Directives) [136]. Research on the selection of a technical fluid exposed to the risk of ignition, the evaluation of the fire risk in the case of technical fluids are also in the specialized literature [48], [51], [128].

Inflamability on hot surfaces, as a property of technical fluids, is becoming more and more researched and related to practical applications, because this (undesirable) event of fluid leakage on hot surfaces, if it occurs, can cause fire, self-ignition and even explosion [52], [53], [62].

6.2. Equipment and test procedure

The equipment is shown in Fig. 6.2 and is called Automatic installation for testing the flammability of fluids on hot surfaces. It is a modulated design solution of an establishment in order to perform tests on the flammability of fluids on hot surfaces, made after the solution offered by the the coordinator of the thesis in 2008.

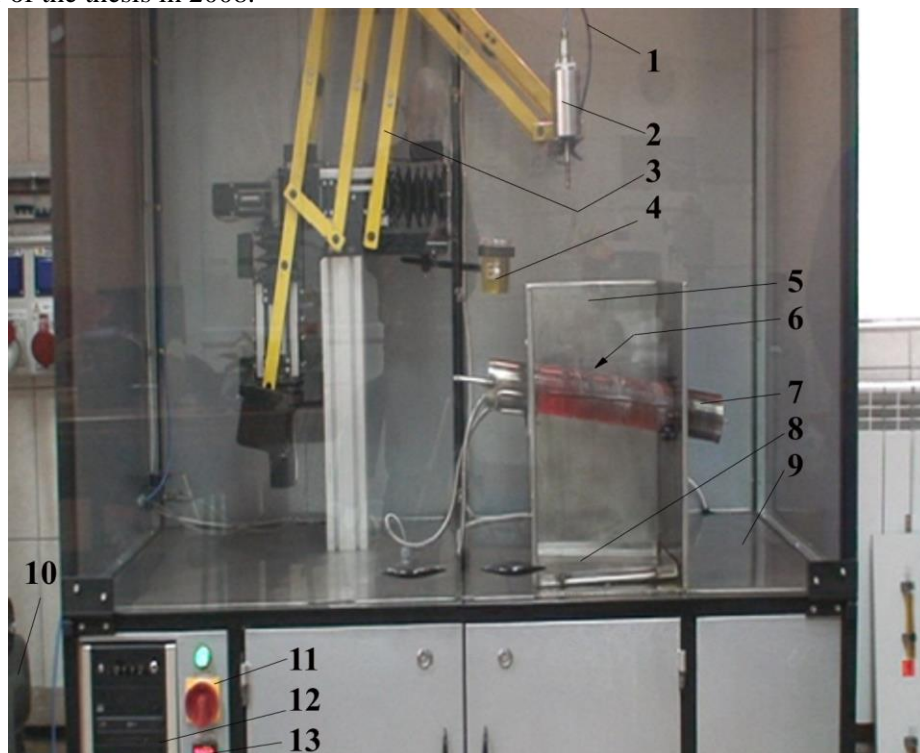


Fig. 6.2. Installation for testing the flammability of fluids on hot surface. 1 – system with cooling tubes for the dispenser, 2 – dispenser with cooling jacket, 3 – 2D manipulator for the dispenser, 4 – tank with the test fluid, 5 – stainless steel enclosure, 6 – thermocouple protected by housing welded to the inclined tube, 7 – the inclined tube, heated with an electrical resistance, positioned inside it, 8 – tray for collecting the fluid falling from the tube, 9 – ventilated enclosure, protected with fire-resistant glass, 10 – the compressor serving the dispenser, 11 – the main switch, 12 – the computer that ensures the adjustment and operation of the installation, 13 – the display for the temperature of the inclined tube

The procedure complies with the standard and offers the possibility of automatic operation of the installation, data recording and filming the test. The test includes the following steps.

1. Cleaning the outer surface of the tube, which must be approximately at room temperature, by rubbing it with a wire sponge, follows a cleaning with absorbent cotton wool soaked with cleaning solvent and finally dry with absorbent cotton wool. To make sure that the metal particles are not left on the surface of the metal particle at all. Cleaning the tube between tests is preferable to be done without removing it from the support, but with the heating element electrically insulated or removed.

2. Mounting the dropper vertically above the axis of the tube and 300 mm above the surface, at the middle of the inclined tube.

3. Filling the dispenser with 10 ml test portion of fluid at 20 °C to 25 °C. All tests were done on the middle of the heated tube in order to avoid small distortions of the temperature field at the tube ends due to air circulation in the stainless box.

4. Testing the drip time of the fluid and adjusting the drip rate with the help of a small tap mounted on the flow pipe

5. Connecting the heating element and balancing the temperature to the value desired by the operator (maximum 700 °C \pm 5 °C) at the estimated point of contact, as indicated by the transducer protected by a metal enclosure welded to the inclined tube.

6. Checking the closing of the explosion-proof windows.

7. Drip the fluid onto the tube at a constant drip rate so that 10 ml of the volume tested is released in 40s to 60s.

8. Observe and film the behavior of the fluid, both on the surface of the tube and when recording any flame or burning on the tube or when the fluid is collected in the tray below.

Repeat the test two more times at the same temperature by observing the steps from point 2 to point 5.

If an ignition temperature is required, select the new temperature below or above 700 °C, as indicated from the result at that temperature, and repeat (procedure) from 1 to 6. Usually, it begins with a temperature close to the flash point of the fluid, if given in the literature. Depending on the result, if the fluid does not ignite, the test is done at a temperature higher by 50...100 °C; if the fluid burns at a certain temperature, the interval halving method is applied to determine the next test temperature value. Repeat the procedure until the fluid stops burning repeatedly at 3 consecutive attempts and the difference between it and the temperature immediately higher at which the fluid ignites, cannot be less than the tolerance field for the temperature measurement system (here 5°C).

6.3. Analysis of Results

From the films made, frames were selected that indicate moments characteristic of the behavior of the oil at the heating temperature of the tube, including the moment of the first drop on the tube, the moment of the start of the smoke release, the moment of ignition of the oil, images with flames of various intensities, on the tube and/or in the tray, the moment of extinguishing the flame (self-extinction, if this happens), the last moment of the duration of the test (dripping), moments of burning after cessation of the test (dripping) if any.

Figure 6.3 shows the unaditivated rapeseed oil tested at 510 °C, with rapeseed oil that ignites.

After the first test at 510 °C, during which the rapeseed oil did not ignited, on the second test carried out at 510 °C, the oil ignited in the 9th second, with a rather large flame, continuing to burn more appeased on the tube, the last drops falling on the tube burning a little lower on the tube and just below it. At this temperature, the oil does not burn and in the tray. Therefore, carrying out as many tests as possible during the range when the probability of ignition exists is important for determining the maximum temperature at which the fluid does not ignite. The standard provides for three consecutive tests, for which the fluid does not ignite, but from the experience of this test campaign, the author has found that the number of tests carried out at the same temperature must be higher, five, six, even 9, so as to increase the degree of confidence in the results obtained.

Recorded videos of the tests are the proof that 495 °C is the maximum temperature at which the rapeseed oil does not burn (three consecutive tests gave the same result), but recent discussions at ISO and in specialists' forums suggest more than 3 tests, even 6... 9 tests.

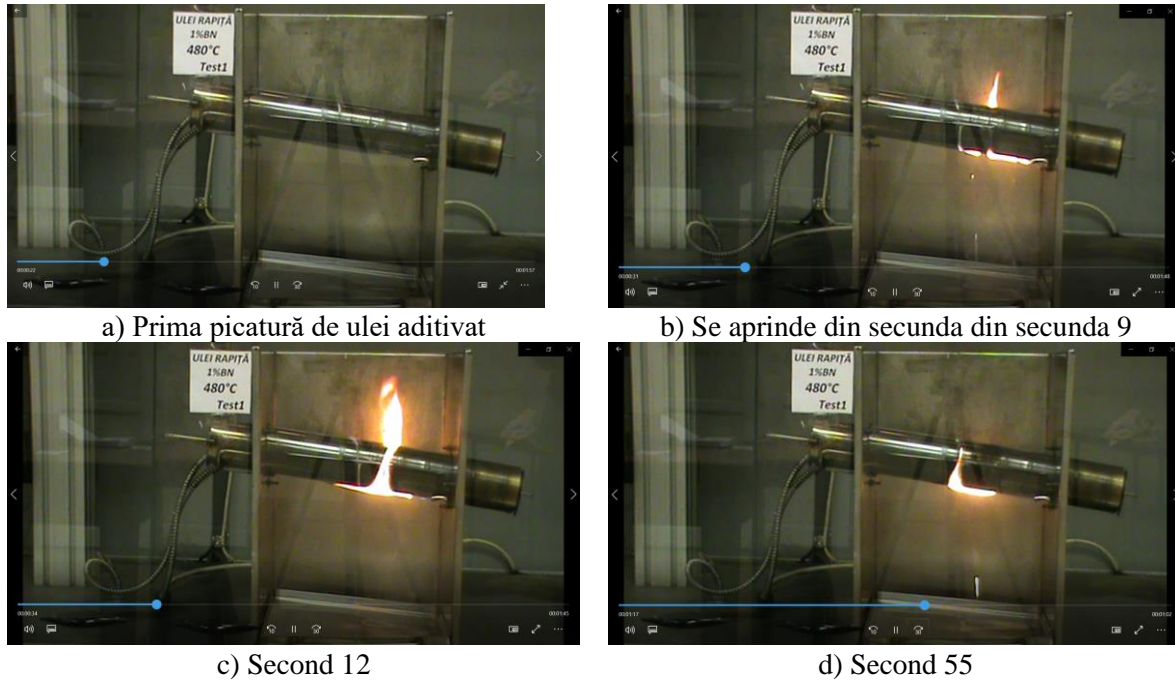


Fig. 6.5. Test 1, with 1 % h-BN additive rapeseed oil at the inclined tube temperature of 480 °C
(the fluid ignites)

Figure 6.5 shows images from a test carried out at a tube temperature of 480 °C, during which the additivated lubricant had ignited. If, after consecutive tests at temperatures lower than several degrees, it is found that the time at which the fluid ignites increases, this is a signal that the tests are approaching the temperature at which the fluid repeatedly stops igniting. Although the addition of 1% h-BN would have been expected to increase the ignition temperature of rapeseed oil, tests have shown that the ignition temperature of the additive lubricant is 10...15 °C lower. Further research is needed, the result is substantiated by tests and must be taken into account when assessing the risk when using this lubricant.

Figure 6.6. present the results of the tests, in the order in which they were carried out and until three consecutive tests have been obtained for which the fluid does not burn.

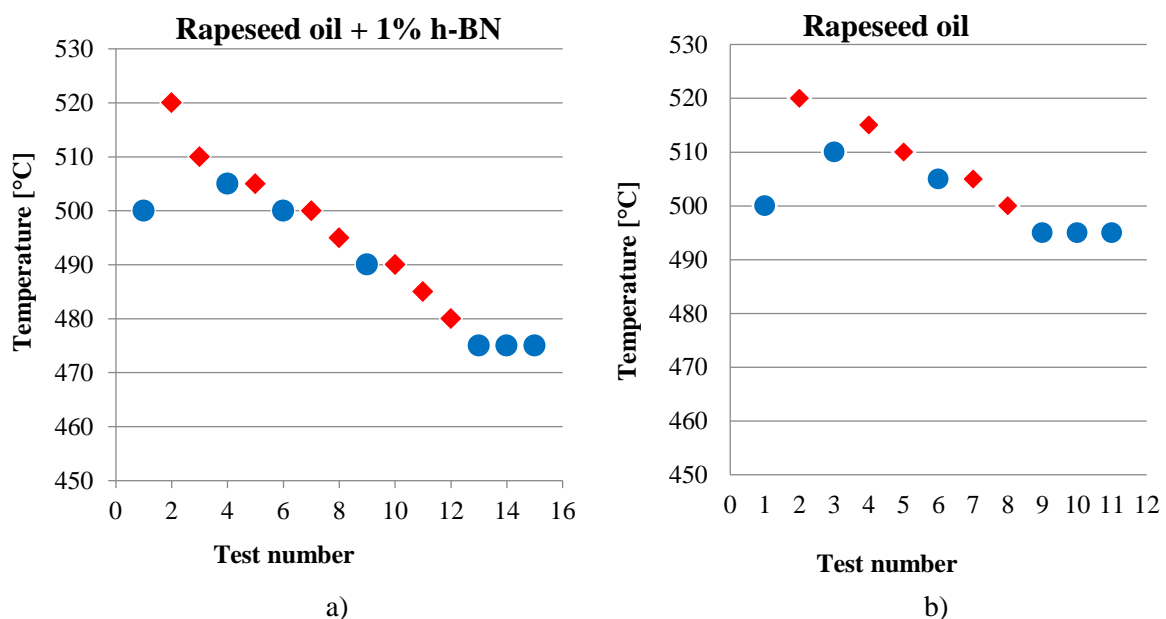


Fig. 6.9. Test results for a) rapeseed oil and b) rapeseed oil additivated with 1 % h-BN

6.4. FTIR Analysis for Lubricant Samples after Flammability Testing on Hot Surfaces

6.4.1. Apparatus and method of analysis

Robinson N. [120] presented a model of the lubricant spectrogram, on which specific changes in used fluid can be identified (Fig. 6.7). Wear particles, compounds resulting from mechanical shear and/or oxidation or chemical radiation of the lubricant components (for base oil and additives) may be pointed out.

In all lubrication systems, organic compounds exposed to high temperatures and pressures in the presence of oxygen will partially oxidize (react chemically with oxygen). There are a variety of by-products produced during the combustion process, such as ketones, esters, aldehydes, carbonates and carboxylic acids, and the exact distribution and composition of these products are very complex.

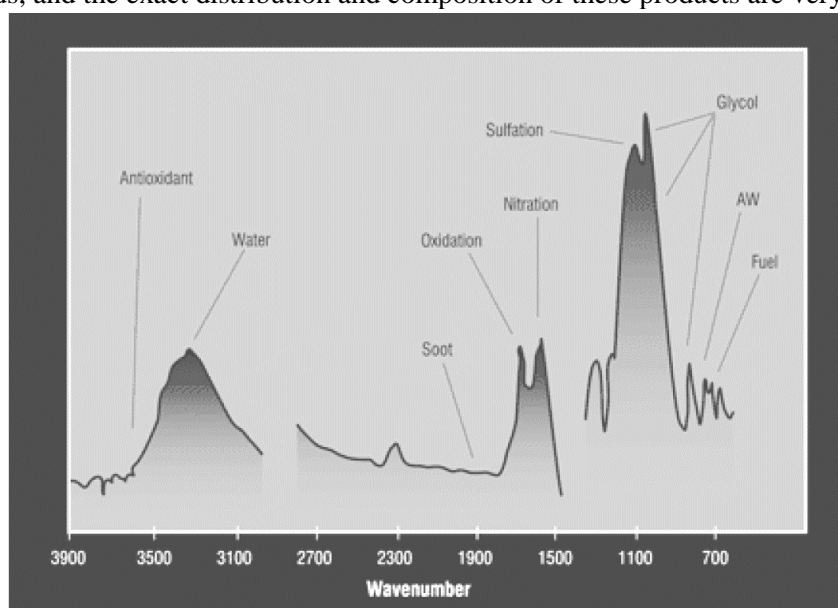


Fig. 6.7. Typical image of an absorbance spectrum for a used lubricant [120]

Some of these compounds are dissolved by the oil or remain in suspension, due to the dispersed additives in the oil. Carboxylic acids contribute to the acidity of the deplete engine oil and their base reserve of additive decreases, as neutralization occurs. The net effect of prolonged oxidation is that, from a chemical point of view, the oil becomes acidic, causing corrosion, while an increase in viscosity occurs.

FTIR spectrometric analysis can determine the oxidation level by the response of the carbonyl group (C=O) in the range of 1,800... 1,670 cm^{-1} . (Fig. 6.7). In this region, IR energy is absorbed due to the oxygen carbon bonds in the oxidized oil. Very few compounds found in new petroleum lubricants have significant absorptions in this area. Thus, monitoring this region is a direct measurement of the level of oxidation, as compared to another method, such as acidity number (AN), which takes into account all acidic species in the oil.

The FTIR analysis provides reliable information on the changes in the spent lubricants, but the information must be supplemented with that obtained through other tests and analyzes, in order to make a more relevant diagnosis of the used oil samples.

The spectrometer used in this study, is ALPHA II, from Faculty of Sciences and Environment, "Dunărea de Jos" University of Galați [446], being successful in all FT-IR applications in any industry, be it quantification, identification of unknowns, raw material verification, quality control or research.

The procedure is simple. Take a little fluid pipette and allow a few drops to fall on the window of the apparatus (previously cleaned). The analysis is rendered on the computer monitor in the form of an absorbance spectrum. The dedicated software can identify the wave number of peaks on the graphs.

6.4.2. Results of FTIR Analysis

Oxidation of vegetal oils produces hydroperoxides and volatile compounds with low molecular weight, such as aldehydes, ketones, carboxylic acids and alkanes and short-chain alkenes. Thermal reactions occur when the fluid contact the hot surface, consisting of monomers and triglyceride polymers [125]. Variations in IR spectra for vegetal oils is not easy to notice because their composition is similar.

Figure 6.8 shows an absorbance spectrum for the rapeseed oil used in this study, with the identification of wave numbers for peaks. Similar results were obtained by Jiang D. et al. [74], [95] and Lu Y et al. [96], with very small differences of thousandths of percent.

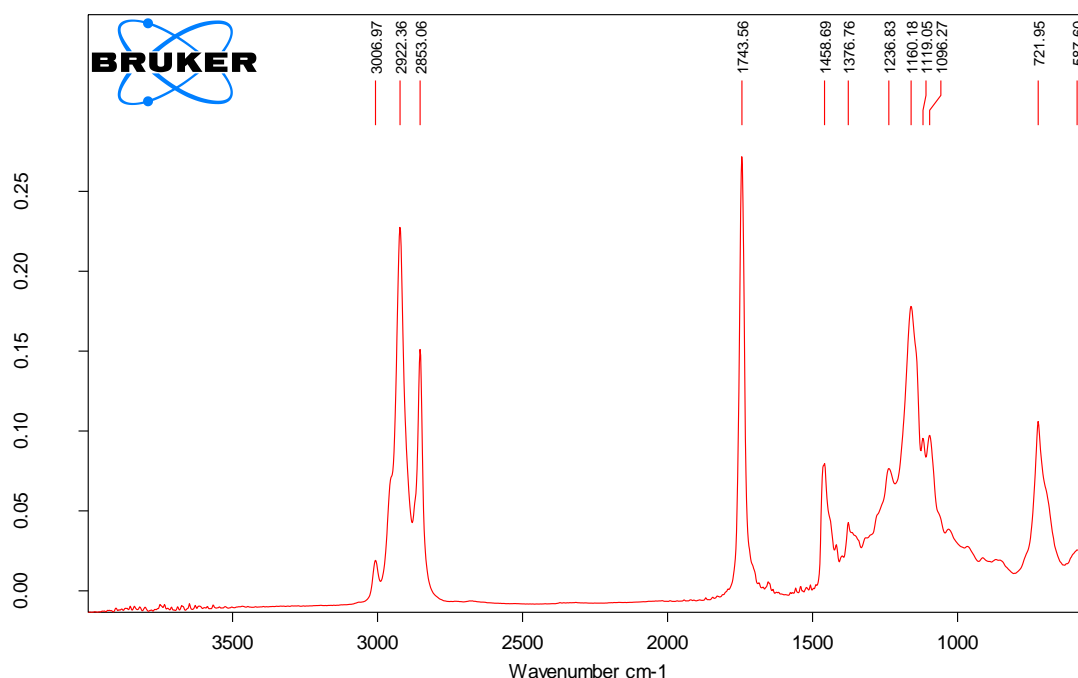
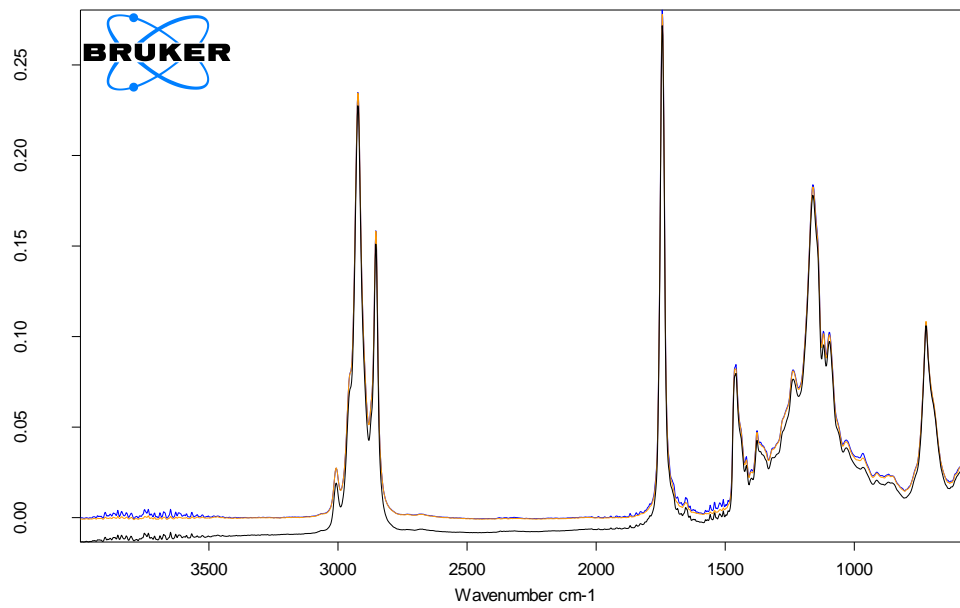


Fig. 6.8. Absorption spectrum of rapeseed oil used in this study

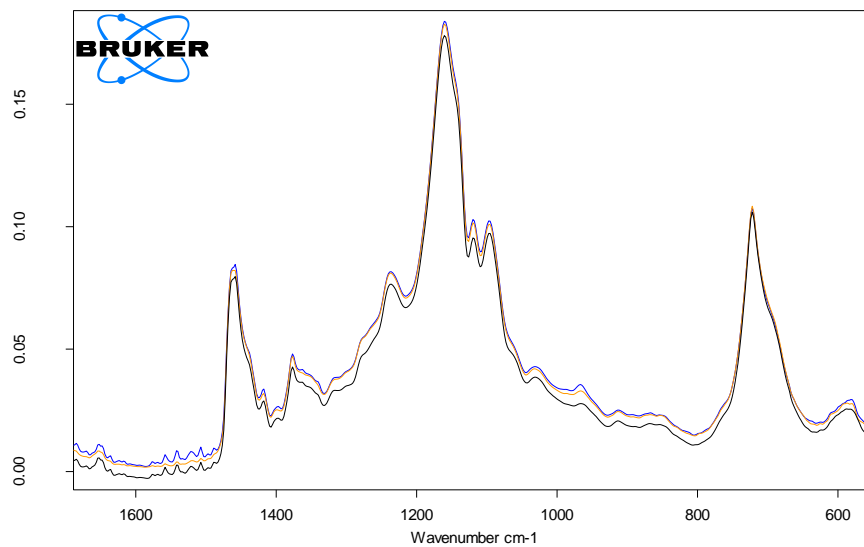
Table 6.1. Allocation of peaks in the FTIR spectrum of the rapeseed oil

Wave number [cm ⁻¹]			Functional grouping	Vibrating mode
Lu Y., 2014 [96]	Fig. 6.8	Δ[%]		
1	2	3	4	5
3010	3006.97	-0.101	=C-H (cis-)	Stretching
2924	2922.36	-0.056		Stretching
2856	2853.06	-0.103	-C-H(CH ₂)	Stretching
1746	1743.56	-0.140	-C-H(CH ₂)	Stretching
1650		-	-C=O (ester)	Stretching
1465	1458.56	-0.442	-C=C- (cis)	Bending
1420			-C-H(CH ₂)	Bending
1375	1376.76	0.128	=C-H(CH ₃)	Symmetrical bending
1240	1236.83	-0.256	-C-O	Stretching
1160	1160.18	0.016	-C-O	Stretching
1120	1119.05	-0.085	-C-O	Stretching
1110	1096.27	-1.252	-C-O	Stretching
966			-HC=CH- (trans-)	Bending out of plane
721	721.95	0.123	-CH ₂ -	Pivory
690			-HC=CH- (cis)	Bending out of plane
	587.60			

$$\Delta[\%] = (\text{column 2} - \text{column 1}) * 100 / \text{column 2}$$



a. IR spectra



b) Detail of the spectra in a).

Fig. 6.9. Untested (black) rapeseed oil, tested, with ignition on the tube (yellow) and tested without ignition on the tube (blue) at 510 °C

The quality of the tested oil (supplied by Expur Bucharest SA) is also highlighted by the overlapping of the absorbance spectra, for three different samples (Fig. 6.9), one of the three 5 l containers delivered.

Figure 6.10 shows spectrum for the oil picked from the tray, after testing the oil on the hot surface, at 510 °C: a) spectra on hole range of wave number, b) detail for range 1600...550 cm^{-1} .

The peaks identified in Fig. 6.9 are correlated with the constituents of rapeseed oil. The major bands associated with functional groups of triglycerides include the peaks in the column 2, Table 6.1.

To differentiate the spectra, they were represented below each other (Fig. 6.13) or superimposed (Fig. 6.14).

Detailing the range of wave numbers 1650... 550 cm^{-1} highlighted the changes. For the oil that burned on the tube there are no peaks (not very high) between 1600... 1475 cm^{-1} , which means that there are no more of those compounds after combustion. The similar shape of the spectra indicates that the oil remaining after combustion does not differ from the untested oil, except for insignificant changes. It follows that the burning of rapeseed oil led to the formation of volatile compounds or fleshy compounds that remained on the tube or evaporated.

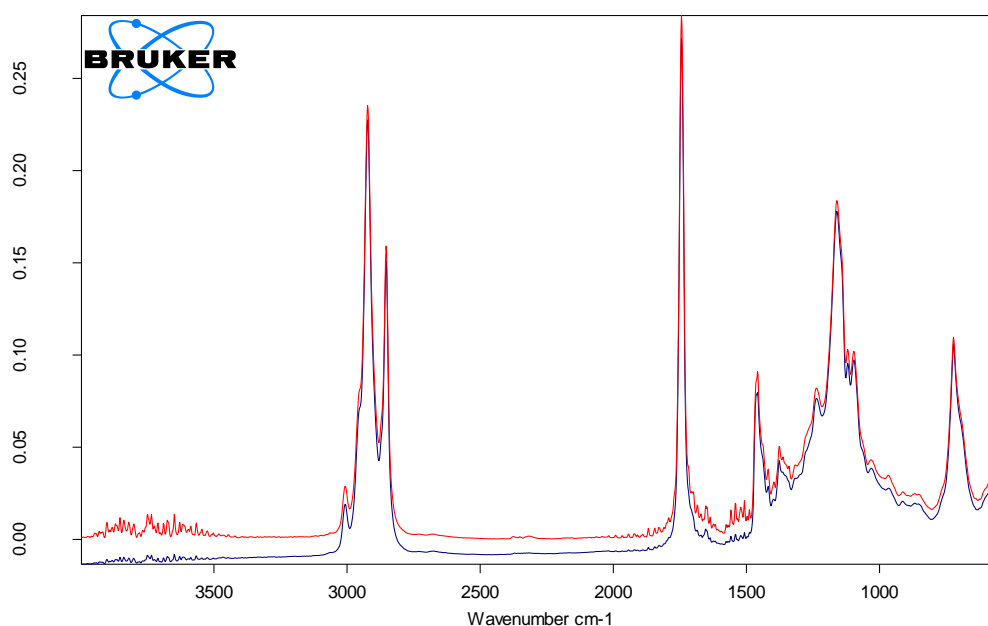


Fig. 6.10. Comparison of the absorbance spectra for rapeseed oil (blue) and rapeseed oil, tested at 520 °C (oil burned on the hot tube) (red)

On the absorbance spectrum of the lubricant based on rapeseed oil, additived with 1% h-BN, in addition to the characteristic spectrum of rapeseed oil, characteristic peaks for h-BN are observed. A comparison between rapeseed oil and the additived lubricant is given in Fig. 6.12.

Sudeep et al. [143] have identified the peaks for h-BN, also called white graphene, with significant peaks in the range of 1500 to 700 cm^{-1} . In the FTIR spectrum of h-BN, it is difficult to find functional peaks because the intense peaks of B-N from 817 cm^{-1} and 1370 cm^{-1} shield other components and, in addition, h-BN has very few impurities and it is a substance with low reactivity in air.

Kostoglou reported [79] a FTIR analysis (with the Thermo Scientific Nicolet 6700 system) for h-BN, for the IR range 4000...400 cm^{-1} , identifying peaks (Fig. 6.11) at 764 cm^{-1} and 1329 cm^{-1} , attributed to vibrations of the B-N bond, with results similar to those in [22].

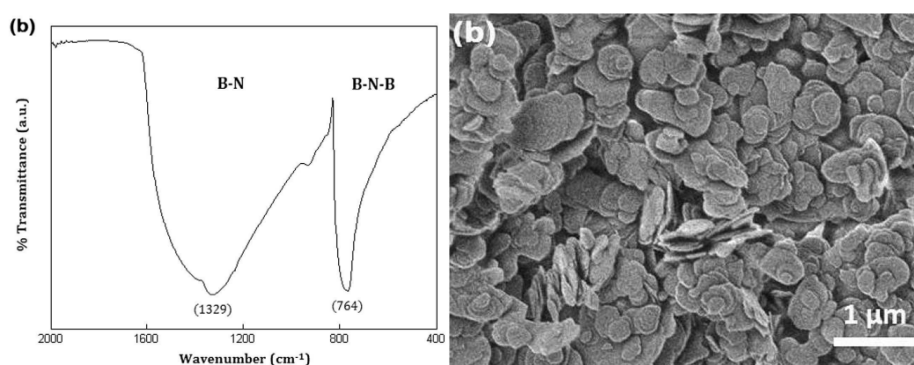
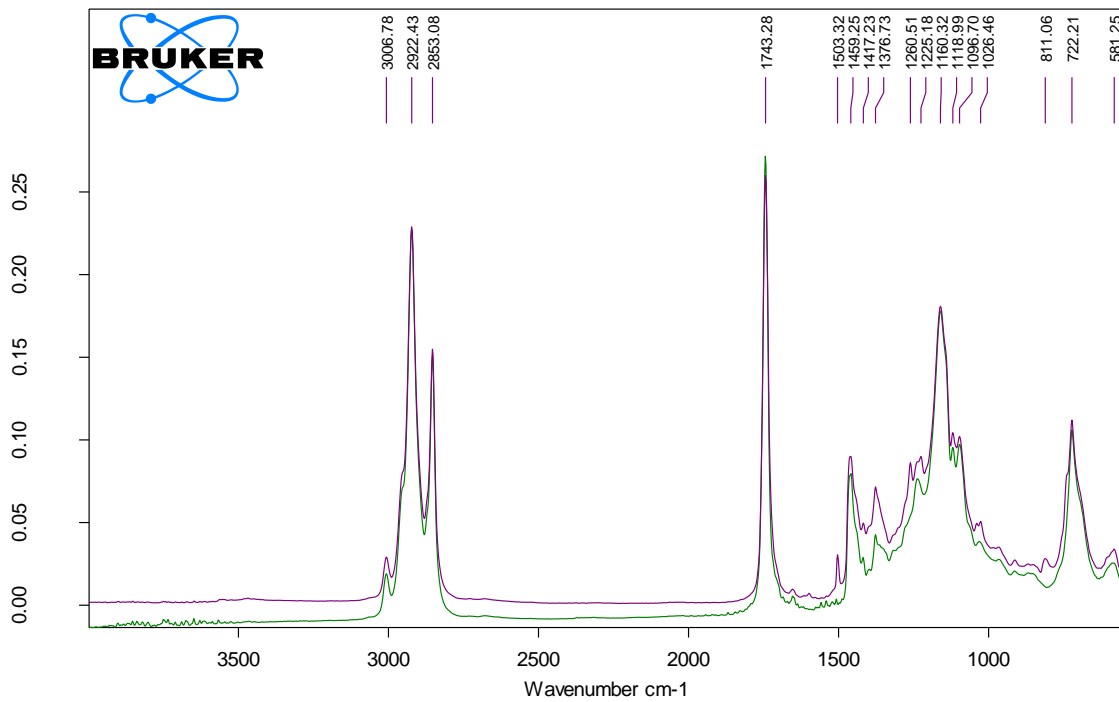
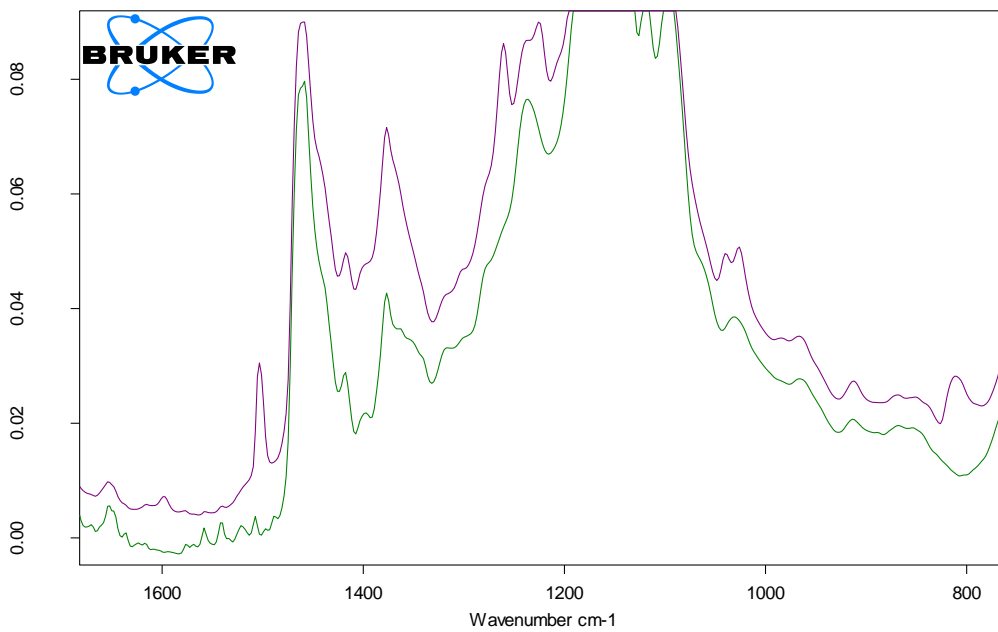


Fig. 6.11. IR spectrum for h-BN and SEM image of h-BN particles [79]

Additional peaks at 1503.32 cm^{-1} , 1376.73 cm^{-1} , 1260 cm^{-1} are observed on the graphs of the absorbance spectra of the additive oil with 1% h-BN (Fig. 6.12).



a) Absorbance spectra for rapeseed oil (green) and rapeseed oil additived with 1% h-BN (magenta)



b) Detail in the range of wave number 1700...750 cm^{-1}

Fig. 6.12. Absorbance spectra for rapeseed oil (green) and rapeseed oil +1% h-BN (magenta) (untested oils)

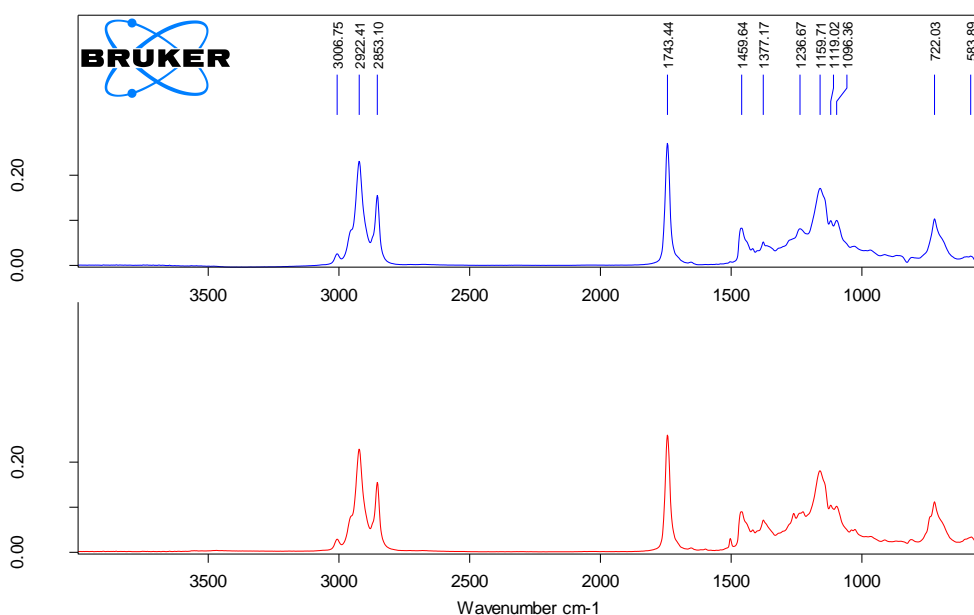


Fig. 6.13. Absorbance spectra for rapeseed oil +1% h-BN: blue - untested lubricant, red - lubricant tested at 475 °C (it does not burn)

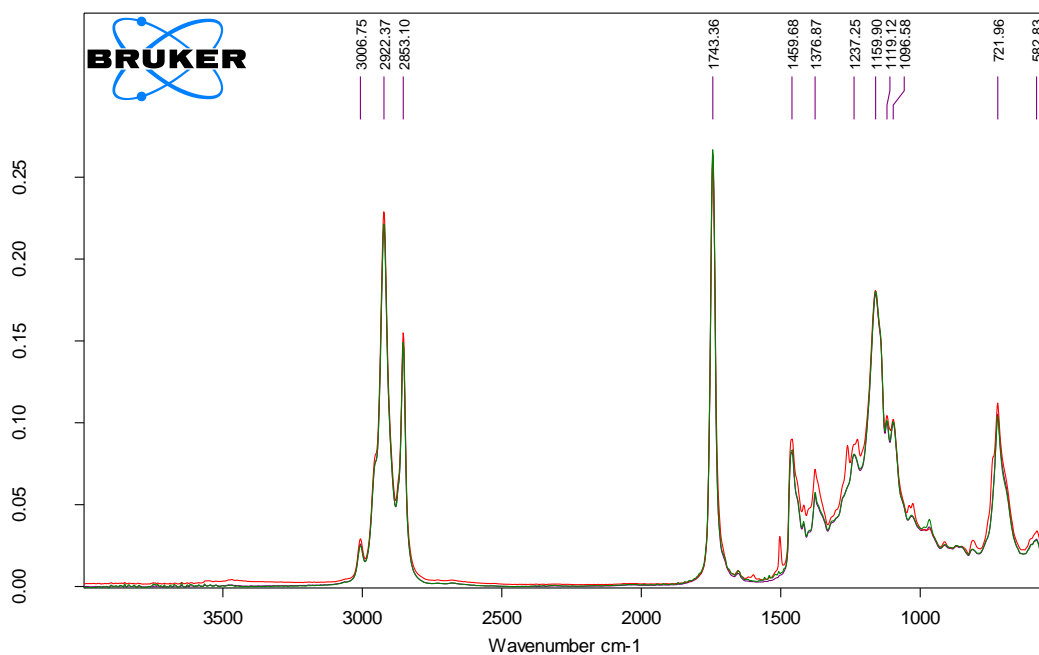


Fig. 6.14. Absorbance spectra for rapeseed oil added with nano h-BN: untested oil (red), oil collected in the enclosure tray, under the tube, tested at 490 °C (the oil burned on the heated tube) (green), oil collected in the enclosure tray, under the tube, tested at 490 °C (the oil did not burn on the heated tube) (magenta)

From Fig. 6.13, it is noted that the spectra of the tested oils (the oil collected in the tray), whether they burn or do not burn, at the same temperature, have no changes, which implies the preservation of the composition of the oil remaining unburned, including the presence of the nano additive. Of course, it is not possible to say what is the remaining concentration of h-BN in the oil leaked into the tray.

FTIR oil samples were analyzed from the tray (leaked from the hot tube) at 490°C (the oil burns in two tests and does not burn in another test) and at 475 °C (in no test out of three, the additivated oil did not ignite), and the spectra revealed the same peaks, which imply that the combustion products were

also volatile products and solid products that were deposited on the tube, the oil leaked from the tube having no significant change in functional groups. From Fig. 6.14, one may see the elimination of C=C groups, of the peak of 1459.68 cm⁻¹. Except this, the spectograms are resembling.

Rapeseed oil has a particular spectrum through the highlighted peaks and this information can be useful for pointing out impurities and additives. The oils collected from the tray after testing had very little modified spectra, which implies that the oil leaked into the tray did not undergo substantial changes, but the amount collected is very small and, so, part of the oil has been subjected to chemical reactions due to the temperature of the tube, resulting in volatile oxidation products or fleshy products that remained on the tube.

These results for an important test in the use of vegetal oils showed that FTIR analysis is good to be applied for identifying differences in composition between the oil that is not put on fire.

6.5. Conclusions on the Flammability of Rapeseed Oil and Lubricant with Rapeseed Oil and 1% h-BN on Hot Surface

The conclusion of this study on two oils, rapeseed oil and rapeseed oil additived with 1% wt nano h-BN, is that vegetal oils have a good resistance to ignition on hot surfaces, since the minimum temperature at which they do not ignite on a hot surface is higher than that of mineral oils (Table 6.2).

Table 6.2. Results of the tests for the determination of the flammability temperature on hot surfaces

Type of oil	Rapeseed oil		Rapeseed oil +1% h-BN		Olive oil		Corn oil		Soybean oil		Hydraulic mineral oil		Hemp oil		Castor oil	
	Guglea, 2022															
					[139]								[138]		[137]	
Temperature, [°C] (±5°C)	495	500	475	480	485	490	510	515	500	510	420	425	500	505	490	495
Qualifier	N	I(T)	N	I(T)	N	I(T)	N	I(T)	N	I(D)	N	I(D)	N	I(T)	N	I(D)
Ignition delay time [s]	3		9		2		5		3		2					

It is noted that, additive or not, vegetal oils have the minimum hot surface ignition temperature between 480 °C and 515 °C, which would result that it is not the concentrations of the constituents that matter, but their presence in the oil in question, even in low concentrations, a conclusion also highlighted in [105]. The short-chain components will ignite first, but they will generate enough energy to further ignite the components with higher molecular weight.

The conditions for the effective use of the results of the fluid resistance tests are the knowledge of the possible tests that can be done, the selection of the appropriate ones for improving the operating safety. Thus, the list of possible fluids to be selected and the list of tests that they "pass", must be known and established at the very design stage of the equipment in order to obtain the solution that reduces the risk of fire. It is important to analyze similar accidents, related to actual applications in the same field of activity (and not only) in order to obtain possible improvements in equipment, technological process, environmental protection and operators' certification.

Rapeseed oil does not burn under the test conditions of SR EN ISO 20823:2004 [186] at 495 °C and the lubricant based on rapeseed oil and 1 % BN-h does not burn at 475 °C. Comparing these values with those obtained for other test fluids on the same test intallation and under the same conditions, these values are higher than the olive oil and hydraulic oil tested in [137].

These results argue once again that experimental results are necessary in assessing the fire risk when using technical fluids and the additivation of a base oil does not guarantee a-priori better flammability characteristics, even if the additive would suggest an improvement.

The small temperature range in which the minimum ignition temperature evolves on hot surfaces for vegetal oils assumes that not the quantity of constituents, but their presence, starts the ignition.

Another pertinent observation is that the temperature range between the tests must not be less than the tolerance for the measured temperatures, for this installation and the range 20 to 700 °C, has been determined as ± 2.5 °C, so the difference between the temperatures determined as the maximum temperature at which the fluid does not ignite on hot surface and the minimum temperature at which the fluid ignites on hot surface cannot be less than 5 °C.

Chapter 7 CONCLUSIONS AND PERSONAL CONTRIBUTIONS

7.1. Final Conclusions

The research in this doctoral thesis was oriented towards the tribological study of non-additivated rapeseed oil and nano additivated with hexagonal Boron nitride and graphene.

The study revealed that the tribological evaluation of a lubricant, especially additivated, should be done according to several variables, including the type of regime (normal, customized for a particular application, or severe), the ranges of the test parameters (load, velocity, duration of the test or other specific conditions, such as load blocks), the lubricant (concentrations of additives, their nature and the base oil, lubricant temperature) and medium (temperature, composition). Comparisons were done between the results obtained on the four-ball machine at $t=ct$ and $L=ct$, the conclusion being that $L=ct$ better reflects the tribological behavior because direct comparisons can be done between measurable parameters, such as wear scar diameter (WSD) and not between calculable parameters, such as wear rate of WSD.

In this work, two working regimes were studied: the severe regime and the normal working regime (applicable in actual systems). For the normal regime, the tests on the four-ball machine were performed for constant duration ($t=ct=1$ h) and for constant sliding distance ($L=ct=1933$ m).

The tribological behavior of rapeseed oil and lubricants formulated by the author, based on rapeseed oil and friction and wear modifying additives (hexagonal Boron nitride and graphene, at nano-sized) was analyzed on the four-ball machine, determining the tribological characteristics:

- friction coefficient (qualitative, as evolution during the test, but also by its average value during a test),
- wear by the wear scar diameter and wear rate of WSD, $w(WSD)$, and
- the temperature in the ball cup during the test and at the end of the test.

For the tested lubricants, these characteristics evolve into narrow ranges for normal regimen, but for severe regime, the lubricant with 1% h-BN performs better. It had WSD lower towards higher loads, as compared to those for rapeseed oil and the OFS parameter – the oil film resistance parameter, introduced by Paleu [107], [110], is more favorable as compared to that of rapeseed oil. The change in the tribological behavior with this type of additive is not significant, at least on the studied range of parameters for velocity, load, additive concentration. But, from the 3D maps of the tribological parameters in the range of the test regime (load, sliding velocity), there is visible the tendency of the two nano additive lubricants (rapeseed oil + 1% h-BN and rapeseed oil + 1% h-BN + 1% graphene) to behave better at regimes with higher values of the pair of variables (load, velocity).

The theoretical minimum thickness of the rapeseed oil film was calculated for the parameters of the working regime, similar to that in the actual tests ($F=100...300$ N, $v=0.23...0.84$ m/s and the temperature of the rapeseed oil in the ball cup 38,9 °C and 60 °C) and the lubrication regime were identified.

By introducing the dynamic viscosity, experimentally obtained for rapeseed oil at different temperatures, at the end of the four-ball tests, and the use of the piezo-viscosity coefficient as reported in the literature, for particular contact pressures specific to performed tests, the theoretical minimum thickness of the film was calculated. For rapeseed oil, the calculated thicknesses of the fluid film are very close and comparable to the Ra roughness values of the initial surfaces of the balls in contact.

Based on the calculations done for the minimum theoretical thickness of rapeseed oil film, suggestively represented in Fig. 7.1 (the color legend has been preserved for both graphs), the following conclusions are drawn:

- for rapeseed oil, h_{min} decreases with increased temperature, but increases with increased velocity and force in contact,
- at the same working regime, the temperature increase causes the reduction of h_{min} .

The following values of h_{min} are coded as follows in parenthesis: (sliding velocity, in m/s; force on tribotester, in N; temperature of rapeseed oil, in °C). There are given the ratios between the values h_{min} at the same temperature, for the lightest working regime ($v=0.23$ m/s and $F=100$ N) and the most severe normal regime ($v=0.84$ m/s and $F=300$ N), regimes that were also applied to the tests on the four-ball machine.

$$\frac{h_{\min(0.84;300;37.8)}}{h_{\min(0.23;100;37.8)}} = \frac{3.28 \times 10^{-8}}{1.54 \times 10^{-8}} = 2.12$$

$$\frac{h_{\min(0.84;300;48.9)}}{h_{\min(0.23;100;48.9)}} = \frac{2.43 \times 10^{-8}}{1.14 \times 10^{-8}} = 2.13$$

$$\frac{h_{\min(0.84;300;60)}}{h_{\min(0.23;100;60)}} = \frac{1.86 \times 10^{-8}}{0.876 \times 10^{-8}} = 2.12$$

It is noticed that, regardless of temperature, this ratio is 2.12...2.13 in favor of the regime with higher load and velocity. Thus, a regime with higher speed and load is favorable for the formation of a film with rapeseed oil, at least for the studied ranges of velocities and forces.

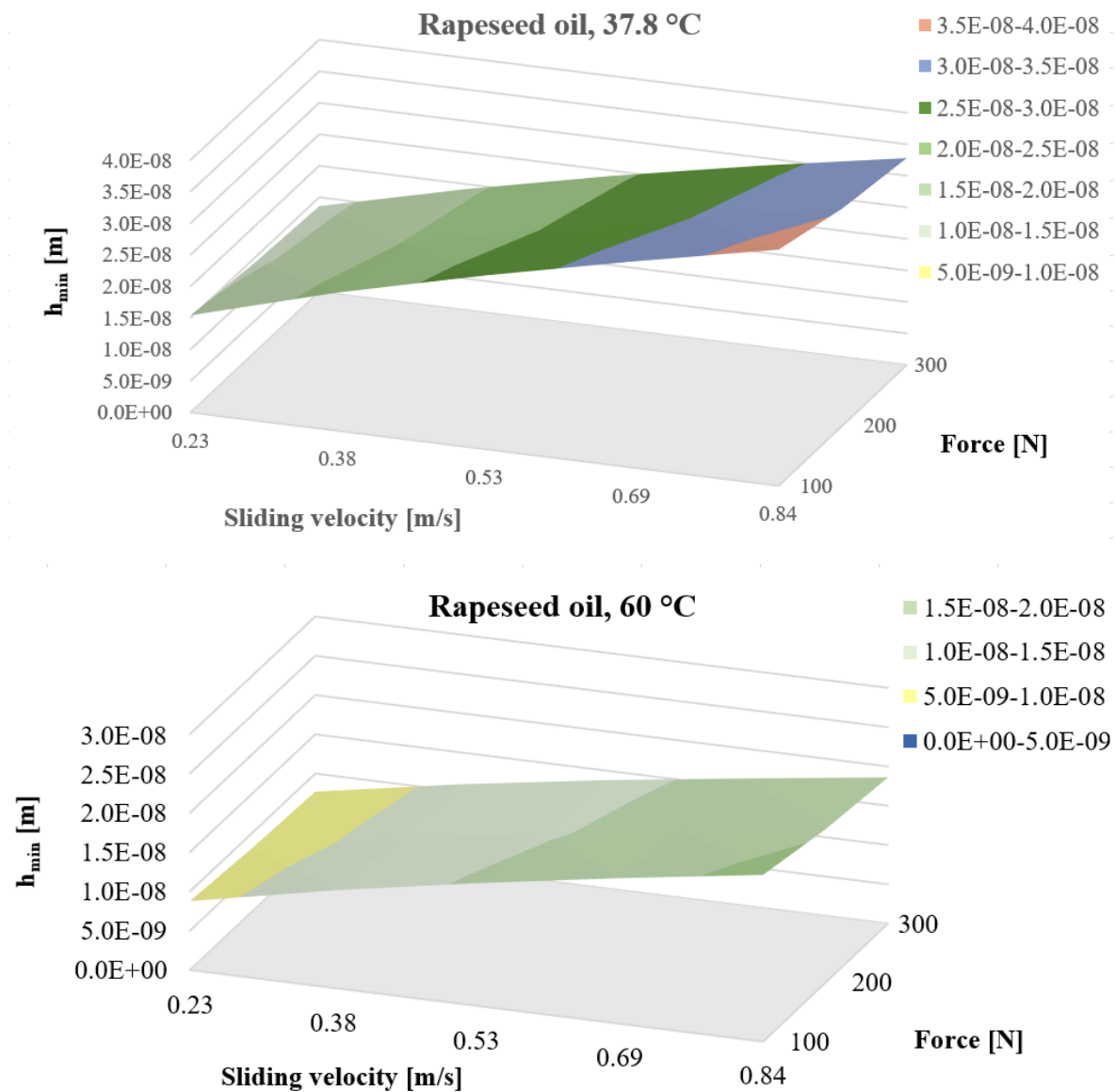


Fig. 7.1. Maps of the calculated minimum thickness of the rapeseed oil film, depending on the working regime of the contact (force, velocity)

If the same ratio is calculated for the same working regime, but at different temperatures, it is observed that lower temperatures favor the generation of the film of rapeseed oil.

$$\frac{h_{\min (0.84;300;37.8)}}{h_{\min (0.84;300;60)}} = \frac{3.28 \times 10^{-8}}{1.86 \times 10^{-8}} = 1.76$$

$$\frac{h_{\min (0.23;100;37.8)}}{h_{\min (0.23;100;60)}} = \frac{1.54 \times 10^{-8}}{0.876 \times 10^{-8}} = 1.75$$

From running of the theoretical model, described above, for the considered intervals of force, sliding velocity and temperature, the following is found. Rapeseed oil can form film under certain working conditions; it is recommended that the metal surfaces in contact to be as finely processed as possible, not to have roughness peaks that interrupt the lubricant film. A theoretical value of the parameter λ was calculated as the ratio between h_{\min} and an equivalent roughness parameter for the contact surfaces and it resulted that the working regime of the tribosystem would be at least mixed or boundary, but from the values of friction coefficient, obtained experimentally, for some sets (v , F) of tests, this parameter falls to 0.05 to 0.08, values specific to the fluid film regime (EHD). This is argued by the fact that elastic deformations and wear change the contact configuration (especially the equivalent radius of curvature increases), which favors the generation of the film.

The influence of the temperature of the lubricant is considerable. The increase in the temperature of the lubricant in contact causes the viscosity of the fluid to decrease, this process of reducing the viscosity of the oil, participating in decreasing the theoretical minimum thickness of the fluid film.

At the same temperature and at the same force in contact, the influence of the sliding velocity is manifested by increasing the minimum thickness with increasing velocity.

When increasing the force in contact, for the same temperature and the same velocity, the minimum thickness decreases, but the influence of the load is less than the influence of the sliding velocity.

Chapter 4 presents the laboratory-scale technology for obtaining additivated lubricants, the test equipment (the four-ball machine and the resistant moment monitoring system), the test campaign developed to highlight the influence of additive concentration, velocity and force applied to the tribotester, with constant duration tests, and with constant sliding distance tests ($L=ct$) for three lubricants (rapeseed oil, rapeseed oil +1% h-BN and rapeseed oil +1% h-BN +1% graphene). The operations included in the technology (mechanical mixing of the additive with a dispersant (guaiacol), mechanical mixing of this initial additive mixture with rapeseed oil and sonication steps and cooling breaks) allowed for achieving a good dispersion of additive(s), but in small quantities, of 200 ml.

Chapter 5 presents the tribological behavior of rapeseed oil and lubricants formulated by the author. Following the first tests carried out with a duration of 1 h, for rapeseed oil and rapeseed oil additivated with h-BN (in concentrations of 0.25%, 0.5% and 1%), it was found that the lubricant with 1% h-BN has the best tribological behavior, analyzing in the first row the wear parameters, then the coefficient of friction and the lubricant temperature, the author considering that these parameters reflect the durability and reliability of the contact. In the next set of tests, $L=ct$ was adopted because with this feature, one can compare the tribological parameters at any force and velocity, which for $t=ct$ was not possible, the comparisons being made only for the same sliding velocity, because at $t=ct$ and different velocities result in different sliding distances and therefore, WSD was no longer a parameter to analyze. These tests with $L=ct$ were performed for three lubricants (rapeseed oil, for comparison, rapeseed oil + 1% h-BN and rapeseed oil + 1% h-BN + 1% graphene). Although tests were performed for three forces applied to the axis of the four-ball ambush, for space reasons only two values are discussed here, the results for the entire test interval being given in Chapter 5. Figure 7.2 shows COF dependence on load, velocity and the nature of the additive. Additivated lubricants have the values more scattered around the trend suggested by the results, given that their distribution in contact may not have a high degree of uniformity. It is noticed, however, that at higher forces (here $F=300$ N), COF of the lubricant rapeseed oil + 1% h-BN + 1% graphene has lower values and the variation with the velocity is in a smaller range, which recommends for applications with variable velocities.

In terms of wear, characterized by the wear scar diameter, WSD, it is noticed that rapeseed oil +1% h-BN + 1% graphene has this parameter almost insensitive to velocity, but increases by almost 40... 50%, if the force increases from $F=100$ N to $F=300$ N (Fig. 7. 3).

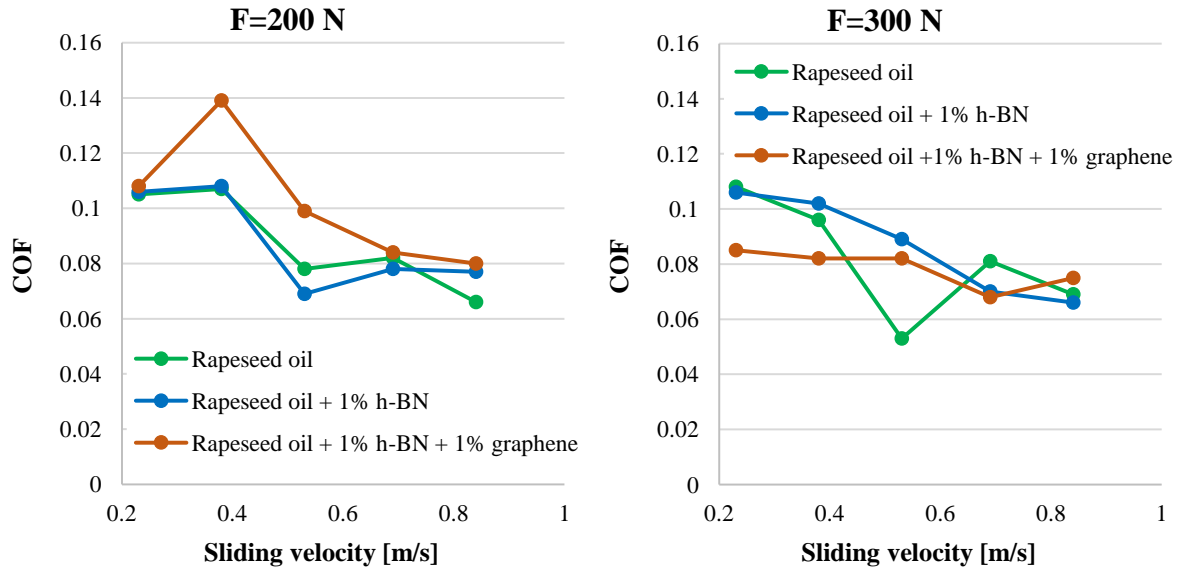


Fig. 7.2. Values and trends of values for the average friction coefficient (COF), for three formulated lubricants (L=ct tests)

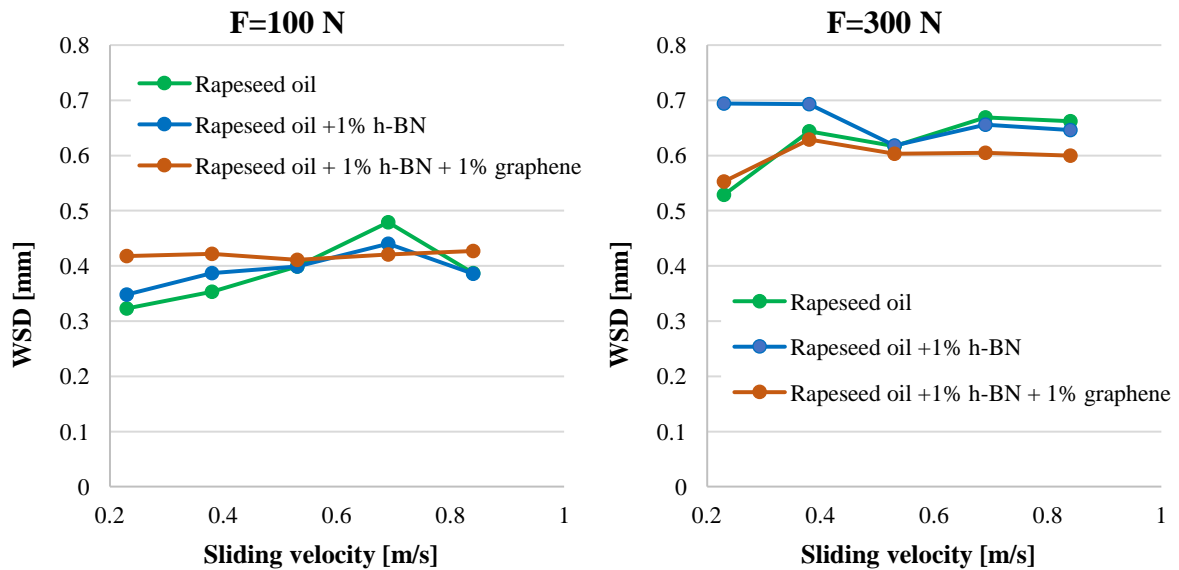


Fig. 7.3. Values and trends of the scar wear diameter (WSD), for three formulated lubricants (L=ct tests)

The wear rate of WSD (Fig. 7.4) indicates the followings:

- at low velocities and low loads, the wear rate of the nano-additivated lubricants is higher than that of non-additivated rapeseed oil, but, for the first, this parameter does not depend so much on the increase in velocity,
- at high loads (here is given the graph w(WSD) only for F=300 N), the value of w(WSD) varies around 1.2×10^{-6} mm/(N·m), the lowest values being obtained for the additivated lubricant with the package 1% h-BN +1% graphene.

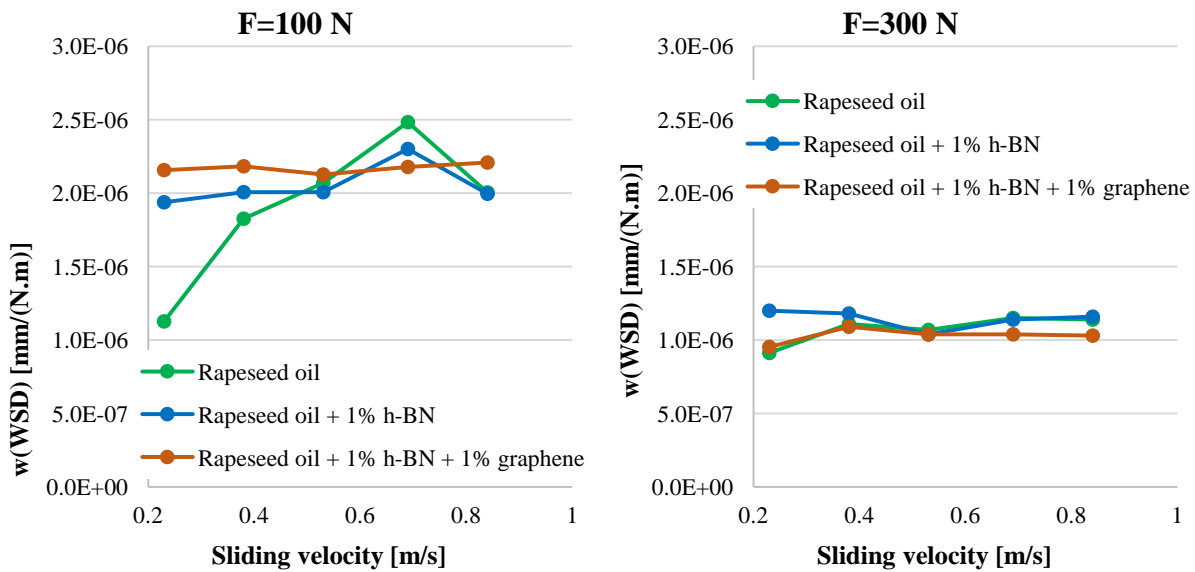


Fig. 7.4. Values and trends of the wear rate of WSD, $w(WSD)$, for three formulated lubricants (tests carried out with $L=ct$)

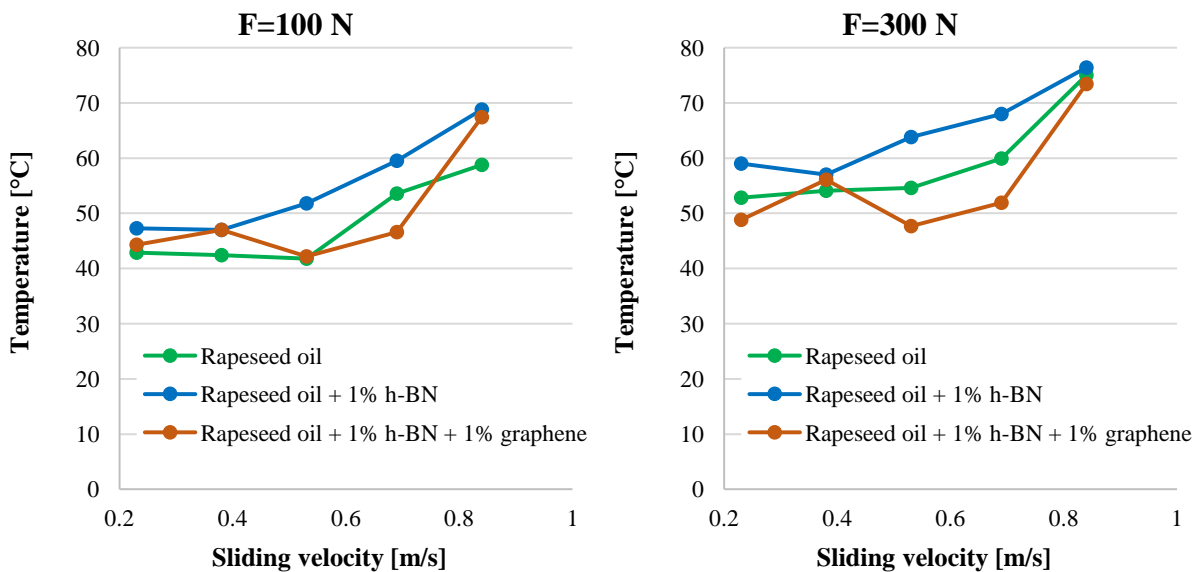


Fig. 7.5. Temperature values and trends recorded at the end of the test for three studied lubricants (tests with $L=ct$)

It is interesting to note that on the domain of working regime, tested with $L=ct$ ($v=0.23... 0.84$ m/s and $F=100...300$ N), the trends of evolution of the analyzed parameters do not change:

- COF decreases with the increase in velocity and load, the generation of a regime with fully lubricant film being recognized by small values; for additivated lubricants, the tendency is weaker at load $F= 300$ N,
- WSD and $w(WSD)$ increase slightly with the load and velocity for rapeseed oil, but for the additivated lubricants, WSD increases visibly only when switching from the mild regime (0.23 m/s, 100 N) to (0.38 m/s, 100 N); the similarity of the curves for the two wear parameters is due to the fact that the tests were done for $L=ct$; this is a "business card" for a lubricant to be inserted into a system that operates with variable regime (e.g. wood cutting and processing machines, textile and paper machines, bearings of the stern tube of small vessels, with regulations for protecting the environment),

- for F=100 N, the temperature curve at the end of the test as a function of velocity is lower for rapeseed oil, the highest being that of the lubricant by 1% h-BN, but at F=300 N the rapeseed oil is situated between the two nano aditivated lubricants, the lower values obtained with the package additive lubricant (1% h-BN +1% graphene) due to the better thermal conductivity properties of graphene (Fig. 5).

Chapter 6 deals with a very rarely analyzed aspect, the flamability of lubricants on hot surfaces, at the same time with the tribological behavior, although the assessment of the fire risk of technical fluids is increasingly required in quality management system, as included in the latest version of the standard, SR EN ISO 9001:2015 Quality management systems. Requirements. The author tested two lubricants, rapeseed oil and rapeseed oil + 1% h-BN, reporting results on the minimum temperature at which the liquid ignites and the maximum temperature for which the fluid does not ignite on hot surface.

Table 7.1. Results of flammability tests on warm surfaces

Type of oil	Rapeseed oil		Rapeseed oil+ 1% BN-h	
	Guglea, 2022			
Temperature, [°C] ($\pm 2.5^\circ\text{C}$)	495	500	475	480
Mark	N	I(T)	N	I(T)
Ignition delay time [s]	3		9	

N – does not burn

I(T) – the fluid ignites or burns on the tube, but does not continue to burn when it is collected in the tray underneath;

The conclusion is that vegetal oils have a good resistance to ignition on hot surfaces, since the minimum temperature at which they do not ignite on a hot surface is higher than that of mineral oils. Additivated or not, vegetal oils have the minimum ignition temperature on hot surface between 480 °C and 515 °C, which would result that it is not the concentrations of the constituents that matter, but their presence in the oil. Short-chain components will ignite first, but will generate enough heat to further ignite the higher molecular weight components.

Based on the results of these ignition tests (but other fire tests may be added), lubricants suitable for reducing the risk of ignition can be selected in order to improve operating safety.

Rapeseed oil does not burn under the test conditions of SR EN ISO 20823:2004 at 495 °C and the lubricant with rapeseed oil and 1 % h-BN does not burn at 475 °C. Comparing these values with those obtained for other test fluids on the same installation and under the same conditions, these values are higher than those for olive oil and a hydraulic oil (which burns at 425 °C, typical of this family of mineral oils).

The author analyzed FTIR spectrograms for lubricant samples taken from the tray (leaked from the hot tube at the end of the test), both for temperatures at which the fluids burned and for temperatures at which ignition was not triggered.

Rapeseed oil has a particular spectrum through the highlighted peaks and this information can be useful for pointing out impurities and additives. The lubricants collected from the tray, after testing, had very little modified spectra, which implies that the oil leaked into the tray did not undergo any substantial modifications, but the amount collected is very small and so, part of the oil was subjected to chemical reactions due to the temperature of the tube, resulting in volatile oxidation products or ashy products that remained on the tube.

These results for such an important test in using vegetal oils showed that FTIR analysis is usable in identifying differences in composition between the oil that is not put on fire.

7.2. Personal contributions

The author of this thesis the followings:

- an analytical study of recent documentation on non-additivated and additivated vegetal oils for lubrication applications, in particular rapeseed oil,

- identification of lubrication regimes and determination from calculation of the theoretical minimum thickness of the lubricant film for rapeseed oil, in order to establish possible test regimes,
- a laboratory-scale technology of lubricants to ensure the dispersion of nano additives by mechanical mixing and sonication; the proposed technology is currently applicable to small amounts of formulated lubricants (200 ml...1 l), because the applied sonication regime heats the lubricant and must be kept below the degradation temperature of the base oil, the rapeseed oil. The used dispersant was effective in obtaining a uniform dispersion until the test was carried out, but the dispersion quality after storage is not known for a long time, characteristic of industrial scale applications;
- the formulation of three new lubricant recipes (rapeseed oil + 1% h-BN), (rapeseed oil + 1% graphene) and (rapeseed oil + 1% h-BN + 1% graphene). The first variant resulted from tests carried out on a concentration range of hexagonal Boron nitride, with tests of $t=ct$, h-BN concentrations of 0.25%, 5% and 1%. The behavior of the lubricant with 1% h-BN being better (by analysing the tribological parameters, but especially by focusing on wear parameters), the study was continued only for this concentration. Taking into account the results obtained by the team of the Research Center "Mechanics and Tribology of the Superficial Layer", by additivating rapeseed oil with graphene, the author elaborated two more lubricants, rapeseed oil +1% graphene and a lubricant with a package of anti-wear and anti-friction additives (1% h-BN +1% graphene) and compared their tribological behaviors using results obtained from tests with the same sliding distance ($L=1933 m=ct$).
- the design of a methodology for evaluating the tribological behavior of lubricants by a set of tests on the four-ball machine: it is worth mentioning how to approach the discussion on tribological parameters: tests with constant duration and tests with constant sliding distance; in the literature, most of the studies on the four-ball machine are performed at the sliding velocity $v=0.53$ m/s, corresponding to a rotational speed of the main shaft of 1400...1450 rpm, recommended in ISO and ASTM standards; the author selected five sliding velocities and performed tests with $L=ct$, for a wider range of sliding velocities (0.23...0.84 m/s), and three forces, which allowed for evaluating the tribological behavior, for operating parameters more commonly met in practice. Even recent research studies choose a single velocity and a few forces, which does not reflect the actual working regime of a lubricated system. The tests were carried out for a constant duration of 1 h (in the literature the normal regime was reported with test durations of 10 minutes, half hour, one hour and even a few hours) and another set of tests was performed for constant sliding distance, $L=1933$ m, distance corresponding to the test of 1 h at the velocity of 0.53 m/s, value commonly used in other studies;
- a complex tribological study on formulated lubricants by:
 - the test campaign (with four variables: nature of the additive, its concentration for nano hexagonal Boron nitride, velocity and load), ensuring, by performing tests twice at the same parameters, a good repeatability and an increased confidence in the obtained results,
 - determination of tribological parameters (friction coefficient as the average value over the duration of a test, the wear scar diameter, WSD, and the wear rate of the wear scar diameter, $w(WSD)$ and temperature at the end of a test),
 - processing and interpretation of experimental data in order to establish the influence of variable parameters (in this study, force, sliding velocity, concentration and nature of nano additive),
 - drawing 3D maps of tribological parameters and using them for evaluating tribological behavior and recommendations on applications in which these lubricants behave well; these 3D maps drawn as a function of the test regime, represented by pairs of values (load, velocity), help to understand and adjust the tendency of a parameter to evolve with the combined variation of two parameters and offer the possibility of identifying working domains with favorable tribological parameters,
 - a study on the flammability of rapeseed oil and rapeseed oil with 1 % h-BN on the hot surface, taking into account the risk of ignition in systems using lubricants and a FTIR analysis of the oil collected after the test (whether it burns or it does not burn) and the determination of the maximum

temperature at which the lubricant does not ignite under the conditions of the dropping test on hot surface and the minimum temperature at which the fluid ignites on the hot surface. These studies that bring together different characteristics of a lubricant are rare, but very useful. For example, in the case of rapeseed oil, it is used for heat treatments on metal parts also and because it hardly ignites. The scenario that the flammability test imitates on hot surface is possible to encounter in practice and the results are useful in the design of fire protection systems,

- interpretation and dissemination of results through scientific articles, published and/or held at international conferences. With preliminary results, the author published three WOS indexed papers and BDI-indexed papers, for several being the first author. He has held papers at international conferences, presented in English (the 16th International Conference on Tribology, Kragujevac, Serbia, the 10th International Conference on Advanced Concepts in Mechanical Engineering – ACME 2022, "Gheorghe Asachi" Technical University of Iasi, Romania, June 09–10, 2022 ACME, the International Conference on Tribology (ROTRIB'19), 19-21 September 2019, Cluj-Napoca),
- during his doctoral studies, the author has developed skills necessary for elaborating a research study, he has learned to use software for the management of experimental data: MathLab, Excel, CurveExpert, (the dedicated software of the four-ball machine), the software serving the optical microscope),
- calibration of the device for real-time measurement and monitoring of the friction moment on the four-ball machine.

7.3. Directions of Future Research

Based on the results obtained, the research can be continued in the following directions:

- extension of the test areas for load and sliding velocity,
- seizure study of the influence of nano additives, because on the wear and friction coefficient maps there is a tendency to reduce the influence of the load for nano additivated lubricants and at high loads, it is likely that the nano additive will move to the right and reduce the slope of the curve load - WSD,
- the use of other methods of investigation to explain the particular rheological and tribological behavior of these lubricants (3D profilometry of wear scars),
- complex additivation of rapeseed oil (by formulating a package of additives including viscosity modifiers and oxidation inhibitors).

List of scientific papers
elaborated by eng. Dionis GUGLEA

WOS and Scopus indexed scientific papers

1. **Guglea, D.**, Georgescu, C., Deleanu, L., Calculating the film thickness for the rapeseed oil in order to evaluate functioning regime, The 10th International Conference on Advanced Concepts in Mechanical Engineering – ACME 2022, “Gheorghe Asachi” Technical University of Iasi, Romania, June 09–10, 2022, Iasi, Romania
2. Ionescu, T. F., Cristea, G. C., **Guglea, D.**, Dima, D., Georgescu, C., Deleanu, L., Wear-load curves in severe regime for rapeseed oil additivated with ZnO, University Politehnica of Bucharest Scientific Bulletin Series B. Chemistry And Materials Science, 83, Issue 4, pp. 151-162, 2021, WOS:000731356100014
3. Ionescu, T. F., **Guglea, D.**, Deleanu, L., Alexandru, P., Georgescu, C., Tribological behavior of coarse rapeseed oil additivated with nanoparticles of Zinc oxide, 17-19 May, 2019, prezentată la 16th International Conference on Tribology, Kragujevac, Serbia, publicată în Proceedings on Engineering Sciences, Volume 1 Number 1, 2019, Publisher: Faculty of Engineering, University of Kragujevac, DOI: 10.24874/PES01.01.002, <http://pesjournal.net/journal/v1-n1/2.pdf>
4. Ionescu, T. F., **Guglea, D.**, Georgescu C., Dima, D., Deleanu, L., Influence of ZnO concentration in rapeseed oil on tribological behavior, International Conference on Tribology, ROTRIB'19, 19-21 septembrie 2019, Cluj-Napoca, IOP Conference Series: Materials Science and Engineering, 724 (2020) 012045, IOP Publishing, doi: 10.1088/1757-899X/724/1/012045, <https://iopscience.iop.org/article/10.1088/1757-899X/724/1/012045/pdf>, WOS:000619349400045
5. **Guglea, D.**, Ionescu, T. F., Dima, D., Georgescu, C., Deleanu, L., Tribological behavior of rapeseed oil additivated with boron nitride, International Conference on Tribology, ROTRIB'19, 19-21 septembrie 2019, Cluj-Napoca, Romania, Book Series IOP Conference Series-Materials Science and Engineering, Vol. 724, Article Number 012046, DOI 10.1088/1757-899X/724/1/012046 Conferința Internațională Rotrib 2019, WOS:000619349400046,
6. Deleanu, L., Georgescu, C., Ionescu, T., **Guglea, D.** Isăcescu, D., SR EN ISO 20623 - A standard for tribological evaluation of lubricants that may bust innovation, Universitatea Tehnică “Gheorghe Asachi”, Iași, Facultatea de Inginerie Mecanică, ACME 2020, 4-5 iunie 2020, Iași, România, IOP Conf. Series: Materials Science and Engineering 997 (2020) 012008, DOI: 10.1088/1757-899X/997/1/012008
7. Ionescu, T., **Guglea, D.**, Dima, D., Georgescu, C., Deleanu, L., Rapeseed oil with anti-wear additives on the four ball tester, Universitatea Tehnică “Gheorghe Asachi”, Iași, Facultatea de Inginerie Mecanică, ACME 2020, 4-5 iunie 2020, Iași, România, IOP Conf. Series: Materials Science and Engineering 997 (2020) 012013, IOP Publishing, doi: 10.1088/1757-899X/997/1/012013
8. **Guglea, D.**, Ionescu, T. F., Georgescu, C., Dima, D., Ojoc, G. G., Deleanu, L., Boron nitride as additive in rapeseed oil, tested on four ball tester, prezentată la 16th International Conference on Tribology, Kragujevac, Serbia, in Proceedings on Engineering Sciences, Volume 1, Number 1, 2019, Publisher: Faculty of Engineering, University of Kragujevac, DOI, 10.24874/PES01.01.076

Published papers in journals and conference proceedings with peer review process (BDI indexed)

9. **Guglea, D.**, Ionescu, T. F., Dima, D., Deleanu, L., Georgescu, C., Nano additivation of rapeseed oil with ZnO and BN, Buletin Științific, no. 5, pp. 281-286, Editura Academiei Forțelor Terestre „Nicolae Bălcescu” Sibiu, 2020, http://cadetanova.ro/documente/Supliment_Inova_20.pdf
10. Ionescu, T. F., Șorcaru, A. A., **Guglea, D.**, Cristea, G. C., Georgescu, C., Deleanu, L., Rapeseed oil additivated with hexagonal boron nitride, INCAS BULLETIN, vol. 12, pp. 63-72, iunie 2020, <https://doi.org/10.13111/2066-8201.2020.12.2>
11. Ionescu, T. F., Șolea, L. C., **Guglea, D.**, Georgescu, C., Deleanu, L., Evaluating seizure on four ball tester for rapeseed oil, Mechanical Testing and Diagnosis, 2019 (IX), Volume 3, pp. 18-23, <https://www.gup.ugal.ro/ugaljournals/index.php/mtd/article/view/2491/2118>
12. Ionescu, T.F., **Guglea, D.**, Deleanu, L., Alexandru, P., Georgescu, C., Tribological behavior of coarse rapeseed tested on four ball tester, 13-14 June, 2019, Scientific Conference of Doctoral Schools, Universitatea “Dunărea de Jos”, Galați, Romania și publicată în Mechanical Testing and Diagnosis, 2021(XI), Vol. 1, pp. 5-10, <https://www.gup.ugal.ro/ugaljournals/index.php/mtd/article/view/4397/3871>

Papers presented at national conferences

13. Ionescu, T. F., **Guglea D.**, Dima, D., Georgescu, C., Deleanu L., Influence of nano particles of ZnO as additive in rapessed oil for evaluationg the tribological behavior, UGAL INVENT, Salonul Cercetării și Inovării organized by “Dunărea de Jos” University din Galați, 16-18 October 2019, <http://www.invent.ugal.ro/ROcatalogue2019.html>
14. **Guglea, D.**, Ionescu, T. F., Dima, D., Georgescu, C., Deleanu, L., Influence of nano particles of hBN as additive in rapeseed oil for evaluating the tribological behavior, „Dunărea de Jos” University of Galați, UGAL INVENT, 16-18 October 2019, Galați, <http://www.invent.ugal.ro/ROcatalogue2019.html>

References¹

1. Abdullah, M. I. H. C., Abdollah, M. F. B., Tamaldin, N., Amiruddin, H., Mat Nuri, N. R., Gachot, C., & Kaleli, H. (2016). Effect of hexagonal boron nitride nanoparticles as an additive on the extreme pressure properties of engine oil. *Industrial Lubrication and Tribology*, 68, 441–445
2. Adhvaryu, A., Erhan, S.Z., & Perez, J.M. (2004). Tribological studies of thermally and chemically modified vegetable oils for use as environmentally friendly lubricants, *Wear*, 257, 359–367
3. Ali, M. K. A., & Xianjun, H. (2015). Improving the tribological behavior of internal combustion engines via the addition of nanoparticles to engine oils. *Nanotechnology Review*, 4, 347–358
4. Ali, M. K. A., Xianjun, H., Mai, L., Qingping, C., Turkson, R. F., & Bicheng, C. (2016). Improving the tribological characteristics of piston ring assembly in automotive engines using Al₂O₃ and TiO₂ nanomaterials as nano-lubricant additives. *Tribology International*, 103, 540–554
5. Allen N., (2009). Hazards of High Flash Point Liquids in Relation to the ATEX 137 Directive, Symposium Series No. 155, Hazards XXI, *Institution of Chemical Engineers*, pp. 271-276
6. Alves, S. M., Barros, B. S., Trajano, M. F., Ribeiro, K. S. B., & Moura, E. (2013). Tribological behavior of vegetable oil-based lubricants with nanoparticles of oxides in boundary lubrication conditions. *Tribology International*, 65, 28–36
7. Ashby, M. F., Brunton, J. H., & Lim, S. C. (1987). Wear-Rate Transitions and Their Relationship to Wear Mechanisms, *Acta Metallurgica*, 35, 1343–1348
8. Ataie, S. A., & Zakeri, A. (2016). Improving tribological properties of (Zn–Ni)/nano Al₂O₃ composite coatings produced by ultrasonic assisted pulse plating. *Journal of Alloys Compounds*, 674, 315–322
9. Bart, J. C. J., Gucciardi E., & Cavallaro S. (2013). *Biolubricants*. Woodhead Publishing Limited, Cambridge UK.
10. Bas, H., & Karabacak, Y.E. (2014). Investigation of the effects of boron additives on the performance of engine oil, *Tribology Transactions*, 57(4), 740-748
11. Berman, D., Erdemir, A., & Sumant, A. V. (2014). Graphene: a new merging lubricant, *Materials Today*, 17(1), 31-42. <https://doi.org/10.1016/j.mattod.2013.12.003>
12. Berman, D., Erdemir, A., & Sumant, A. V. (2018). Approaches for achieving superlubricity in two-dimensional materials. *ACS Nano*, 12, 2122–2137
13. Berman, D., Erdemir, A., Zinovev, A. V., & Sumant, A. V. (2015). Nanoscale friction properties of graphene and graphene oxide. *Diamond & Related Materials*, 54, 91-96
14. Bernard, S., & Miele P. (2014). Nanostructured and architected boronitride from boron, nitrogen and hydrogen-containing molecular and polymeric precursors, *Materials Today*, 17, 450
15. Binu, K. G., Shenoy, B. S., Rao, D. S., & Pai, R. (2014). A variable viscosity approach for the evaluation of load carrying capacity of oil lubricated journal bearing with TiO₂ nanoparticles as lubricant additives. *Procedia Materials Science*, 6, 1051–1067
16. Biresaw, G., & Bantchev, G. B. (2013). Pressure viscosity coefficient of vegetable
17. Bockisch, M. (1998). *Fats and Oils Handbook*. AOCE Press, Champaign, Illinois, SUA
18. Bogatu L., Dragomir R. E. (2016). Influence of additives on antiwear and extreme pressure behaviour of the vegetable oils, *Revista de chimie*, 67(4), 630-633
19. Bondarev, A. V., Kovalskii, A. M., Firestein, K. L., Loginov, P. A., Sidorenko, D. A., Shvindina, N. V., Sukhorukova, I. V., & Shtansky, D. V. (2018). Hollow spherical and nanosheet-base BN nanoparticles as perspective additives to oil lubricants: Correlation between large-scale friction behavior and in situ TEM compression testing. *Ceramic International*, 44(6), 6801–6809
20. Borda, F. L. G., Oliveira, S. J. R., Lazaro, L. M. S. M., & Leiróz, A. J. K. (2018). Experimental investigation of the tribological behavior of lubricants with additive containing copper nanoparticles. *Tribology International*, 117, 52–58
21. Brazhkin, V. V., & Solozhenko, V. L. (2019). Myths about new ultrahard phases: Why materials that are significantly superior to diamond in elastic moduli and hardness are impossible. *Journal of Applied Physics*. 125 (13), 130901. doi:10.1063/1.5082739.
22. Bunk, O. Corso, M., Marto, D., Herger, R., Willmott, P.R., Patterson, B.D., Osterwalder, J., van der Veen, J.F., & T. Greber (2007). Surface X-ray diffraction study of boron-nitride nanomesh in air. *Surface Science*, 601(2), L7–L10. doi:10.1016/j.susc.2006.11.018
23. Cameron, A. (1983). *Basic Lubrication Theory*, 3rd Edition (Ellis Horwood Ltd)
24. Çelik, O.N., Ay, N., and Göncü Y. (2013). Effect of nano hexagonal boron nitride lubricant additives on the friction and wear properties of AISI 4140 steel, *Particulate Science and Technology*, 31(5), 501-506

¹ Bibliographic references are written in APA style (7th edition), Common Reference Examples Guide, <https://apastyle.apa.org/instructional-aids/reference-examples.pdf>

25. Cristea, G. C. (2017). *Tribological characterization of soybean oil additivated with nano materials based on carbon (black carbon, graphite and graphene)*, PhD thesis, "Dunărea de Jos" University of Galați, Romania
26. Cristea, G. C., Cazamir, D., Dima, D., Georgescu, C., Deleanu, L. (2018). Influence of TiO₂ as nano additive in rapeseed oil, ACME 2018, *The 8th International Conference on Advanced Concepts in Mechanical Engineering*, Iasi, Romania <http://www.mec.tuiasi.ro/acme2018/files/Conference%20Program%20Outline.pdf>
27. Cristea, G. C., Dima, C., Georgescu, C., Dima, D., Solea, L., Deleanu, L. (2018). Evaluating lubrication capability of soybean oil with nano carbon additive, 15th International Conference on Tribology, Kragujevac, Serbia. *Tribology in Industry*, 40(1), 66-72, DOI: 10.24874/ti.2018.40.01.05
28. Cristea, G. C., Dima, D., Dima, D., Georgescu, C., Deleanu, L. (2017). Nano graphite as additive in soybean oil, *21st Innovative Manufacturing Engineering & Energy International Conference – IManE&E*, 112, DOI: <https://doi.org/10.1051/mateconf/201711204023>
29. Cristea, G. C., Georgescu, C., Dima, D., Alexandru, P., & Deleanu L. (2016). Tribological evaluation of soybean oil additivated with nano graphene. *Mechanical Testing and Diagnosis*, (VI)4, 5-11, http://www.om.ugal.ro/mtd/download/2016-4/1%20MTD_2016_Volume%204_Cristea%20grafen.pdf
30. Cursaru, D.-L., Andronescu, C. Pirvu C., & Ripeanu R. (2012). The efficiency of Co-based single-wall carbon nanotubes (SWNTs) as an AW/EP additive for mineral base oils. *Wear*, 290, 291133–139
31. Czichos, H., Saito, T., & Smith, L. (2006). *Springer Handbook of Materials Measurement Methods*, Berlin, Springer Science-Business Media
32. Dang, R. K., Goyal, D., Dhami, S. S., & Chauhan, A. (2017). Effect of nanoparticles-based lubricants on static thermal behaviour of journal bearings: A review. *Research Journal of Engineering and Technology*, 8, 149–153
33. Dowson, D., & Higginson, G. R. (1977). *Elasto-hydrodynamic lubrication* (Oxford, Pergamon Press)
34. Du, P., Chen, G., Song, S., Zhu, D., Wu, J., Chen, P., & Chen, H. (2017). Preparation and tribological properties of Cu-doped muscovite composite particles as lubricant additive. *Chemical Research in Chinese Universities*, 33, 430–435
35. Ealias, A. M., & Saravanakumar, M. P. (2017). A review on the classification, characterisation, synthesis of nanoparticles and their application. *IOP Conference Series Materials Science and Engineering*, 263, 032019
36. Engler M., Lesniak C., Damasch R., Ruisinger B., Eichler I. (2007). Hexagonal Boron Nitride (hBN). Applications from Metallurgy to Cosmetics. *Ceramic Forum International*, 84(12), 49-53
37. Essien, N. M., Ofem, O. E., & Bassey, S. C. (2014). Comparative physical characterization, physico-chemical and fatty acid composition of some edible vegetable oils, *Journal of Advances in Biology & Biotechnology*, 1(1), 30-39, JABB.2014.003
38. Eswaraiah, V., Sankaranarayanan, V., & Ramaprabhu, S. (2011). Graphene-Based Engine Oil Nanofluids for Tribological Applications. *ACS Applied Materials Interfaces*, 3(11), 4221–4227. <https://doi.org/10.1021/AM200851Z>
39. Fasina, O. O., & Colley, Z. (2008). Viscosity and specific heat of vegetable oils as a function of temperature: 35°C to 180°C. *International Journal of Food Properties*, 11, 738–746, DOI: 10.1080/10942
40. Fukunaga, O. (2002). Science and Technology in the Recent Development of Boron Nitride Materials. *Journal of Physics: Condensed Matter*. 14(44), 10979. doi:10.1088/0953-8984/14/44/413.
41. Georgescu, C., Cristea G. C., Solea C.L., Deleanu L., & Sandu I.G. (2018). Flammability of Some Vegetal Oils on Hot Surface, *Revista de chimie*, 69(3), 668-673. <http://www.revistadechimie.ro/pdf/29%20GEORGESCU%20C%203%2018.pdf>
42. Georgescu, C., Cristea, C. G., Dima, S., Deleanu, L. (2017). Evaluating lubricating capacity of vegetal oils using Abbott-Firestone curve, *IOP Conference Series Materials Science and Engineering*, 17401205, DOI 10.1088/1757-899X/174/1/012057
43. Georgescu, C., Deleanu, L., & Cristea, C. G., (2018). The tribological behavior of soybean oil, (36 p) in Minobu Kasai (editor) *Soybean - Biomass, Yield and Productivity*, IntechOpen, <https://cdn.intechopen.com/pdfs/64105.pdf>
44. Georgescu, C., Solea, L. C., & Deleanu, L. (2018). Additivation of vegetal oils for improving tribological characteristics, *Xth Product Design, Robotics, Advanced Mechanical & Mechatronic Systems and Innovation Conference, PRASIC'18*, November 8 - 9, 2018 Brasov, Romania
45. Georgescu, C., Solea, L. C., & Deleanu, L. (2019). Additivation of vegetal oils for improving tribological characteristics. *IOP Conference Series Materials Science and Engineering*, 514(1), 012012, DOI: 10.1088/1757-899X/514/1/012012

46. Georgescu, C., Solea, L. C., Cristea, G.C., Deleanu, L. (2015). On the lubrication capability of rapeseed oil, paper 5533, *Recent Advances in Mechanics and Materials in Design, M2D'2015*, 26-30 July 2015, Ponta Delgada, Azores, Portugal
47. Georgescu, C., Solea, L.C., Cristea, G.C., & Deleanu, L. (2015). On the lubrication capability of rapeseed oil, *Recent Advances in Mechanics and Materials in Design, M2D'2015*, 26-30 July 2015, paper 5533, Ponta Delgada, Azores, Portugal
48. Gere R., & Hazelton T. (1993) Rules for choosing a fire-resistant hydraulic fluid. *Hydraulics & pneumatics*, 46, 4 37-42
49. Gnanasekaran, D., & Chavidi, V. P. (2018). *Vegetable Oil based Biolubricants and Transformer Fluids*. Springer, Singapore.
50. Gold, P. W. (2002). *Basics of Tribology (Lectures Notes)*. Institut für Maschinenelemente (IME) der RWTH-Aachen, Germany
51. Goode, M. J., Phillips D. W., & Winkeljohn, R. D. (2000). *Proceedings of the 48th National Conference on Fluid Power*, paper 100-1.12
52. Grasso S., Little Leaks Can Cause Big Problems, *Process Heating*, April 2001.
53. Grosshandler, W. (2001). (editor), *Work on Fire Testing Measurement Needs*, Proceedings, https://tsapps.nist.gov/publication/get_pdf.cfm?pub_id=861084
54. Gu, Y., Zhao, X., Liu, Y., & Lv, Y. (2014). Preparation and tribological properties of dual-coated TiO₂ nanoparticles as water-based lubricant additives. *Journal of Nanomaterials*, Article ID 785680
55. Guglea, D., Ionescu, T. F., Dima, D., Deleanu, L., & Georgescu, C., (2020). Nano additivation of rapeseed oil with ZnO and BN, *Academia Forțelor Terestre „Nicolae Bălcescu” din Sibiu, Buletin științific supliment*, 281-285, Catalogul oficial al salonului „Cadet INOVA”® Nr. 5/2020, Cercetări și inovații în viziunea tinerilor cercetători. http://37.251.175.30/documente/Supliment_Inova_20.pdf
56. Guglea, D., Ionescu, T.F., Georgescu, C., Dima, D., Ojoc, G.G., & Deleanu, L. (2019). Boron nitride as additive in rapeseed oil, tested on four ball tester. *International Conference on Tribology, SerbiaTrib 2019*, Kragujevac, Serbia
57. Gulzar, M., Masjuki, H. H., Varman, M., Kalam, M.A., Mufti, R.A., Zulkifli, N.W.M., Yunus, R., & Zahid, R. (2015). Improving the AW/EP ability of chemically modified palm oil by adding CuO and MoS₂ nanoparticles. *Tribology International*, 88, 271–279
58. Gulzar, M., Masjuki, H., Kalam, M., Varman, M., Zulkifli, N., Mufti, R., Zahid, R., & Yunus R. (2017). Dispersion stability and tribological characteristics of TiO₂/SiO₂
59. Hamrock B. J., , C. V., Han, H. G., & Kong, H. (2010). Tribological evaluation of selected biodegradable oils with long c York, Marcel Dekker Inc)
60. Hamrock, B. J., & Dowson, D. (1978). *Minimum film thickness in elliptical contacts for different regimes of fluid-film lubrication*, NASA Technical paper 1342, <https://ntrs.nasa.gov/archive/nasa/casi.ntrs.nasa.gov/19780025504.pdf>
61. Harper, C. A. (2001). *Handbook of Ceramics, Glasses and Diamonds*. McGraw-Hill.
62. Hatamura, Y. (2005). *Structure and Expression of Failure Knowledge Database*, (Explanation of Failure Mandalas), Failure Knowledge Database Project, Japan Science and Technology Agency, <http://www.sozogaku.com/fkd/en/>
63. Herdan, J.M. (2000). Friction modifiers in engine and gear oils, *Lubrication Science*, 12(3), 265-276
64. Honary, L. A. T., & Richter, E. (2011). *Biobased Lubricants and Greases: Technology and Products*, First Edition (John Wiley & Sons Ltd)
65. Holmberg, K., Andersson, P., Erdemir, A. (2012). Global Impact of Friction on Energy Consumption, Economy and Environment. *Tribology International*, 47, pp. 221–234.
66. Hwang, Y., Lee, C, Choi, Y. et al. (2011). Effect of the size and morphology of particles dispersed in nanooil on friction performance between rotating discs. *J Mech Sci Technol*, 25(11), pp. 2853-7.
67. Ilie, F., & Covaliu, C. (2016). Tribological properties of the lubricant containing titanium dioxide nanoparticles as an additive. *Lubricants*, 4, 12
68. Ionescu, T. F. (2021). *A tribological study of lubricants based on rapeseed oil and nano additives for reducing friction and wear*, PhD thesis, ”Dunărea de Jos” University of Galați, Romania
69. Ionescu, T. F., Cristea, G. C., Guglea, D., Dima, D., Georgescu, C., & Deleanu L. (2020). Wear-Load Curves in Severe Regime for Rapeseed Oil Additivated with ZnO, *8th International Conference on Materials Science and Technologies – RoMat 2020*, November 26-27, 2020, Bucharest, Romania, http://www.mse.pub.ro/images/RoMAT2020/RoMAT-2020_Program-Stiintific.pdf
70. Ionescu, T. F., Guglea, D., Dima, D., Georgescu, C., & Deleanu, L. (2020). Rapeseed oil with anti-wear additives on the four ball tester, *IOP Conference Series: Materials Science and Engineering*, 997 012013, The 9th International Conference on Advanced Concepts in Mechanical Engineering - ACME 2020 4-5 June 2020, Iași, Romania

71. Ionescu, T. F., Şolea, L. C., Guglea, D., Georgescu, C., & Deleanu, L. (2019). Evaluating seizure on four ball tester for rapeseed oil, *Mechanical Testing and Diagnosis*, (IX)3, 18-23
72. Ionescu, T. F., Sorcaru, A.-A., Guglea, D., Cristea, G. C., Georgescu, C., & Deleanu, L. (2020). Rapeseed oil additivated with hexagonal boron nitride. *INCAS Bulletin*, 12(2), 63-72, doi: 10.13111/2066-8201.2020.12.2.6.
73. Irtegov, Y., An, V., Machekhina, K., & Lemachko, N. (2016). Influence of copper nanoparticles on tribological properties of nanolamellar tungsten disulfide. *Key Engineering Materials*, 712, 133–136
74. Jiang, D., Wang, X., Liu, S., & Guo, H. (2011). Rapeseed Oil Monoester of Ethylene Glycol Monomethyl Ether as a New Biodiesel. *Journal of Biomedicine and Biotechnology*, Article ID 293161, doi:10.1155/2011/293161
75. Kim, S., Mansurov C., Yu, N., & Li, S. H. (2017). The method for producing copper nanoparticles and analysis of their lubricating ability. *Solid State Phenomena*, 265, 738–744
76. Kosbe, P., Patil, P., Manickam, M., & Ramamurthy, G. (2020) Effect of hexagonal boron nitride (h-BN) inclusion on thermal characteristics of disc brake friction composites. *Diamond & Related Materials*, 107, 107895
77. Kong, L., Sun, J., Bao, Y., & Meng, Y. (2017). Effect of TiO₂ nanoparticles on wettability and tribological performance of aqueous suspension. *Wear*, 376–377, 786–791
78. Korlipara, P. V. (2017). Chapter 16 Vegetable Oil-Based Lubricant Additives, pp. 315-334, in *Environmentally Friendly and Biobased Lubricants*, Editors: Sharma B. K. and Biresaw G., (Boca Raton, USA, CRC Press, Taylor & Francis Group)
79. Kostoglou, N., Polychronopoulou, K., & Rebholz, C. (2015). Thermal and chemical stability of hexagonal boron nitride (h-BN) nanoplatelets. *Vacuum*, 112, 42–45. <https://doi.org/10.1016/J.VACUUM.2014.11.009>
80. Kumar N., Bhaumik S., Sen A., Shukla A. P., Pathak S. D. (2017). One-pot synthesis and first-principles elasticity analysis of polymorphic MnO₂ nanorods for tribological assessment as friction modifiers. *The Royal Society of Chemistry Advances* 7: 34138–34148.
81. Kumara C., Luo H., Leonard D. N., Meyer H. M., Qu J. (2017). Organic-modified silver nanoparticles as lubricant additives. *ACS Applied Materials & Interfaces* 9: 37227–37237.
82. Laad M., Jatti V. K. S. (2018). Titanium oxide nanoparticles as additives in engine oil. *Journal of King Saud University - Engineering Sciences* 30: 116–122.
83. Laad M., Ponnamma D., Sadasivuni K.K. (2017). Tribological studies of nanomodified mineral based multi-grade engine oil. *International Journal of Applied Engineering Research* 12: 2855–2861.
84. Lee, J., Cho, S., Hwang, Y., Cho, H.-J., Lee, C., Choi, Y., B.-C., Ku, Lee, H., Lee B., Kim D., Kim, S. H. (2009). Application of fullerene-added nano-oil for lubrication enhancement in friction surfaces. *Tribology International*, 42, 440–447
85. Lee, K., Hwang, Y., Cheong, S., Choi, Y., Kwon, L., Lee, J. et al. (2009). Understanding the role of nanoparticles in nano-oil lubrication, *Tribology Letters*, pp. 35-127.
86. Li S., Bhushan B. (2016). Lubrication performance and mechanisms of Mg/Al-, Zn/Al-, and Zn/Mg/Al-layered double hydroxide nanoparticles as lubricant additives. *Applied Surface Science*, 378, 308–319
87. Li, J. J., Gao T. Y., Luo J. B. (2018). Superlubricity of graphite induced by multiple transferred graphene nanoflakes. *Advanced Science* 5(3): 1700616.
88. Li, S., Qin H., Zuo R., Bai Z. (2015). Friction properties of La-doped Mg/Al layered double hydroxide and intercalated product as lubricant additives. *Tribology International*, 91, 60–66.
89. Li, S., Qin H., Zuo R., Bai Z. (2015). Tribological performance of Mg/Al/Ce layered double hydroxides nanoparticles and intercalated products as lubricant additives. *Applied Surface Science* 353: 643–650.
90. Li, Y., Zhang S., Ding Q., Li H., Qin B., Hu L. (2018). Understanding the synergistic lubrication effect of 2-mercaptobenzothiazolate based ionic liquids and Mo nanoparticles as hybrid additives. *Tribology International*, 125, 39–45.
91. Lin, J., Wang, L., & Chen, G. (2011). Modification of graphene platelets and their tribological properties as a lubricant additive. *Tribology Letters*, 41(1), pp. 209-215.
92. Liu, W., & Wang, X. (2008). Nanolubricants Made of Metals, p 175, in *Nanolubricants*, Martin J. M, Ohmae N. (editor), 2008 John Wiley & Sons, Ltd.
93. Liu, Y. M., Song A. S., Xu Z., Zong R. L., Zhang J., Yang W. Y., Wang R., Hu Y. Z., Luo J. B., Ma T. B. (2018). Interlayer friction and superlubricity in single-crystalline contact enabled by twodimensional flake-wrapped atomic force microscope tips. *ACS Nano*, 12(8): 7638–7646.
94. Liu, Y., Mateti S., Li, C., Liu, X., Glushenkov, A. M., Liu, D., Li, L. H., Fabijani, D., & Chen, Y. (2018). Synthesis of composite nanosheets of graphene and Boron nitride and their lubrication application in oil. *Advanced Engineering Materials*, 20(2) 1700488. <https://doi.org/10.1002/adem.201700488>

95. Lu, Y., Du C., Shao Y. and Zhou J., (2014), Characterization of Rapeseed Oil Using FTIR-ATR Spectroscopy. *Journal of Food Science and Engineering* 4, 244-249, doi: 10.17265/2159-5828/2014.05.004
96. Lu, Y., Du C., Shao Y. and Zhou J., Characterization of Rapeseed Oil Using FTIR-ATR Spectroscopy, *Journal of Food Science and Engineering* 4 (2014) 244-249, doi: 10.17265/2159-5828/2014.05.004
97. Manu, B. R., Gupta, A., & Jayatissa, A.H. (2021). Tribological Properties of 2D Materials and Composites—A Review of Recent Advances. *Materials*, 14, 1630. <https://doi.org/10.3390/ma14071630>
98. Meng, Y., Xu, J., Jin, Z., Prakash, B., & Hu, Y. (2020). A review of recent advances in tribology. *Friction*, 8(2), 221–300, <https://doi.org/10.1007/s40544-020-0367-2>
99. Miller, M. (2008). *Additives for bioderived and biodegradable lubricants* *Lubricant Additive Chemistry and Applications*, 2nd edition, Chapter 18, (Rudnick L R, Erhan S. Z., Ed.), CRC Press, Taylor and Francis Group
100. Najan, A. B., Navthar, R. R., & Gitay, M. J. (2017). Experimental Investigation of tribological properties using nanoparticles as modifiers in lubricating oil. *International Research Journal of Engineering and Technology (IRJET)*, 4, 1125–1129
101. Nasser, K. I., Liñeira del Río, J. M., López, E. R., & Fernández, J. (2020). Synergistic effects of hexagonal boron nitride nanoparticles and, phosphonium ionic liquids as hybrid lubricant additives, *Journal of Molecular Liquids*, 311 113343
102. Nasser, K. I., Lineira del Río, J. M., Marino, F., E. R. Lopez, & Fernandez, J. (2021). Double hybrid lubricant additives consisting of a phosphonium ionic liquid and graphene nanoplatelets/hexagonal boron nitride nanoparticles, *Tribology International*, 163, 107189
103. Nazare, M I., Paleu, V., Bhaumik, S., Ianuş, G, & Olaru, D. N. (2018). Performances of automotive lubricants – tests on four ball machine. *IOP Conference Series: Materials Science and Engineering* 444, 022013. doi:10.1088/1757-899X/444/2/022013
104. Nouredini, H., Teoh, B. C., & Clements L. D. (1992). Viscosities of vegetable oils and fatty acids. *Biomaterials* 10. http://digitalcommons.unl.edu/chemeng_biomaterials/10
105. Olaru D. (2002). *Fundamente de lubrificație*, Editura Gheorghe Asachi, Iasi, Romania
106. Paleu V, Bercea I, Cretu Sp, Bercea M 2005 Lubricant Oils Additived With Polymers in EHD Contacts: Part 2. Tests using a Four-Ball Machine *Lubrication Science* 17 - 2 pp 173-184. Doi: 10.1002/ls.3010170205
107. Paleu V. (2002). Cercetări teoretice și experimentale privind dinamica și fiabilitatea rulmenților hibridi (Theoretical and experimental research on the dynamics and reliability of hybrid rolling bearings), PhD thesis, Technical University “Gheorghe Asachi” Iasi, Romania
108. Paleu V. (2020). Tribological analyses of a new optimized gearbox biodegradable lubricant blended with reduced graphene oxide nanoparticles, *Mechanical Engineering, Materials Science Proceedings of the Institution of Mechanical Engineers, Part J: Journal of Engineering Tribology*
109. Paleu, V., Bercea, I., Cretu, S., & Bercea, M. (2005). Lubricant oils additivated with polymers in EHD contacts: Part 2. Tests using a four-ball machine. *Lubrication Science*, 17(2), 173-184
110. Paleu, V. (2009). Steel on silicon nitride hybrid tribological systems lubricated by kerosene. tests on a four-ball machine, *The Annals of University “Dunarea de Jos” of Galati, Fascicle VIII, Tribology*, XV, , ISSUE 2, 2009
111. Pawlak Z., Kaldonski T. J., Macko M., Urbaniak W. (2017). h-BN lamellar lubricant in hydrocarbon and formulated oil in porous sintered bearings (iron + h-BN). *Archives of Civil and Mechanical Engineering*, 17, 687–693
112. Park, J. H., Park, J. C., Yun, S. J., Kim, H., Luong, D. H., Kim, S. M., Choi, S., Yang, H. W., Kong, J., Kim, K. K., & Lee, Y. H. (2014). Large-area Monolayer hexagonal Boron nitride on Pt foil. *ACS Nano*, 8(8), 8520-8528
113. Patil S. J., Patil D. P., Shrotri A. P., Patil V. P. (2014). A review on effect of addition of nano particles on tribological properties of lubricants. *International Journal of Mechanical Engineering and Technology (IJMET)* 5, 120–129.
114. Peña-Parás L., Maldonado-Cortés D., Taha-Tijerina J. (2019). *Handbook of Ecomaterials*. Martínez L, Kharissova O, Kharisov B, eds. Springer, Cham
115. Peña-Parás L., Taha-Tijerina J., Garza L., Maldonado-Cortés D., Michalczewski R., & Lapray C. (2015). Effect of CuO and Al₂O₃ nanoparticle additives on the tribological behavior of fully formulated oils. *Wear*, 332–333, 1256–1261
116. Perez J. M., Rudnick L. R., Erhan S.Z., Sharma B. K. and Kohli K. (2017). Chapter 23 Natural Oils as Lubricants pp 387-399, in *Synthetics, Mineral Oils and Bio-Based Lubricants. Chemistry and Technology*, 3rd Edition, Editor Rudnick L R (Boca Raton, USA, CRC Press)
117. Qiao S.Z., Liu J., Max Lu G. Q. (2017). *Modern Inorganic Synthetic Chemistry*, 2nd edn. Xu R, Xu Y, eds. Elsevier, Amsterdam

118. Quinchia, L. A., Delgado, M. A., Valencia, C., Franco, J. M., & Gallegos, C. (2010). Viscosity modification of different vegetable oils with EVA copolymer for lubricant applications. *Industrial Crops and Products*, 32, 607–612
119. Rahmati, B., Sarhan, A. A., Sayuti, M. (2014). Morphology of surface generated by end milling AL6061-T6 using molybdenum disulfide (MoS₂) nanolubrication in end milling machining. *Journal of Cleaner Production* 66: 685–691
120. Robinson N. (2022). Monitoring Oil Degradation with Infrared Spectroscopy. *Machinery Lubrication*, <https://www.machinerylubrication.com/Read/1109/oil-degradation-spectroscopy>
121. Rudnick, L. R., & Erhan, S. Z. (2006). Natural oils as lubricants in Synthetics, mineral oils, and bio-based lubricants: chemistry and technology (Rudnick L R, Erhan, S Z, Ed.) New York, CRC/Taylor & Francis Group
122. Rudnik L. R. (ed.) (2009). *Lubricant Additives. Chemistry and applications*, Second Edition (CRC Press, Taylor & Francis Group)
123. Rudolph, S. (2000). Boron Nitride (BN). *American Ceramic Society Bulletin*. 79: 50.
124. Rusak, D. A., Brown L. M., & Martin S. D. (2003). Classification of Vegetable Oils by Principal Component Analysis of FTIR Spectra, *Journal of Chemical Education*, 80(5), 541-543
125. Sahin, S., & Sumnu, S. G. (2009). *Advances in deep fat frying of foods* (1st ed.). Boca Raton, USA: Taylor & Francis Group (Chapter 3)
126. Sahu, J., Panda, K., Gupta, B., Kumar, N., Manojkumar, P.A., & Kamruddin, M. (2018). Enhanced tribochemical properties of oxygen functionalized mechanically exfoliated hexagonal boron nitride nanolubricant additives. *Materials Chemistry and Physics*, 207, 412–422. <https://doi.org/10.1016/j.matchemphys.2017.12.050>
127. Salles, V., Bernard, S., Chiriac, R., & Miele, P. (2012). Structural and thermal properties of boron nitride nanoparticles, *Journal of the European Ceramic Society*, Volume 32, Issue 9, July, Pages 1867-1871
128. Santamaria-Ramiro J. M., & Braña-Aísa, P. A. (1998). Risk analysis and reduction in the chemical process industry. New York: *Chapman & Hall*
129. Satyanarayana, K., & Kakati M.C. (1991). Correlation of flash points. *Fire and Materials*, 15, 97-100
130. Schein, L. B. (1988). Electrophotography and Development Physics. *Physics Today. Springer Series in Electrophysics. 14. Berlin: Springer-Verlag.* pp. 66–68. doi:10.1063/1.2811250
131. Scherge, M., Böttcher, R., Kürten, D., & Linsler, D. (2016). Multi-Phase friction and wear reduction by copper nanoparticles. *Lubricants*, 4, 36
132. Shafi, W. K., Raina, A., & Haq M. I. U. (2018). Friction and wear characteristics of vegetable oils using nanoparticles for sustainable lubrication. *Tribology - Materials, Surfaces and Interfaces*, 12(1), 27–43
133. Shafi, W. K., & Charoo, M.S. (2019). Rheological Properties of Sesame Oil Mixed With H-Bn Nanoparticles As Industrial Lubricant, *Materials Today: Proceedings 18 4963–4967, the 9th International Conference of Materials Processing and Characterization, ICMPC-2019*
134. Shahmohamadi, S. H., Rahmani, R., Rahnejat, H., Garner, C. P., & Balodimos, N. (2017). Thermohydrodynamics of lubricant flow with carbon nanoparticles in tribological contacts. *Tribology International*, 113, 50–57.
135. Sharma, B. K., Karmakar, G., & Erhan, S. Z. (2020). Chapter 24 Modified Vegetable Oils for Environmentally Friendly Lubricant Applications, pp 400-430, in Synthetics, Mineral Oils and Bio-Based Lubricants. *Chemistry and Technology*, 3rd edition, editor Rudnick L R (Boca Raton, USA, CRC Press)
136. Snyder, C. E., & Krawetz, A. A. (1981). Determination of the flammability characteristics of aerospace hydraulic fluids, *Lubrication Engineering*, 37, 705-714
137. Şolea L. C., Deleanu L. (2020). Flammability tests on hot surface for castor oil. *Mechanical Testing and Diagnosis*, (X)4, 30-34
138. Şolea, L. C., Deleanu, L. (2021). Flammability tests for hemp seed oil, *Mechanical Testing and Diagnosis*, (XI), Vol. 2, pp. 5-9
139. Şolea, C.L., (2013). *Contribuții la studiul comportării reologice și tribologice a unor lubrifianți biodegradabile pe bază de uleiuri vegetale*. PhD thesis, Universitatea „Dunărea de Jos” din Galați, România
140. Soma, T. et al. (1974). Characterization of Wurtzite Type Boron Nitride Synthesized by Shock Compression. *Materials Research Bulletin*. 9(6), 755. doi:10.1016/0025-5408(74)90110-X.
141. Song, H., Huang, J., Jia, X., & Sheng, W. (2018). Facile synthesis of core-shell Ag@C nanospheres with improved tribological properties for water-based additives. *New Journal of Chemistry*, 42, 8773– 8782
142. Stachowiak, G. W., & Batchelor, A. W. (2005). *Engineering tribology*. Butterworth-Heinemann, Team Lrn

143. Sudeep, P. M., Vinod, S., Ozden, S., Sruthi, R., Kukovecz, A., Konya, Z., Vajtai, R., Anantharaman, M. R., Ajayan, P. M., & Narayanan, T. N. (2015). Functionalized boron nitride porous solids, *RSC Advances*, 5, 93964, DOI: 10.1039/c5ra19091f
144. Sustere, Z., Murnieks, R., & Kampars, V., (2016). Chemical interesterification of rapeseed oil with methyl, ethyl, propyl and isopropyl acetates and fuel properties of obtained mixtures, *Fuel Processing Technology* 149 320–325.
145. Suzuki, T., Ohtaguchi, K., & Koide, K. (1991). A method for estimating Flash points of organic compounds from molecular structures. *Journal of Chemical Engineering of Japan*, 24(2), 258–261.
146. Tao, C., Wang, B., Barber, G. C., Schall, J. D., & Lan, H. (2018). Tribological behaviour of SnO₂ nanoparticles as an oil additive on brass. *Lubrication Science* 30: 247–255
147. Thachnatharen, N., M. Khalid, Arulraj, A., & Sridewi, N. (2022). Tribological performance of hexagonal boron nitride (hBN) as nano-additives in military grade diesel engine oil. *Materials Today: Proceedings*, 50(1), 70-73
148. Thakre, A. A., & Thakur, A. (2015). Study of behaviour of aluminium oxide nanoparticles suspended in SAE20W40 oil under extreme pressure lubrication. *Industrial Lubrication and Tribology*, 67, 328
149. Thampi, A. D., Prasanth, M. A., Anandu, A. P., Sneha, E., Sasidharan, B., & Rani, S. (2021). The effect of nanoparticle additives on the tribological properties of various lubricating oils. Review, *Materials Today: Proceedings*, 47(15), 4919-4924, <https://doi.org/10.1016/j.matpr.2021.03.664>.
150. Thottackkad, M. V., Rajendrakumar, P. K., & Prabhakaran Nair, K. (2014). Experimental studies on the tribological behaviour of engine oil (SAE15W40) with the addition of CuO nanoparticles. *Industrial Lubrication and Tribology*, 66, 289–297
151. Veluri R., Types of Lubricant Additives, 03.02.2022, <https://www.tribonet.org/wiki/lubricant-additives/>
152. Wan Q., Jin Y., Sun P., and Ding Y. (2015) Tribological behavior of a lubricant oil containing boron nitride nanoparticles, *Procedia Engineering* 102, pp. 1038-1045.
153. Wan Q., Jin Y., Sun P., Ding Y. (2014). Rheological and tribological behaviour of lubricating oils containing platelet MoS₂ nanoparticles. *Journal of Nanoparticle Research* 16: 2386.
154. Wang B., Tang W., Liu X., Huang Z. (2017). Synthesis of ionic liquid decorated multi-walled carbon nanotubes as the favorable water-based lubricant additives. *Applied Physics A: Materials Science and Processing* 123: 680.
155. Wu, Y. Y., Tsui, W. C., & Liu, T. C. (2007). Experimental analysis of tribological properties of lubricating oils with nanoparticle additives. *Wear*, 262(7-8), 819–825
156. Xiao H., S. Liu (2017) 2D nanomaterials as lubricant additive: A review, *Materials and Design*, 135, pp. 319–332
157. Xue, M., Wang Z., Yuan F., Zhang X., Wei W., Tang H. & Li C. (2017) Preparation of TiO₂/Ti₃C₂T_x hybrid nanocomposites and their tribological properties as base oil lubricant additives, *RSC Adv.*, 7, 4312–4319, DOI: 10.1039/c6ra27653a
158. Yadav A., Singh Y., Negi P. (2021). A review on the characterization of bio based lubricants from vegetable oils and role of nanoparticles as additives, *Materials Today, Proceedings* 46, pp 10313-10517
159. Yıldırım Ç. V., M.Sarıkaya, T. Kıvık, Ş. Şirin, (2019). The effect of addition of hBN nanoparticles to nanofluid-MQL on tool wear patterns, tool life, roughness and temperature in turning of Ni-based Inconel 625. *Tribology International*, 134, 443-456, <https://doi.org/10.1016/j.triboint.2019.02.027>.
160. Zaimovskaya T. A., Oganeseva E., Yu, Kuzmina G. N., Ezhov A. A., Ivanov V. K., Parenago O. P. (2013). Titanium-containing compounds as efficient triboadditives to oils. *Journal of Friction and Wear*, 34: 487–493.
161. Zareh-Desari B., Davoodi B. (2016). Assessing the lubrication performance of vegetable oil-based nano-lubricants for environmentally conscious metal forming processes. *Journal of Cleaner Production* 135: 1198–1209.
162. Zhang S. W. (2013). Green tribology: Fundamentals and future development. *Friction*, 1, 186–194.
163. Zhang X. M., Yang X.P., & Ouyang P. (2014). Research progress in copper-containing micro and nano particles as lubricating additives. *Xiandai Huagong/Modern Chemical Industry*, 34, 53–56.
164. Zhang Z., Simionesie D., Schaschke C., (2014). Graphite and hybrid nanomaterials as lubricant additives, *Lubricants*, 2 (2) 44–65.
165. Zhang, R., Zhao, J., Pu, J., & Lu, Z. (2018). First-principles investigation on the tribological properties of h-BN bilayer under variable load. *Tribology Letters*, 66 124
166. Zhang, W., Zhou, M., Zhu, H., Tian, Y., Wang, K., Wei, J., Ji, F., Li, X., Li, Z., Zhang, P. (2011). Tribological properties of oleic acid-modified graphene as lubricant oil additives. *Journal of Physics D: Applied Physics*, 44(20), paper 205303.

167. Zhou, C., Li, Z., Liu, S., Zhan, T., Lie, W., & Wang, J. (2022) Layered double hydroxides for tribological application: Recent advances and future prospective. *Applied Clay Science*, 221, May, 106466, <https://doi.org/10.1016/j.clay.2022.106466>
168. Zink, M. D. (2000). Fire resistant hydraulic fluids: shifting definitions and standards, *Proceedings of the 48th National Conference on Fluid Power*, paper 105-8.3
169. *** Approval Standard for Flammability Classification of Industrial Fluids (Class 6930), Factory Mutual Global, January 2002.
170. *** Boron Nitride,
https://en.wikipedia.org/wiki/Boron_nitride#:~:text=Boron%20nitride%20is%20a%20thermally,a%20similarly%20structured%20carbon%20lattice
171. *** British Coal Specification 570:1981 Fire Resistant Fluids for use in Machinery and Hydraulic Equipment (Safety requirements and physical characteristics only)
172. *** Catalogue, PlasmaChem, 2016
173. *** Council Directive 91/339/EEC, amending for the 11th time Directive 76/769/EEC on the approximation of the laws, regulations and administrative provisions of the Member States relating to restrictions on the marketing and use of certain dangerous substances and preparations, Official Journal L 186 , 12/07/1991 P. 0064 – 0065.
174. *** Council Directive 98/37/EC, 22 June 1998, on the approximation of the laws of the Member States relating to machinery, OJ L 207, 23.7.1998.
175. *** Directiva 2014/34/UE A Parlamentului European și a Consiliului din 26 februarie 2014 privind armonizarea legislațiilor statelor membre referitoare la echipamentele și sistemele de protecție destinate utilizării în atmosfere potențial explozive (reformare), (ATEX), Jurnalul Oficial, L 96. P. 309, <https://eur-lex.europa.eu/legal-content/RO/TXT/PDF/?uri=CELEX:32014L0034&from=EN>
176. *** Directiva 92/104/CEE a Consiliului din 3 decembrie 1992 privind cerințele minime pentru îmbunătățirea securității și protecției sănătății lucrătorilor din industria extractivă de suprafață și în subteran [a douăsprezecea directivă specială în sensul articolului 16 alineatul (1) din Directiva 89/391/CEE] (JO L 404, 31.12.1992, p. 10), modificată prin: M1 Directiva 2007/30/CE a Parlamentului European și a Consiliului din 20 iunie 2007 Jurnalul Oficial L 165, p. 21 27.6.2007, <https://eur-lex.europa.eu/legal-content/RO/TXT/PDF/?uri=CELEX:01992L0104-20070627&from=EN>
177. *** Graphene and Boronitrene (White Graphene). physik.uni-saarland.de
178. *** HSE Approved specifications for fire resistance and hygiene of hydraulic fluids for use in machinery and equipment in mines, Reference HSE (M) File L11.6/3, October 1999, <https://www.hse.gov.uk/mining/frfluid.pdf>
179. *** Lubricant Additives and the Environment ATC Document 49 (revision 1), Technical Committee of Petroleum Additive Manufacturers in Europe (ATC)
180. *** Infrared, Near Infrared and Raman Spectroscopy, Routine FT-IR Spectrometers (2022). www.bruker.com/en/products-and-solutions/infrared-and-raman/ft-ir-routine-spectrometer/alpha-ii-compact-ft-ir-spectrometer.html
181. *** Physical Properties of fats and Oils (accessed March 2022)
http://www.dgfett.de/material/physikalische_eigenschaften.pdf
182. *** The directive on dangerous substances, Comisia Europeană, https://ec.europa.eu/environment/archives/dansub/home_en.htm
183. *** US Army Corps of Engineers, Engineering and Design, Lubricants and Hydraulic Fluids, Engineer Manual, 1110-2-1424, Washington, DC, 1999
184. *** ASTM D2783-21 Standard Test Method for Measurement of Extreme-Pressure Properties of Lubricating Fluids (Four-Ball Method)
185. *** SR EN ISO 20623:2018 Produse petroliere și produse înrudite. Determinarea proprietăților de extremă presiune și antiuzură ale lubrifianților. Metoda cu patru bile (condiții europene)
186. *** SR EN ISO 20823:2004 Produse petroliere și produse înrudite. Determinarea caracteristicilor de inflamabilitate a fluidelor în contact cu suprafețe calde. Încercarea de inflamabilitate pe metal cald
187. ASTM D2596:2020 Standard Test Method for Measurement of Extreme-Pressure Properties of Lubricating Grease (Four-Ball Method)